Master of Science Thesis

An exploration into the potential of microturbine based propulsion systems for civil Unmanned Aerial Vehicles

Anna Marcellan

13 May 2015

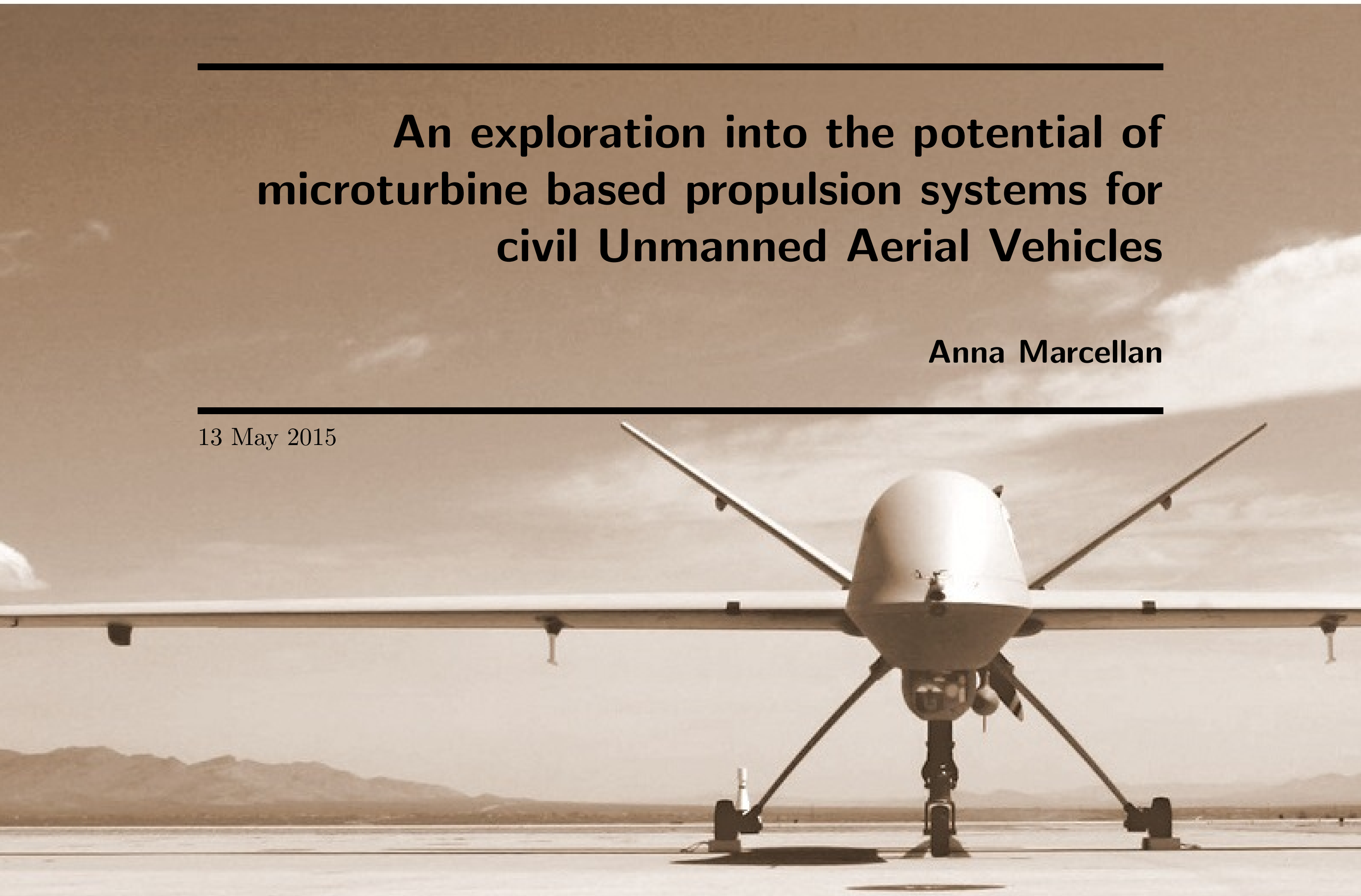

Faculty of Aerospace Engineering · Delft University of Technology

TU Delft Delft University of Technology

Challenge the future

An exploration into the potential of microturbine based propulsion systems for civil Unmanned Aerial Vehicles

Master of Science Thesis

For obtaining the degree of Master of Science in Aerospace Engineering at Delft University of Technology

Anna Marcellan

13 May 2015

Thesis number = 030#15#MT#FPP

Faculty of Aerospace Engineering · Delft University of Technology

Delft University Of Technology
Department Of
Flight Performance and Propulsion

The undersigned hereby certify that they have read and recommend to the Faculty of Aerospace Engineering for acceptance a thesis entitled **"An exploration into the potential of microturbine based propulsion systems for civil Unmanned Aerial Vehicles"** by **Anna Marcellan** in partial fulfillment of the requirements for the degree of **Master of Science**.

Dated: 13 May 2015

Head of department: ______________________
Prof. Dr. Ir. P. Colonna

Supervisor: ______________________
Dr. Ir. W. P. J. Visser

Reader: ______________________
Dr. Ir. M. Voskuijl

Reader: ______________________
Dr. Ir. R. Pecnick

Summary

A Master Thesis Research has been undertaken with the goal of investigating the potential of micro gas turbines as propulsion system of choice for small Unmanned Aerial Vehicle (UAV) used in civil applications.

An Exploration Study is performed both in the fields of UAV technology and of Micro Gas Turbine technology. These two areas are covered in order to understand the possible advantages and limitations of micro gas turbine engines compared to alternative propulsion concepts (e.g. electric and reciprocating engines) when used for a specific application.

After the identification of a significant Case Study, a conceptual design of a high-potential UAV micro gas turbine based propulsion system is performed. Prediction of scale effects is important within the framework of turbine conceptual design where the power output is varied in order to optimize the mission performance in which the turbine is integrated. To this end, engine cycle optimization using Gas turbine Simulation Program (GSP) is carried out.

Furthermore, an "Aircraft Study" is performed in a correlated Master Thesis Project in which the aerodynamic and flight performance model of a baseline UAV is developed. After the model validation, results from the micro gas turbine model are integrated and the performance of the new UAV configuration is investigated.

Acknowledgements

Foremost, I would like to express my gratitude to my supervisor Wilfried Visser for his availability and support, for his motivation, enthusiasm, and great knowledge. Besides my supervisor, I would like to thank my thesis committee, Prof. Piero Colonna for his kind approval and guidance during the structuring of the project and for providing arguments and encouragement during this research, Mark Voskuijl, for his support and invaluably constructive criticism and advice during the project work, and Rene Pecnik for taking the time to asses my thesis work.
I would like to thank Sander Beuselinck for being part of this venture, I enjoyed collaborating and discussing with him both our work and many other topics during the months that passed. My sincere thanks also goes to Adam J. Head for his constant support and help in uncountable things during the development of this thesis, and to the other PhD candidates of the Department of Flight Performance and Propulsion for their kind support and guiding.
I also want to extend my gratitude to my friends, who are my source of energy and inspiration, for being there when it was most needed and for creating a wonderful environment for me to grow as a person and as an engineer. I thank my fellow course mates for the stimulating discussions, for the sleepless nights we were working together before deadlines, and for all the fun we have had in the last two years. I also want to place on record my sense of gratitude to all the persons, who directly or indirectly, have lent their hand for the successful completion of this report.
Last but not the least, I would like to thank my family: my parents Massimo and Carla, for supporting me with love throughout my life; my brother Marco, for reminding me to always follow my dreams and fight for my beliefs; and my sister Elena, whose courage and kindness I will always admire.
With gratefulness,

Delft, The Netherlands — Anna Marcellan
13 May 2015

Contents

List of Figures

List of Tables

List of Symbols

Greek Symbols

η_∞	Polytropic Efficiency	[-]
η_b	Combustion efficiency	[-]
η_c	Compressor Isentropic efficiency	[-]
η_m	Shaft Mechanical Efficiency	[-]
η_n	Exhaust Nozzle efficiency	[-]
η_{pr}	Propeller Efficiency	[-]
η_t	Turbine Isentropic Efficiency	[-]
γ	Heat Capacity Ratio	[-]

Acronyms

AIAA	American Institute of Aeronautics and Astronautics
APP	Aerospace Propulsion and Power
CAS	Calibrated Air Speed
CR	Close Range UAV
DP	Design Point
EADS	European Aeronautic Defence and Space Company
EASA	European Aviation Safety Agency
EN	Endurance UAV
EPR	Engine Pressure Ratio

GSP	Gas turbine Simulation Program
HALE	High Altitude Long Endurance
IAI	Israel Aerospace Industries
IR	Infrared
ISTAR	Intelligence, Surveillance, Target Acquisition and Reconnaissance
LHV	Lower Heating Value
LR	Long Range UAV
MALE	Medium Altitude Long Endurance
MAV	Micro UAV
MCL	Maximum climb
MCT	Maximum continuous
MGT	Micro Gas Turbine
MR	Medium Range UAV
MTOW	Maximum Take-Off Weight
MTO	Maximum take-off
MUAV	Mini UAV
NLR	Nationaal Lucht- en Ruimtevaartlaboratorium
OD	Off-design
RC	Rating Code
RF	Radio Frequency
RPAS	Remotely Piloted Aircraft Systems
RPV	Remotely Piloted Vehicles
SAE	Society of Automotive Engineers
SAR	Search and Rescue
SFC	Specific Fuel Consumption
SF	Scaling Factor
SR	Short Range UAV
TIT	Turbine Inlet Temperature
TL	Technology Level
TSFC	Thrust Specific Fuel Consumption
UAS	Unmanned Air System
UAV	Unmanned Aerial Vehicle
VTOL	Vertical Take-Off and Landing

Other Symbols

R	Gas Constant
$\dot{m}_a$	Air Mass flow

CO_2	Carbon Dioxide
PR_c	Compressor Pressure Ratio
c_m	Exit meridional velocity
dP_{pt}	exit-to-ambient relative pressure drop
∞	Infinity
V_j	Jet Velocity
LiS	Lithium Sulphur
LiPO	Lithium-ion-polymer
Ma	Mach Number
V_0	True Air Speed
C_{pw}	Power Coefficient
PW	Power
D_{pr}	Propeller Diameter
Re	Reynolds Number
N	Rotational Speed
u_t	Rotor Tip speed
W_t	Specific Weight
v_{0t}	Theoretical spouting velocity
C_t	Thrust Coefficient
T	Thrust

Chapter 1

Introduction

The term UAV is an acronym for Unmanned Aerial Vehicle, an aircraft with no pilot on board. The UAV market is likely to develop great economic and technological importance on a near future because of the wide variety of applications and the added value related to these unmanned vehicles. Over the last decade, UAV manufacturers have moved beyond the military sector and have shown a significant amount of interest in potential UAV applications in civil and commercial markets. The military has acted as a first adopter of UAV systems and has demonstrated their utility, encouraging the idea of their use in a large number of non-military applications.
New multi-disciplinary technologies, not only from the sphere of aeronautics but also from many other disciplines, will considerably promote UAV improvements. In this regard, research focused on improving UAV capabilities is strictly related to UAV propulsion systems; as a matter of fact, aircraft performance is dependent on the mass of the powerplant and its specific fuel consumption since these can have a very significant effect on the reduction in size or increase in range of the UAV.

The following Master Thesis Project has been performed with the goal of investigating the potential of micro gas turbine based propulsion systems for a UAV used for a civil application. Firstly, an Exploration Study has been carried out focusing on analysing both UAV and micro turbine technologies in order to establish the potential of their integration for a civil mission. This requires the definition of a Case Study to set a significant framework for the investigation: it will allow the development of the research objectives and the clear assessment of the results.

The work is developed in nine main chapters. Chapter 1 presents the project proposal, where the research question and the objectives of the study are addressed in detail. Chapter 2 focuses on the Exploration Study, where UAV technology and micro gas turbine technology State of the art are extensively analysed. Chapter 3 explains the methodology adopted in the investigation and the specific planning of the project. The aforementioned Case Study is defined in Chapter 4, followed by the micro gas turbine model development described in Chapter 5. Analysis of the results of the engine cycle optimization are discussed in Chapter 6. According to the mission performance of different engine models, in Chapter 7 a micro gas turbine conceptual design is concluded for the selected Case Study. Chapter 8 addresses the results of the investigation, and the main conclusions and recommendations are summarised in Chapter 9.

1.1 Project Rationale

UAVs represent a rapidly growing activity in commercial aviation that will have a very significant economic impact in the near future. The use of small UAVs in performing civil and commercial operations such as photography, wild life research and survey, agriculture surveying and mapping, and others, has stimulated the demand for UAVs in the commercial sector. The strong growth of this market will come along with the increase in functionalities such as higher endurance, lower noise and emissions, extended mission range, among others.
The type and performance of the air vehicle is principally determined by the needs of the operational mission. Significant determinants in the design of the aircraft configuration are the operational range, flight speed, and endurance demanded by the mission requirements. The endurance and range requirements will determine the fuel load to be carried. Achievement of small fuel consumption and maximised performance will require an efficient propulsion system and optimum airframe aerodynamics. For this reason, developments are taking place to advance the technology of power plants. The high power to weight ratio of gas turbines could benefit new UAV concepts, provided that their efficiency will be sufficiently high for specific requirements in terms of range and endurance, especially when compared to other possible propulsion systems available. Even though micro turbines are becoming increasingly popular for small-scale power generation, and they are gradually emerging as the propulsion system of choice for small aircraft with power ratings down to 200 kW, it is speculated that the full potential of this technology for civil UAVs has not been explored yet.
Given the experience of the Delft Universitys Propulsion and Power group in micro turbine technology, it is considered an interesting opportunity to investigate the potential of micro turbines for civil UAVs. Results of the study may well lead to interesting research questions and solutions that will contribute to the development of competitive novel gas turbine propelled UAV concepts for various applications. Results of the investigation will be used for to assess requirements for experimental facilities in the envisaged new Aerospace Propulsion and Power (APP) Lab.

1.2 Research question, aims and objectives

The goal of the project is to investigate the potential of micro gas turbines as propulsion system of choice for small UAV used in civil applications. The research question to be answered can be structured as follows:

'Which design options may allow a micro turbine based propulsion system to arguably showcase a competitive edge compared to alternative propulsion concepts (e.g. electric and reciprocating engines) when used as power propulsion system for a small civil UAV?'

In order to answer this question, several subquestions are identified and further investigated.

- What is the definition of UAV?
- How are the different types of UAVs classified?
- What is the current regulation regarding UAV deployment in the civil air space?
- Which civil missions can they perform?
- Which requirements should a civil UAV satisfy for each mission?
- How are those requirements translated into design specifications?
- What is the current State of the art in UAV technology?
- Which propulsion systems are currently used by existing UAVs?
- What is the definition of micro gas turbine technology?
- Which applications currently make use of micro gas turbines?
- What are the pros and cons of micro gas turbines compared to alternative propulsion systems for a civil UAV?
- Which design considerations should be taken into account when downscaling a micro gas turbine?
- How is the efficiency of the components affected by downscaling?
- How should a valuable Case Study be developed?

By answering these questions, the State of the art in UAV technology is determined with a clear overview of current UAV types and classifications. Analysis of civil applications with potential to meet demands from society and/or the market is performed. This requires an investigation both in the academic environment and in the market scene, with particular attention to development trends for the future generations of UAV systems, regulations and certifications, and analysis of key technologies which challenge the market expansion. In addition, in depth investigation on micro gas turbine technology will allow the understanding of the possibilities of their utilisation as propulsion system of choice for a small UAV. This needs to be set against the analysis of other possible propulsion systems, in particular considering their performances in terms of power range, power-to-weight ratios, efficiencies, and suitability according to the requirements that civil UAVs dictate. Effects of downscaling on the design parameters such as specific fuel consumption and efficiency of turbomachinery components represent a fundamental part of the investigation.

Chapter 2

Exploration Study

The following Exploration Study provides an overview of UAV and micro gas turbine technologies. In section 2.1, the State of the art on UAV technology is discussed. An introduction of the current definitions and classifications used for UAVs is given in paragraph 2.1.1. In paragraph 2.1.2, market and development trends analysis are presented, followed by an overview of current regulations and certifications in paragraph 2.1.3. Current and foreseen civil applications are discussed in paragraph 2.1.4, while paragraph 2.1.5 briefly presents the existing UAVs.
In section 2.2, a review of different propulsion system requirements and configurations is performed, with detailed section for electric motors 2.2.1, reciprocating engines 2.2.2, and gas turbine engines 2.2.3. A structured analysis of micro gas turbine design considerations follows (2.3) with a discussion of pros and cons of their utilization and a developed review of the main effects of downscaling in the turbine design(2.3.1).

2.1 UAV Overview

2.1.1 Definition and Classifications

Literature presents many different definitions of an UAV. Vehicles that fly without pilots are commonly defined as Unmanned Aerial Vehicles (UAVs), Remotely Piloted Vehicles (RPVs), and drones. While RPVs are characterized by being controlled from a remote location, UAVs differentiate since they may also perform autonomous or preprogrammed missions. In the past, they were all are called drones, that is a *"an unmanned aircraft or ship guided by remote control or onboard computers"* according to Merriam-Websters Dictionary [3]. Today the UAV developer and user community does not use the term drone except for vehicles which have limited flexibility for their missions and fly in a dull, monotonous, and indifferent manner, such as a target drone. Another common definition is Unmanned Air System (UAS) which highlights the fact that nowadays this kind of technology includes more sophisticated ground control systems, payloads, and other components. Throughout this document, the terms UAV, UAS and RPV will be considered

interchangeable terms.
The Department of Defense and AIAA Committee of Standards [4] give the following definition for an Unmanned Aerial Vehicle :
"A powered, aerial vehicle which is designed or modified not to carry a human operator/pilot, uses aerodynamic forces to provide vehicle lift, can fly autonomously or be piloted remotely, can be expendable or recoverable, and can carry one or multiple designated payload(s)"

As a minimum, Gundlach [5] states that a typical UAV system is composed of air vehicle(s), one or more ground control station and/or mission planning and control stations, payload, and data link. In addition, many systems include launch and recovery subsystems, air-vehicle carriers, and other ground handling and maintenance equipment. The air vehicle includes the airframe, the propulsion system, flight controls, and electric power unit. The air data terminal is mounted in the air vehicle, and is the airborne portion of the communications data link. The payload is also on-board the air vehicle, but it is recognized as an independent subsystem that often is easily interchanged with different air vehicles and uniquely designed to accomplish one or more missions. Payload types can be classified as follows [6]:

- Camera: optical cameras, low-light-level cameras and thermal imaging cameras.
- Sensor: a lot of options possible like pollution monitoring, weather sensors, distance measurements, etc.
- Radio relay system: radio receiver, amplifier and transmitter used to increase the range of radio communication.
- Non-disposable: a lot of options possible like radar, public addressing system, etc.
- Disposable (Solid): medical supplies, surviving equipment, postal packages, seeds, etc.
- Disposable (Liquid): Fire retardant liquids, water, fertilizers and pesticides, etc.

The aircraft itself has much in common with manned aircraft, but presents also several differences. Those mainly result from the differences in operational requirements compared with manned aircraft, for example the need to take off from remote, short, unprepared runway or to fly for long periods at very high altitudes. The performance of the aircraft is often enhanced by not having to carry the weight of equipment and structure required to accommodate the aircrew, and by having a lower aerodynamic drag for the same reason [6].

There are several ways used by academics to categorize different kinds of UAV. These classifications are commonly based on UAV size and/or mission. However, these definitions are constantly being changed as technology developments allow smaller systems to perform the roles of bigger ones. The boundaries, therefore, are often blurred and the following classes (based on [7]) should be considered as working definitions for the scope of the present study.
The terms currently in use cover a range of systems, from the HALE with an aircraft of

	Altitude [m]	Endurance [hr]	Range [km]	MTOW [kg]	Examples
HALE - High Altitude Long Endurance	15000-20000	24 - 48	> 2000	2500-12500	*GlobalHawk, Xianglong, Soar Dragon, EuroHawk, Hamaseh, Buraq , Global Observer*
MALE - Medium Altitude Long Endurance	5000-15000	24 - 48	> 500	1000-1500	*Predator, Orion , CyberEye II, BZK-005, Pterodactyl, Harfang, Barracude, European UAS, Dominator*
EN - Endurance UAV	5000 - 8000	12 - 24	> 500	500 - 1500	*Aerosonde, Vulture II Exp, Shadow II, Searcher II*
LR - Long Range UAV	5000	6 - 12	200 - 500	-	*Hunter, Vigilante 502*
MR - Medium Range UAV	3000 - 5000	6 -10	70 - 200	150 - 500	*Aerostar, Eagle Eye+, Sniper, Firescout (VTOL), Camcopter S100 (VTOL), Seagull (VTOL)*
SR - Short Range UAV	3000	3 - 6	30 - 70	200	*Scorpi 6/30, Firebird, Luna, Copter 4*
Close-Range UAV	3000	2 - 4	10 -30	150	*Scan Eagle, Observer, Phoenix, Sprite (VTOL)*
MUAV - Mini UAV	150 - 300	< 2	< 10	< 30	*Desert Hawak III, Bluebird Skylite, Indago (VTOL)*
MAV - Micro UAV	250	< 1	< 10	0.10	*Wasp, MinO, Maveric, Quadrotor (VTOL)*

Table 2.1: UAVs classification according to flight altitude, endurance, range, and MTOW

35 m or greater wing span, down to the MAV which are of only 150 mm span. Therefore, different UAVs can be defined according to table 2.1.

For each class of UAV, requirements in terms of flight altitude, endurance, range and maximum take-off weight are specified. Some examples of existing UAVs which belong to each class are given. This categorization will be useful in a further stage to assess which UAV class is suitable for each civil application as identified in the following paragraph.

2.1.2 Market and Development Trends

Military investment in UAV research, systems, and applied technologies is increasing and potential uses for UAVs in civil operations are currently being investigated. These developments, along with growing scientific research in automation and sensor technologies, are

proving the potential for costs savings and causing commercial interest in the unmanned market. Indeed, these vehicles offer a unique range of features, among which ultra-long endurance and high-risk mission acceptance.
How the demand for UAVs will manifest itself in a future market remains highly speculative. Indeed, market forecasts for the UAV industry are tempered by the fact that they do not include the projections for payload costs or operational costs. Table 2.2 lists various forecasts based on the number of units of demand for basic systems; these forecasts do not reflect the total market including operations and sensor suites [4].

Source	Date	Forecast	Uses
Department of Defense	F.Y. 2001 budget	Strike force to be 1/3 UAVs by 2010	Military
Teal Group	Dec 2002	Market to double by 2014	Military, science, homeland security
Frost and Sullivan	Oct 2003	5.5B EUR by 2012	Military, science, homeland security
Forecast Intl	Oct 2003	\$10.6B by 2013 Massive growth 2010	Military, science, homeland security
Teal Group Date	Aug 2004	\$4.5B/year by 2014	Military, science, homeland security
Frost and Sullivan	Oct 2005	\$1.45B /year by 2015	Civil and commercial
Frost and Sullivan	Mar 2006	\$17B by 2011	Military, civil and commercial

Table 2.2: UAV Market Forecasts

Of interest to this effort is the fact that all indicate a high rate of growth in the number of units demanded over the next ten years. By extension, the growth in the support market could be considered explosive as well. UAV price structure will be the major influence in the civil sector growth rate.
According to Lucintel Brief market forecast [8], approximately 70% of global growth and market share is currently in the USA, while in terms of production, European development of dual-use systems for military and civilian applications is broadening the market demand of UAV systems. In the Mid-East region, Israel is the pioneer for many of the current tactical UAV efforts and major player in UAV sales to armed forces around the globe, and Asia-Pacific countries have increased their actives in UAV development, showing great potential in the coming years.
The creation of a UAV market is a combination of the emergent technology revolution together with emergent market opportunities. Evolving technologies in the fields of computation, propulsion, communications, payloads, materials and manufacturing, feed the motivation to develop new UAV products. New multi-disciplinary technologies, not only from the sphere of aeronautics, will considerably advance UAV improvements, and the emphasis during the coming years will be on affordability, performance, safety and readiness.
Key Technologies for a successful development of UAVs include the following:

- Airframes - the flight platform is the main component of a UAV system. Given the unique requirements for specific tasks, the airframes and their flight performance should be developed to suit them, e.g. high maneuvering performance required for low level terrain-following.

- Propulsion units - this is particularly significant for high altitude and/or long endurance requirements. Likewise, there may be special fuel or engine material-property requirements.
- Autonomous Flight Controllers - the key to wide application potential of UAVs. Globally, there has not yet been many UAVs capable of completely autonomous operations.
- Launch and Recovery - key phases of UAV flight. Launch and recovery requirements are often dependent on task and operational requirements. Current launching techniques range from the use of runways, catapults, rockets, to the use of trucks.
- Navigation and Guidance - the common availability of Global Positioning Satellite Navigation Systems has had a prominently positive impact on navigation in general, and likewise their use in UAVs. The integration of satellite navigation and inertial sensor data with flight control systems enable wider application potential for UAVs.
- Self-Protection - safety for the possibly valuable on-board sensors and airframes, from external interference and damage, to keep costs low.
- Ground Control Station - the UAVs would need to be monitored from base in some form, and the possibility to update task requirements mid-way through a mission.
- Payloads - innovation and imagination remains the key to using UAVs to carry payloads and sensors, ranging from surveillance sensors to possibly express parcel delivery systems.
- Data Communication, Storage, Processing, and Dissemination - secure data links, and information technology.

However, several prerequisites must be satisfied to render the UAV a viable, cost-effective and regulated alternative to existing resources. According to [4], major civil and commercial market barriers include:

- Lack of airspace regulation that covers all types of UAV systems (encompassing 'sense and avoid', airspace integration and airworthiness issues)
- Affordability - price and customization issues (e.g. commercial off-the-shelf, open modular architecture)
- Liability for civil operation
- Capacity for payload flexibility
- Lack of sufficient secure non-military frequencies for civil operation
- Perceived reliability (e.g. vehicle attrition rate vs. manned aircraft)
- Operator training issues

- Recognition/customer perception of the UAV market
- Technology developments for multi-mission capability

The market demands for better performance push the technology to continually provide improved solutions. With respect to body design, it is important for a UAV to have a light structure, high-stabilty construction, high thrust-to-weight ratio, and a general design that is well-suited for autonomous flight. With regard to autonomous control, a UAV requires a highly reliable data link and advanced sensors.
Important UAV research topics include: formation flight control, such as for civil use observation work, data relay, and in-air refueling; integrated hierarchical control of UAVs and micro air vehicles (MAVs) (for example, highly precise missions can be carried at by coordinating small UAVs with a larger supervisory UAV); high-altitude flight (since a UAV does not carry people, it is well-suited for prolonged flight in the stratosphere for scientific observation missions); all weather flight; installation of collision-avoidance radar systems and other equipment; intelligent flight control and management systems [9, 7]. Current research focuses on improved-cost-effectiveness of small class UAV, with more than 24 hours endurance. Long endurance has numerous benefits for UAV operation, like flexibility, effectiveness, reduced ground operation (returning to base less frequently) etc. Improved configurations and improved propulsion systems, with higher lift to drag ratio, higher fuel fraction, lower empty weight and lower payload weight are currently investigated [10]. Research in advanced high lift aerodynamics includes improved take-off and landing performance (steep glide angles), flight safety at reduced airspeeds (mild stall characteristics), and the capability of continuing the mission in unfavorable weather and icing conditions.
In order to overcome atmospheric pollution problems, researchers worldwide are seeking alternative propulsion methods which will utilize other fuel sources as an alternative to petroleum. Research in this direction includes fuel cells and solar cells which create a potential for new propulsion systems for long endurance UAVs [10, 11].

2.1.3 Regulations and Certifications

Even thou nowadays' UAVs are almost entirely used for military deployment, the potential application of UAVs for civil and commercial use has generated considerable interest worldwide. As a matter of fact, in the long term the market potential on the civil side is considerably larger than the military sector. Currently, the major constraints are the lack of a central authority and the absence of legislation and regulations for safe flight in integrated airspace [12].
Over the last few years work has began to stimulate the civil UAV market through a number of initiatives also in cooperation with military users. These initiatives primarily aim to deal with the key problems which are the lack of a framework of rules governing the flight safety on the one hand, and insertion of civil and military UAVs in non-segregated airspace on the other [13]. A whole range of legislative and regulatory measures need to be designed, find common approval, and then implemented. Until this goal is reached, UAVs are required to fly either with a special military or a Civil Aviation Authority exemption, or in segregated airspace. At the moment, rules vary from one country to another, an incoherence which makes things more difficult for manufacturers and operators. However,

some rules have already been issued. On 20 June 2013, the European RPAS Steering Group (ERSG) of the European Commission published the *"Roadmap for the integration of civil remotely-Piloted aircraft Systems into the European Aviation System"*, covering the development and integration into non-segregated airspace of civil RPAS in the next 15 years. The roadmap is articulated in three pillars: research and development; safety regulation and technical standardisation; and complementary measures including privacy and data protection, insurance and liability. According to Regulation (EC) No 216/2008 [14], airframes with a mass of more than 150 kilos are now required to obtain airworthiness certification at a European level from the European Aviation Safety Agency (EASA).
Another important issue is that of radio frequency allocation. Currently, there are no particular areas of the RF spectrum allocated exclusively to UAV operations, which has already caused significant problems in the military use of UAVs.
Another issue to be considered is the pilot training and certification. As with the UAV platform, future users have to prove that UAV pilots can train and operate with an equivalent level of safety as the on-board pilots. As was the case with development of UAS platforms, it is the militaries that have been leading the way in terms of pilot certification processes and training requirements. This is particularly the case in the U.S., which has the largest operational fleet of large UAVs. The current approach in Europe has been set by EASA, which divides UAV pilots into two classes: line of sight (Class 1) and beyond line of sight (Class 2), and is working on pilot certification issues. The current view is that UAV pilots will be treated differently from on-board pilots in terms of skills and requirements but that their training curriculum will be similar.

2.1.4 Civil Applications

Although UAV development for civil use is in the early stages, it appears that there are many uses being proposed for them. UAS are popularly commended as being well suited to civil applications that are dull, dirty or dangerous, tasks that entail monotony or hazard for the pilot of a manned aircraft[15]. Unmanned Air Systems are now finding operational applications to peacetime public and private industry security and surveillance, detection and monitoring missions related to environmental protection, natural disasters and law enforcement [16, 17]. Because of their relatively low cost and propensity for providing accurate information (some UAS are able to keep station for days, weeks or even months, making them particularly well suited for use as communication relays) numerous UAV development programs have been initiated worldwide. Several studies discuss potential civil applications for UAVs. Possible missions are: forest management [18, 9]; urban highway traffic monitoring [9, 19]; fire-fighting [20, 9]; meteorological observation (surveys of the ozone layer, air pollution, snow coverage, polar zones, rivers, conditions for typhoon and hurricane generation, tornado formation, etc.)[9]; life search and rescue [20]; law enforcement (border surveillance, police surveillance, counter terrorism operations); large scale public outdoor events surveillance; environmental control and monitoring (including air and sea pollution); telecommunications [20]; disaster assessment and management [21]; crop spray and monitoring [22, 9]; fisheries protection; mineral exploration and magnetic surveys [23], [9]; ground mapping and photography [24]; pipeline and power line monitoring [16, 23, 20, 9].

The civil UAV capability assessment performed by NASA [4] classified civil UAV applications into three identifiable groupings: Commercial and Land Management, Homeland Security, and Earth Science. For each application, requirements in terms of range, endurance, flight altitude, speed, and vertical take-off and landing (VTOL) capability, have been determined based on the literature available. Table 2.3 presents the definitions used to define the requirements values for each application.

Range	**Endurance**	**Altitude**	**Speed**
Short = 0 - 70 km	Short = 0 - 3 hr	Low = 0 - 3,000 m	Low = 0 100 km/h
Medium = 70 - 500 km	Medium = 3 - 12 hr	Medium = 3,000 - 5,000 m	Medium = 100 km/h - 350 km/h
Long = 500 - 20,000 km	Long = 12 - 48 hr	High = 5,000 - 20,000 m	High = >350 km/h
Ultra long= 20,000 - ∞ km	Ultra long = 48 - ∞ hr		

Table 2.3: Requirements values definition

As it is shown in tables 2.4, 2.5, 2.6, all the applications proposed are defined following the same criteria used for the UAV types classification 2.1. By doing this, each application is matched with the most suitable UAV type/types. This is the first step of the analysis for the selection of the possible civil UAV missions for the case study of the Master Thesis Project. However, propulsion systems investigation is still required to determine which applications (and, therefore, which UAV classes) could competitively perform when powered by a micro gas turbine.

Application			**Requirements**					**Type**
			Range	***Endurance***	***Altitude***	***Speed***	***VTOL/Hover***	
Commercial and Land Management	Aerial photography	Urban	Short	Short	Low	Low	Yes	MAV to CR
		Mapping	Medium to Long	Medium to Long	Medium to high	Low to medium	No	SR to HALE
	Agriculture	Crop monitoring and spraying	Short to medium	Short to medium	Low to medium	Low to medium	Yes	MAV to MR
		Herd monitoring and driving	Short to medium	Medium to long	Low	Low to medium	Yes	CR to SR
	Utility companies (Gas, Oil & Electricity) - Pipeline and powerline inspection		Medium to long	Medium to long	Low to medium	Low to medium	No	MR to LR
	Mining Companies - Looking for minerals		Medium to long	Medium to long	Medium	Low to medium	No	MR to LR
	Courier Service - Delivering packages		Short to long	Short to Medium	Low to high	Low to high	Yes	MAV to EN
	Information services - News information and broadcasting		Short	Short	Low	Low	Yes	MAV to CR
	Telecommunications		Long	Long	High	Medium to high	No	EN to HALE

Table 2.4: Commercial and Land Management UAVs applications

2.1.5 Existing UAVs

In order to understand possible trends in the design of UAVs, all the existing UAV have been analysed as listed in the 2013 Worldwide UAV Roundup done by the American Institute of Aeronautics and Astronautics [1]. For each of them, all the information available has been gathered for a complete overview of the current status of the existing UAV technology.

Application			Requirements					Type
			Range	*Endurance*	*Altitude*	*Speed*	*VTOL/Hover*	
Homeland Security	Coastguard	SAR and Coast and sealine monitoring	Long	Medium to long	Medium to high	Low to high	No	EN to HALE
	Police Authorities	Security and incident surveillance	Short to medium	Short to medium	Low to medium	Low to medium	Yes	MAV to MR
	Emergency support	SAR and Delivering emergency supplies	Short to long	Short to medium	Low to medium	Low to high	Yes	MAV to LR
	Fire Service	Forest fire detection and damage assessment	Long	Medium to long	Medium to high	Low to medium	No	EN to HALE
		Forest fire fighting	Short to medium	Short to medium	Low to medium	Low to medium	Yes	MAV to MR
		Communication						
	Lifeboat Institutions - Incident investigation, guidance and control		Long	Medium to long	Medium to high	Low to high	No	EN to HALE
	Customs and Excise - surveillance for illegal imports		Long	Medium to long	Medium to high	Low to high	No	EN to HALE
	Local Authorities - disaster control		Short to medium	Short to medium	Low to medium	Low to medium	Yes	MAV to MR
	Traffic Agencies - Monitoring and control of traffic		Short to medium	Short to medium	Low	Low	Yes	MAV to SR

Table 2.5: Homeland security UAVs applications

Application			Requirements					Type
			Range	*Endurance*	*Altitude*	*Speed*	*VTOL/Hover*	
Earth Science	Conservation - Pollution, land and wildlife monitoring		Long	Medium to long	Medium to high	Low to medium	No	EN to HALE
	Fisheries - Fisheries protection		Long	Medium to long	Medium to high	Medium to high	No	EN to HALE
	Meteorological services - Sampling and analysis of atmosphere		Long	Medium to long	Medium to high	Low to high	No	EN to HALE
	Survey	Geographical	Long	Medium to long	High	Low to medium	No	EN to HALE
		Geological					No	
		Archaeological	Short	Short	Low	Low	Yes	MAV to CR
	River Authorities - Water course and level monitoring		Medium to long	Medium to long	Low medium	Low to medium	No	MR to LR
	Atmospheric Satellite		Ultra long	Ultra long	High	High	No	HALE
	Ice reconnaissance		Medium to long	Medium to long	Low to medium	Medium to high	No	MR to LR

Table 2.6: Earth Science UAVs applications

As it is shown in figure 2.1, U.S. is the first worldwide UAVs manufacturer, followed by China and Israel. Few European countries follow, namely France, Germany, Russia and UK. Developing countries are also showing a strong interest in this market, especially Pakistan, Brazil, and India. However, it should be highlighted that the majority of the existing UAVs are currently military.

Figures 2.2, 2.3, 2.4, present some results of this preliminary analysis. From the graphs, it is clear that UAVs are not an established technology yet since most of the existing UAVs are still in development phase. It is also interesting to notice that the majority of the existing ones currently employ reciprocating engines or electric motors as propulsion systems. This topic will be later addressed in section 2.2. Finally, we can see that VTOL/hover capability is implemented in almost 20% of the existing UAVs, proving a growing interest in this function. This fact is also noticeable from the civil applications analysis carried out in section 2.2.

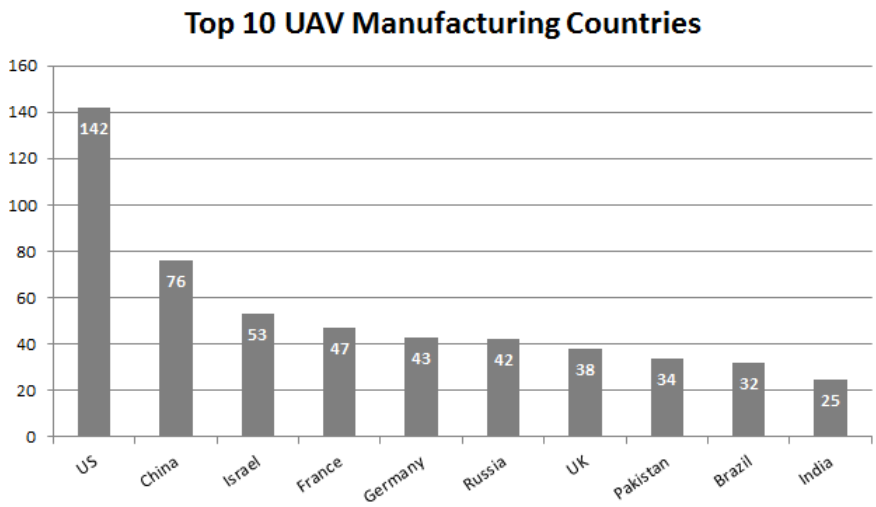

Figure 2.1: Top 10 UAVs manufacturing Countries according to the 2013 Worldwide UAV Roundup done by the American Institute of Aeronautics and Astronautics

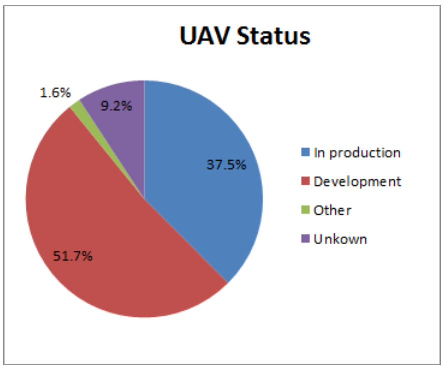

Figure 2.2: Existing UAVs status according to the 2013 Worldwide UAV Roundup done by the American Institute of Aeronautics and Astronautics [1]

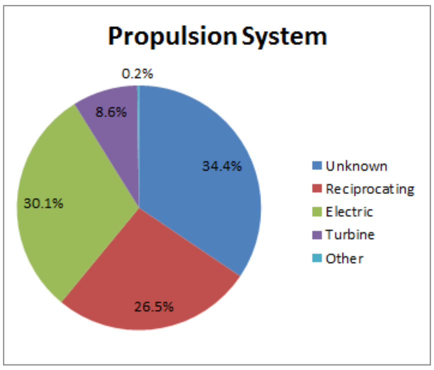

Figure 2.3: Propulsion systems employed by existing UAVs according to the 2013 Worldwide UAV Roundup done by the American Institute of Aeronautics and Astronautics

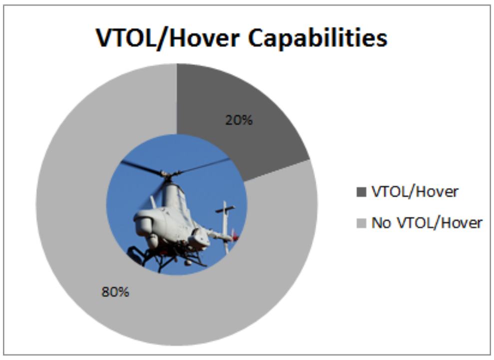

Figure 2.4: Vertical take-off and landing (VTOL) and hover capability of existing UAVs according to the 2013 Worldwide UAV Roundup done by the American Institute of Aeronautics and Astronautics

2.2 Propulsion Systems

The power system for a UAV, as for any aircraft, includes an energy source, a means of converting that energy into mechanical energy and a means of converting that into a lift or thrust force. A power-plant will include engine speed and/or power output controllers, engine temperature controller and, usually for fixed-wing aircraft, an electrical power generator.
Both unmanned and manned aircrafts are frequently powered by jets, turboprops, and reciprocating engines. However, unmanned aircraft commonly use battery-propeller propulsion, and occasionally fuel-cell power plants, while solar-powered aircraft technologies are now maturing. In fact, engines for UAV have certain special requirements compared to manned aircraft: long endurance, duty cycle characterized by heavy weight and/or high altitude flight (completely different than for light aviation), compactness translated in high power-to-weight ratio and low volume. Moreover, simple maintainability is often required in terms of robustness due to often lower skills ground crews [25, 26].
As a general approximation, according to Austin [6] the mass of the power-plant in most aircraft of moderately high performance is about 10% of the maximum take-off weight (MTOW) of the aircraft. Typically, the fuel carried is about 10-15% of the MTOW for light aircraft of medium range. The payload of these aircrafts usually is in the order of 40-50% of the MTOW. In the case where the payload may be of imaging sensors or other light electronic systems, and so of a lower fraction of MTOW, more fuel may be carried to extend the range. The fuel load in a UAV may therefore be 20-25% of the MTOW, raising the proportion of total power-plant and fuel mass to one-third or more of the MTOW. Any reduction in the mass of the power-plant or in its specific fuel consumption can have a very significant effect on the reduction in size or increase in range of a UAV. Therefore, developments are taking place to advance the technology of power-plants, with these being internal combustion engines (reciprocating or gas turbine) and electric motors.
In the following sections the State of the art of electric motors, reciprocating engines, and gas turbines technology are discussed. Attention is given to analyse their performance when used as propulsion system for an unmanned aircraft in comparison with manned aircraft.

2.2.1 Electric Motors

Electric motors convert electrical energy into mechanical energy to drive a propeller, fan or rotor. The electrical power may be supplied by battery, a solar-powered photovoltaic cell or a fuel cell. The propulsor is the motor-propeller combination and the power source can be a battery, solar array, turbine-driven generator, or fuel-cell stack, among others.
According to [6] and [5], electric motors have multiple advantages. Unlike internal combustion engines, there is very little maintenance and no consumables such as liquid fuel and lubricants. Electric motors can be stored for very long periods of time and no starters are required, and so UAV air-launch is simplified. The performance characteristics are independent of altitude and they have the particular advantage of being the quietest of all the engines and with the smallest thermal signature. Electric motor systems are also simple to design, integrate, and test. Electric motors apply nearly constant torque to the propeller and their smooth operation reduces the structural loads on the propeller. Properly balanced electric motors have low vibration levels compared to well-designed reciprocating engines. This quality can support low vibration levels at the payload for better pointing accuracy. Also, the motor frontal area is less than a reciprocating engine producing equivalent power, permitting lower drag fairings.
Electric motors have no emissions, and so the UAV emissions depend upon the power source type. Batteries and solar arrays produce no emissions, and hydrogen fuel cells emit only water (this will be discussed in more detail in paragraph 2.2.1), showing potential for very limited environmental impact. Hydrocarbon-based power sources for electric motors have complex emissions that include CO_2 and water, among many other constituents.
The biggest limitation for electric flight is the short endurance that can result from the power source. Modern batteries have low specific energy relative to liquid hydrocarbon fuel, resulting in UAVs with only 0.5-3 hr endurance. The demand on the battery is made not only by the motor, but also by the payload and communication system. Therefore, the flight endurance and speed of such UAV systems and the capability of their payload and communication systems are limited. Back-up batteries must be carried and regularly charged to ensure an electrical supply. Other means of obtaining a continuous electrical supply are being sought in order to extend the range and capability of electrically powered systems and to this end research is underway to develop solar-powered photovoltaic cells and fuel cells compatible with UAV systems requirements. Both systems have been flown in a UAV, but the technology is still under development. Currently only micro- and mini-UAV which weight about 9 kg (or less) are powered by batteries and electric motors with less than 1 kW output power.
The following paragraphs analyse more in detail batteries, fuel cells, and solar cells technologies.

Battery Power

A battery is an electrochemical device that converts stored chemical energy into electrical power. It can be rechargeable or single use. Non rechargeable batteries are known as primary, and rechargeable batteries are called secondary. Primary cells may have superior performance characteristics but the cost of replacing batteries is generally prohibitive for multi-use UAVs, and so secondary batteries are used for those applications. Secondary

batteries are also required for multiday duration solar-powered UAVs that use batteries to power the motors at night.
Several battery chemistries have been used for unammaned aircraft propulsion systems [5]. Nickel- cadmium (NiCd) batteries were dominant in the 1980s and 1990s. Nickel metal hydride (NiMH) made were available in the late 1990s and early 2000s. However, lithium-ion (Li-Ion) and lithium-ion-polymer (Li-Po) batteries are the main type in use today for small UAS propulsion systems. Improvements in rechargeable battery performance through use of LiS (lithium sulphur) technology has reduced the mass-to-energy ratio to about one quarter that of other battery types [6]. Unfortunately a down-side of the system is the large volume of the batteries. For a given energy storage, even LiS batteries occupy four times the volume of that of fossil fuels, presenting a problem for all other than short-range UAV. Todays unmanned aircraft using LiPo batteries might have practical flight durations of about 2 hrs.

Fuel Cells Technology

Fuel cells are electrochemical devices that use chemical reactions of a fuel source and oxidizer to generate electrical power. The fuel and oxidizer are consumed in the conversion process, and the by-product (pure water when the hydrogen is the fuel) are either exhausted from the fuel cell or stored onboard the UAV [1] [27]. The reaction occurs in the presence of an electrolyte, which is not consumed.
Recent developments by companies such as Protonex [28] indicate a power-to-weight ratio for a hydrogen-powered fuel cell in the order of 1 kW/kg. To this, the mass of an electric motor must be added reducing the ratio for the installation to 0.8 kW/kg, making the installation heavier than any of the other systems. It is claimed, that the process is very efficient with energy conversion being about 95% compared with that of about 35% for most internal combustion engines. Although there is little information available on the fuel consumption, the hydrogen must be contained in pressure vessels which must weigh more per mass of fuel compared with the tanks for fossil fuels.
Stated advantages [6] for the fuel cell based system are higher efficiency than any other fossil-fuel-based technology, modular and easy installation, in most cases zero-emission devices, zero or very low noise (except for occasional vibrations). Disadvantages are the high production costs due to exotic materials and complicated design and assembly, their high sensibility to fuel contamination adding expense for filters and cleaners, and their need for skilled personnel for maintenance and overhaul.

Solar Power

Solar cells use the photovoltaic effect to convert the sun radiated power into electrical power. This power does not require onboard energy storage for peak daylight operations. However, multiday flights require that extra energy is stored to power the UAV through the night, allowing the UAV to operate almost indefinitely, bounded only by reliability and component life.
Integrating solar arrays on an aircraft involves compromises across a number of disciplines

[1] At present, emissions of CO_2 are however nearly always involved into the production of hydrogen that is needed as a fuel.

[5]. Solar arrays cause structural challenges since they comprise a large portion of the UAV wing weight. Most of the solar-array weight is aft of the wing torsional axis, which can require additional structure or active aeroelastic control along the wing to prevent flutter. Moreover, many solar-powered aircraft designs find that the wing area required to generate propulsion power is greater than the optimum wing area for minimum power flight. The increased area results in higher UAV weight, more drag, and hence more power required to fly. The wing sizing is often solved through optimization, but this topic is out of the scope of the current literature review.

2.2.2 Reciprocating Engines

The great majority of UAVs in operation are powered by internal combustion engines and most of those have reciprocating engines. These are the most common form of propulsion for UAVs with maximum take off weight (MTOW) values between 10 and 1100 kg, with commercial off-the-shelf engines widely available between 1-150 kW [5]. However, it is speculated that the popularity of reciprocating engines is driven by the lack of suitable jet and turboprop engines for the most prolific UAV classes.
UAV reciprocating engines come from a variety of sources ranging from model aircraft to general aviation. The majority of UAVs use modified engines from other sources. Model aircraft engines mostly generate less than 9 kW output power, with the greatest selection around 0.4-1.5 kW [5]. High power-to-weight ratio and low cost are the most important considerations, while fuel consumption can be high because the typical flight time is between 5 to 20 min and the small fuel weight has negligible impact on the flight performance. Moreover, power specifications from model aircraft engine manufacturers should be verified and fuel flow data are rarely available. They are not designed to meet any defined manufacturing or reliability standards, and therefore the manufacturers do not usually measure the performance data of their products.
Large aviation engines such as those used on ultralights and general aviation aircraft are readily adaptable to UAV applications. Ultralight engines start at approximately 15 kW with mostly two-stroke piston engines. Larger ultralight engines usually are four-strokes, with the Rotax 912 and 914 series seeing widespread use on MALE UAVs [5]. General aviation engines are less common on UAVs, primarily because of their higher power output which is normally not required.
Reciprocating engines may be categorized in three main types, although there are sub-types of each.

- Two-stroke engines
- Four-stroke engines
- Rotary engines

These are outlined in the following paragraphs.

Two-stroke and Four-stroke Engines

The only basic difference between two-stroke and four-stroke engines is that the two-stroke engine has a power-stroke on each revolution of the crank-shaft whereas the four-stroke has a power-stroke every other revolution. Hence, the two-stroke tends to produce twice the power in unit time at the same rotational speed compared with the four-stroke unit. For a given power level, two-stroke engines tend to be half the displacement and weight of their four-stroke counterparts (power-to-weight of the two-stroke engine ranges from 0.8 to 2 kW/kg [5]). The two-stroke unit tends to run hotter than the four-stroke and may require more cooling facilities than the four-stroke, while the four-stroke unit tends to be heavier than the two-stroke. Moreover, two-stroke engines are generally less expensive than four-stroke engines, but are less efficient. The specific fuel consumption ranges from 0.45-1.2 kg/kWh as compared to an average of 0.3-0.4 for four-stroke engines [5]. Therefore, both types will pay for higher performance and higher fuel efficiency with greater complexity, weight and cost. Moreover, two-stroke engine rotational speeds generally vary between 5,000 and 9,000 rpm, which generates higher-frequency noise. Finally, neither type produces power with smooth torque (as does a turbine engine), but the torque of both varies during each revolution [6]. However, the torque peaks of the two-stroke unit are much smaller than those of the comparable four-stroke unit. This is of particular concern for a rotorcraft transmission and rotor system (to a lesser extent this will affect the design of propeller too) which must be the more robust if driven by a four-stroke engine.

Rotary Engines

Todays rotary engines are reported to offer a long life and low specific fuel consumption (0.35 kg/kWh)[6]. Although the basic engines are of high power-to-weight ratio, because the engines operate at a high rotational speed, a reduction gearbox is usually necessary. This, together with high levels of cooling equipment required, increases the mass towards that of a conventional four-stroke engine. Currently, there appear to be no rotary engines below a power rating of about 28 kW or above 60 kW available for aircraft. Moreover, the limited data on rotary engines does indicate a strong scale effect where smaller units are far less efficient than equivalent two- or four-cycle engines.

2.2.3 Gas Turbine Engines

Gas turbine engines may be divided into two generic types:

- turbo-jet units which are designed to produce thrust from a high-velocity jet for direct propulsion;
- Turbo-shaft units which produce power in an output shaft which may drive a propeller or helicopter rotor to provide thrust.

Gas turbines produce much less noise than piston engines and have a smooth power at high power-to-mass ratios. They usually operate with heavy fuel (Jet A for civilian airports and JP-5 or JP-8 for military operations). These attributes make jets and turboprops especially desirable for military applications. According to Gundlach [5], gas turbines can be very reliable and have long mean time between overhauls compared with reciprocating engines. There are relatively few moving parts to fail. The combustion is continuous

rather than oscillatory, and the rotational speed is steady; therefore, the vibration is low relative to reciprocating engines.
With the heavy fuel compatibility, good altitude performance, ability to generate thrust at high speeds, high reliability, and long life, turbines certainly have suitable characteristics to be used on UAVs, despite the current scenario. Most of the time, turbines simply are not available with the necessary performance for smaller UAVs, especially when long endurance at low speed is required. In addition, reciprocating engines tend to have a lower acquisition cost.
In the following paragraphs, turbo-jet units and turbo-shaft units are briefly presented along with their current applications as propulsion systems for UAVs.

Turbo-jet units

Turbofan and turbojet engines are generically referred to as jet engines. These propulsion systems maintain thrust at high speeds and high altitudes better than propeller-driven alternatives. The high-speed capabilities of jet engines make them suitable for UAVs flying at equivalent airspeeds greater than 370 km/h and at Mach numbers greater than 0.6 [5].
The simplest form of jet engine is the turbojet. The oncoming air enters the engine in an inlet, which helps diffusing the air. A compressor slows the air to near static conditions, while increasing the pressure and temperature. The compressed air enters a burner where fuel is injected and ignited. This heated air is then expanded in a turbine, which provides power to drive the compressor. This power is mechanically transferred between the turbine and compressor via a shaft. The air exits the turbine and is accelerated in a nozzle to provide high velocity flow for thrust generation.
Turbofans are similar to turbojets, except that a second turbine is added to drive a ducted fan. The fan turns at a much slower rate than the compressor, and so two separate shafts are used. A turbo-fan unit is in effect a mixture of the turbo-jet and turbo-shaft engines in so far as some of the combustion energy is extracted as a jet whilst some energy is converted to mechanical power to drive a fan which produces a slower-flowing, but larger volume, jet of air. A thrust-producing jet is at its most efficient when the minimum amount of jet velocity is left in the ambient air mass after the aircraft has passed.
Mature jet-units are generally selected for UAS programs because development budgets are rarely available and UAV production quantities are usually insufficient to justify a commercial development by engine manufacturers [5]. However, there are very few manned aircraft engines below 4 kN thrust, requiring engines built specifically for UAVs. The largest markets for military small turbine engines are targets and cruise missiles, where thrust class ranges from 0.13-4.45 kN. Cruise missile engines are designed to operate for a single flight and must start rapidly. Moreover, these engines tend to have a short design life and are difficult to tailor to other UAV applications such as long-duration ISR (Intelligence, Surveillance and Reconnaissance) missions.
At the smallest end of the jet-engine thrust spectrum are engines designed for model aircraft. These engines are intended for aircraft weighing 4.5-25 kg, and so the thrust class is generally less than 0.13 kN. Like target and cruise missile engines, the design life is low, and the TSFC (Thrust Specific Fuel Consumption) is high.

Turbo-shaft units

Turbo-shaft units are divided into turboprops and turboshafts. Turboprop engines are quite similar to turbofans, except that the low-pressure turbine drives a propeller instead of a ducted fan. A reduction gearbox is usually required to match the speed of the propeller and low-pressure turbine. Turboshaft engines are similar to turboprops, except the shaft does not drive a propeller and is available for other uses such as powering a generator. In their simplest form they employ a compressor set and turbine set on a single output shaft.

Their disadvantage is that any increased load on the power output which slows the turbine will also slow the compressor set, thus reducing the power available to accelerate the engine back to operating speed (until an increase in fuel injection can take effect). The result is a lag in response which is bad for a propeller-driven aircraft, but can be disastrous for a helicopter. Most turbo-shaft engines of today therefore are of the free-power-turbine (FPT) configuration. Here the output shaft is a second separate shaft from that mounting the power-generating compressor/turbine sets. Thus when the output demand is increased, the compressor is not slowed and an increase in injected fuel accelerates the compressor spool more rapidly, giving a speedy response to extra power demand [6].

Turboprop engines have many favorable attributes. Like jets, these engines usually operate on heavy fuels such as Jet A, JP-5, and JP-8. The vibration level is low, and reliability is high relative to reciprocating engines. Quite importantly, turboprops have low weight for their power and are scalable to very large power levels. Their power-to-weight ratios range between 3.5 and 4.8 kW/kg, while turboshafts are approximately 4.3-9 kW/kg [5]. Manned aircraft turboprop engines have mean time between overhauls of approximately 3,000 to 4,000 hrs, which is over twice that of reciprocating engines. The performance is suitable for UAVs operating at a height of 7 to 15 km, which is above the operable range of reciprocating engines. Turboprops are used at flight speeds of less than Mach 0.6 due to propeller tip compressibility constraints.

It is speculated that the main reason why turboprops are not used more frequently on UAVs is the lack of available engines in the desired power class [5]. Most turboprop engines are intended for large general-aviation aircraft, regional commercial transports, and military transports. This engine class has much more power than is necessary for most UAV applications. Smaller, medium- and close-range aircraft are usually powered by piston engines, but they would benefit from the high power-to-weight ratio of the turbine engine [6]. Unfortunately, there are no small turboshaft/turboprop engines available below the approximately 200 kW power. A turbine engine is at its most fuel efficient when operating near maximum power, and its specific fuel consumption deteriorates sharply if operated at part-load. Therefore attempting to use an over-size engine for the smaller aircraft would impose not only a mass and bulk penalty, but an unacceptable level of fuel consumption. Of the current medium- and short-range aircraft, a few would require installed power levels of about 120 kW, several in the 30-40 kW range and a number as low as 5-10 kW.

At power levels lower than 200 kW, which would be relevant to most UAV other than MALE or HALE UAS, none of this type of engine is available for serious use. In smaller sizes they have, due to scale effects, a higher fuel consumption than piston engines. This, together with higher acquisition costs, makes them uncompetitive, in spite of their

smoother power output and ability to use a range of 'heavy' fuels, with the alternative engine types. Altogether, due to their diverse attributes, especially in the free-power-turbine configuration for VTOL aircraft, turboprop engines showcase very desirable features for UAV applications.
As mentioned before, very small turboprop engines are available for model aviation. These engines are of the same kind as model aircraft turbojets. These engines generally use centrifugal compressors and are designed for low cost and high power-to-weight ratios, which comes at the expense of fuel consumption, reliability, and engine life.
Modern materials and fuel monitoring together with new manufacturing techniques and the increasing demand for UAV systems may yet make the development of small turbine engines viable [5].

2.2.4 Propulsion Systems Comparison

Table 2.7 shows a complete overview of the UAV propulsion systems as discussed in section 2.2. Limiting flight altitude and speed are specified accordingly to the engine type performance requirements, and important parameters for engines performance comparison such as State of the art specific fuel consumption (SFC), power or thrust range, and power-to-weight/power-to-thrust ratio are presented when available.

POWER PLANT		Altitude [km]	Speed	SFC @ Cruise [kg/kWh]	Power (or Thrust) [kW]	P/W [kW/kg]
Electric Motors	Battery	0 -15	<Mach 0.6	N.A.	N.A.	0.1-1
	Fuel cell				N.A.	<1
	Solar-powered photovoltaic cell			0.090.15 (where the reference fuel is H2)	N.A.	N.A.
Reciprocating Engines	Two-stroke engines	0 - 9	<Mach 0.6	0.4 - 1.2	1 - 150	0.8-2
	Four-stroke engines			0.3 - 0.4		0.4 - 1
	Rotary engines			0.35	15 - 70	N.A.
Gas turbine engines	Turbo-jet	medium to high altitude (see table 2.3)	>370 km/h	N.A.	>4 kN (0.13-4.45 kN for target/cruise missiles)	N.A.
	Turbo-fan				N.A.	
	Turbo-prop	7 -15	<Mach 0.6	0.3 0.5	>200	3.5-4.8
	Turbo-shaft			N.A.		4.3-9

Table 2.7: UAV propulsion systems overview

As it can be seen, even though UAV powered by electric motors do not have altitude limitations due to possible performance deterioration, they are constrained to fly below a certain Mach number due to compressibility effects of the propeller (the propulsor). On the other hand, turbo-jet units do not have this limitation but they better perform at medium/high altitudes and high speeds.
Power level is difficult to be specified for electric motors since it strictly depends on the batteries/fuel-cells/photovoltaic-cells specific configuration. In comparison with gas turbine engines, which are usually not available at power level below the 200 kW, reciprocating engines output power can reach 150 kW while also lower levels are covered

down to 1 kW. On the other side, the table clearly shows that neither electric motors nor reciprocating engines can achieve a competitive power-to-weight ratio compared to gas turbines when this is required.

2.3 Micro Gas Turbines

Different research projects have been recently carried out by academics in the field of micro turbine for propulsion and power generation, mostly with turbine power output lower than 100 W [25, 29, 30]. Relatively bigger turbofan and turbojets are being developed as propulsion systems of choice of UAVs and missiles for military applications [31]. The extreme compactness demanded of such stealthy advanced vehicles requires relatively higher power density combined with increased payload and endurance.
Many model aircrafts use gas turbine as their propulsion system. However, available values of engine power and efficiency are based on manufacturer's published data, which usually report only peak power at a particular operating speed. Since these engines are primarily produced for hobbyists, fuel consumption information and efficiency must be estimated and are therefore not reliable [17].
According to Pilavachi [32], the main advantage of small gas turbine engines lies in the high energy density potential of the fuel-based systems. It is considered that even with relatively low overall system efficiency the power per unit of weight of a gas turbine system will be much higher compared to existing or in the near future available batteries. Fuel-based power generating systems also have a power density advantage compared to batteries and fuel cells. This means that a relatively short period is needed to withdraw the energy to the system, unlike batteries which have a high impedance. Moreover, batteries naturally discharge over time while a fuel provides a long storage time without the loss of potency.
Additional potential advantages compared to other technologies are a small number of moving parts, lower noise, multi-fuel capabilities as well as opportunities for lower emissions. By reducing the overall system weight significantly, they appear to be the preferred choice for missions requiring a high power output and a long duration.
Main technical barriers to the implementation of micro-turbine technology are that, at present, the gas turbine has a lower efficiency in its basic configuration than an equal power output reciprocating engine. In addition, the efficiency of the gas turbine decreases at partial load and burning of lower heating value fuels may not be feasible, depending on the type of the turbine.
High efficiency can only be obtained when the machine operates at high pressure and temperature conditions, which challenge the skills of engineers and materials technologists [32, 31]. When the size of the engine is small, the high turbine inlet temperature will lead to a high overall temperature of the engine structure. Several safety measurements will be needed and the situation is even further aggravated by the high temperature of the exhaust gases. However, it is speculated that the incorporation of a recuperator in the engine cycle could reduce these issues and at the same time further increase the power output of the device [16].
Ways to improve the performance of several types of gas turbine cycle will be a major objective in the coming years.

2.3.1 Downscaling Effects

In this chapter attention is given to the main issues encountered by academics when scaling down a turbine. This is needed in order to provide useful insight of the design problems to be considered in the development of micro gas turbines.
The reduction of scale has several effects on the performance and construction of the turbine. Dimensional analysis shows that the power generated by a gasturbine is proportional to the density of the gas, the fifth power of the diameter, and the third power of the rotational speed [33]. For a known pressure ratio and constant inlet conditions, the speed of the fluid at the exit of the nozzles is a constant, independent of the size of the nozzles. Therefore, the circumferential speed of the turbine is constant, independent of the turbine size. This means that at optimal working conditions, size and rotational speed are inversely proportional. The power density of turbine increases thus with miniaturisation, and this mass reduction is advantageous for aeronautical and space applications.
Previous studies [25, 29, 30], showed that although maximizing the power-to-weight ratio is important for all aerospace power systems, two factors make it absolutely critical to micro air vehicles. First, the overall aerodynamic efficiencies of conventional fixed-wing vehicles using steady-state analysis tools decreases with size. Second, the efficiency of the power/propulsion system appears to degrade with decreasing size. Together, these factors conspire to make the power-to-weight ratio and efficiency of the power system critical [17].
Military research focusing on advanced gas turbine engines with diameter of 10 cm has been carried out [31]. Attention has been given in increasing gas turbine power density and fuel economy through improved aerothermodynamic component technologies and higher temperature, lower density materials. The goals being to decrease engine size and frontal area for a given power output, and to decrease engine fuel consumption, in order to improve engine affordability. Several engine design configuration options are considered for the impending UAV applications including turbojets and turbofans, with centrifugal and axial turbomachinery. The study showed that the lower limit in size is dictated by the feasibility of stable combustion operation throughout the mission profile, and high speed bearing life in the 100 to 250 krpm speed range [31, 34]. Current state of the art small gas turbines exhibit rotational speeds from 60 to 150 krpm with both conventional antifriction and air bearings. The very high rotational speed needed to obtain the enthalpy and pressure changes prescribed by the gas turbine cycle, is one of the major mechanical problems [34].

Scaling is a common technique to define larger or smaller geometries with similar characteristics. However, a simple scaling of a high performance large gas turbine will not result in a good micro gas turbine. Although many of the effects presented here are encountered when extreme downscaling is executed (micro turbine total volume in the order of 1 cubic cm [33]), it is considered important to acknowledge the main issues encountered in previous researches.
According to Van den Braembussche [34], the main factors perturbing such a scaling are:

- The large change in Reynolds number
- Massive heat transfer between the hot and cold components (negligible in large machines)

- Geometrical restrictions related to material and manufacturing of miniaturized components

These effects are here discussed in more details.

Reynolds Number In order to understand the impact of Reynolds Number on the performance losses of small gas turbine engine, it is interesting to analyse its effect on micro gas turbine with power output as low as 80 W, where the diameter of the compressor can be as short as 4 mm [29]. In this context, the role played by the low Reynolds numbers on engine performance is significant and indicates the dominance of frictional forces over inertial ones. The Reynolds number is a key parameter when considering the effects of scaling on a micro engine. Since Reynolds number scales linearly with the length scale factor of the turbine, it is several orders of magnitude less than that of a conventional engine, indicating that viscous effects will be more pronounced. In particular, laminar flow will be prevailing, whereas turbulent flow predominates in large scale engines. This means that the viscous friction losses are expected to be higher and that mixing of the fuel-air mixture in the combustor will be slower, both having a negative impact on efficiency and power density [35, 34]. The 4 mm diameter compressor of the MEMS-based (Micro Electro Mechanical Systems) gas turbine generator in [29] appears to be close to the borderline of suitability according to the study in [33]; at Re=2600 the three-dimensional efficiency of the compressor is predicted to be much less than 50%, a value that is insufficient for the engine to generate net power.

Heat Transfer Reducing size means increasing surface-to-volume ratio, resulting in higher heat transfer. The higher thermal losses have a negative effect on the efficiency of the turbine, and may even cause flame extinction. At very small sizes, the heat generated by the combustion minus the heat loss is no longer sufficient to ignite the mixture. Therefore, thermal insulation between the hot parts and the cold parts becomes critical [34].

Internal heat transfer has an important impact on the performance of very small turbomachines, used in micro- and nano- gas turbines. The heat flux from the hot turbine to the colder compressor results in a cooling of the flow in the turbine and a heating of the flow in the compressor. The performance changes and can no longer be evaluated by the flow conditions measured at inlet and outlet of the components. This problem has first been recognized and studied for small turbochargers where it was shown that the distance between the hot turbine and the cold compressor might have a considerable impact on the flow conditions [34].

Geometrical restrictions The power density of a miniature turbine is also limited for technological reasons. Small turbines cannot be made with the same relative accuracy and detail as large ones, so the performance will be worse than predicted by the scale laws.

One of the major problems in micro gas turbines is the decrease of compressor and turbine efficiency with decreasing dimensions. This is further enhanced by the effect of larger roughness resulting from materials and manufacturing techniques. It is known that gap-to-blade height ratios increase as the engine size decreases and compressor efficiency

is sensitive to small increases in tip clearance [35]. Geometric similarity is generally not maintained when decreasing scale and this may well introduce additional deviations. These may be reflected in changes of velocity ratio (ratio of rotor tip speed to theoretical spouting velocity), and exit flow coefficient (ratio of exit meridional velocity to tip speed). The velocity ratio is a direct measure of the blade loading. The exit flow coefficient is an indirect measure of the specific speed [35].
The resulting decrease in cycle efficiency does not make micro gas turbines to ecological devices. More than any other criterion, performance might define the lower limit for these engines. Therefore, special attention should be given to compressor and turbine optimization [34].

Chapter 3

Methodology

The Exploration Study presented the framework of the research project. Main flight parameters such as service ceiling, maximum take-off power, and cruise speed are defined for each civil UAV application identified, as well as for each propulsion system examined, and for every different typology of UAV. Those determine the kind of propulsion system that will be further analysed. Besides this, all the existing UAVs with accessible information (deployed, in production, or in development) are considered based on their power level, specific fuel consumption, and critical characteristics. Consequently, identification of possible trends and/or relations among features such as MTOW (Maximum Take Off Weight), wing span, and range, will be feasible and may be further used in the design process.

From the Exploration Study, it is clear that gas turbine engines have many advantages compared to typical reciprocating engines and electric motors. Smoother power output, low vibration levels, heavy fuel compatibility, high reliability (small number of moving parts), to name a few. In particular, turboprops are suitable for UAVs operating between 7 and 15 km height, which is above the operable range of reciprocating engines, at high speeds of less than Mach 0.6. With a power-to-weight ratio four times higher than that of reciprocating engines and electric motors, they appear to be the preferred choice for missions requiring a high power output and a long duration. Moreover, the turboprop engine, especially in the free-power-turbine configuration, appears to be suitable for a broader range of possible applications. However, most turboprop engines are intended for large general-aviation aircrafts, regional commercial transports, and military transports, with power output much higher than that required for most UAV applications. Since turbine engine performance deteriorates sharply if operated at part-load, attempting to use an over-size engine for a smaller aircraft would impose not only a mass and bulk penalty, but an unacceptable level of fuel consumption. Therefore, a gap in the current available technology has been identified which is speculated to be potentially filled by the development of small gas turbine based engines.

A Case Study needs to be defined in order to specify a significant environment for the investigation: it allows the development of the research objectives and the clear assessment of the results. The Case Study has to be consistent with the three main topics of the research: UAV, propulsion systems, and Micro Gas Turbine (MGT) technologies. These are further translated into, respectively, future potential UAV Civil Applications, unexplored advantage of a gas turbine based propulsion system, and design considerations of a MGT. The first two topics are developed in the definition process of the Case Study. Next, the MGT design considerations will be applied in the modeling of the gas turbine engine. The Case Study definition is performed according to the following procedure:

1. Based on the results of the trade-off between UAV types, possible civil missions requirements, and propulsion systems performances, the application which presents the highest potential to meet the demands from society and/or the market when propelled by a micro gas turbine is proposed for a case study.

2. An existing UAV is selected with similar requirements to those established for the application in the Case Study. This UAV is further used as a reference for a parallel Master Thesis project [36], the "Aircraft Study", which focuses on the modeling of the UAV platform and mission performance. The selected UAV has to make use of a different propulsion system suitable for further comparison with the gas turbine model performance.

3. An existing gas turbine with the same power level of the current propulsion system employed in the reference UAV is selected, which will be used as baseline for the downscaling procedure.

Eventually, the Case Study enables the investigation of different possibilities at a conceptual design phase, which should characterize the micro gas turbine as a competitive alternative to the current propulsion system employed in the specific application.
Analysis of design considerations of micro gas turbine engines showed that the design of a small gas turbine with positive power output is a challenging task. The trend towards diminishing size requires to maintain the high levels of component efficiencies needed to achieve the improved engine performance goals. The main challenge of the project is to improve the propulsion system efficiency for specific requirements in terms of range and endurance. The goal of the study is to optimize the maximum takeoff power, still satisfying the cruise power required, while performing a competitive specific fuel consumption. For the modeling and optimization, the NLR[1]'s Gas turbine Simulation Program (GSP) will be used to determine the best choice of engine flow path and components types, identifying the critical parameters in the thermodynamic process. Figure 3.1 shows the research process layout described in this chapter.

[1]The Nationaal Lucht- en Ruimtevaartlaboratorium (NLR) is the National Aerospace Laboratory of the Netherlands, an independent non-profit organisation that provides high-quality technical support to the aerospace sector (NLR is ISO 9001:2000/AQAP-110 certified).

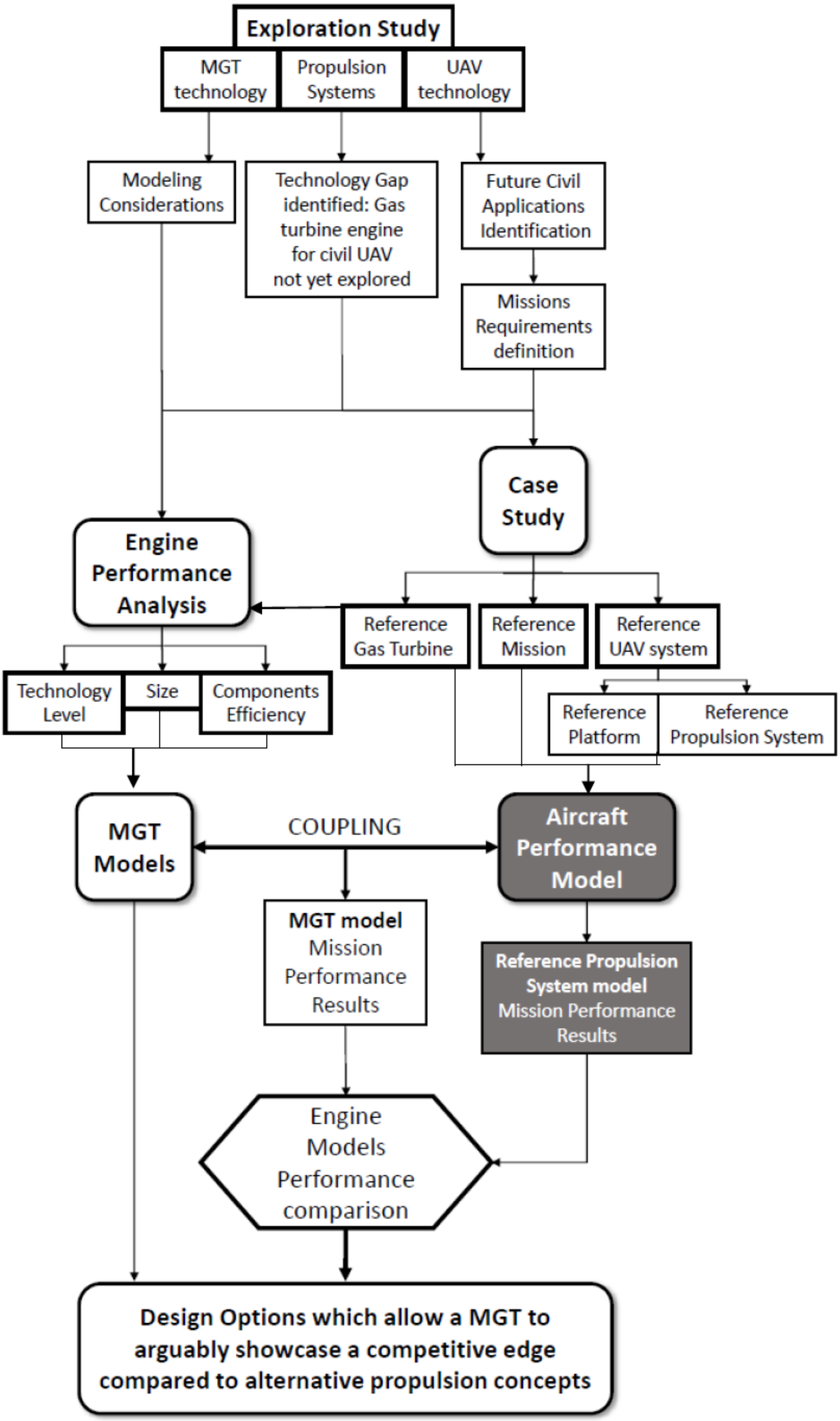

Figure 3.1: Research Process Layout

Chapter 4

Case Study

In this chapter, the development of a Case Study is elaborated. Section 4.1 explains how a reference mission is selected from the potential applications previously identified. Based on this, an existing UAV is chosen to be used as a reference model for the study. This choice is explained in detail in section 4.2. Finally, section 4.3 illustrates the importance of selecting an existing gas turbine as baseline for the design of the Case Study engine model.

4.1 Application

The possible civil UAV applications identified showed a great variety of possible requirements to be satisfied by the system. In the Exploration Study 2.1.4, an effort has been done to translate mission objectives into standardized requirements in terms of range, endurance, flight altitude, speed, vertical take-off and landing capability. Definitions used to establish comparable values for the requirements for each application have been proposed. According to this criteria, a first selection of UAV types which could perform each mission has been performed. This represents the starting point for the identification of a Case Study application. The selection process is explained in detail in section 4.1.1, while the applications proposal and the selected mission requirements are discussed in section 4.1.2.

4.1.1 Selection Procedure

In the Case Study definition process, it is fundamental to identify the elements which play a key role in the research, and to carefully define the relations among them. These elements are:

- Application
- Type of Propulsion System

- Type of UAV

Their relations are based on the application requirements, propulsion system performance, and agreed UAV type definition, as described in figure 4.1.

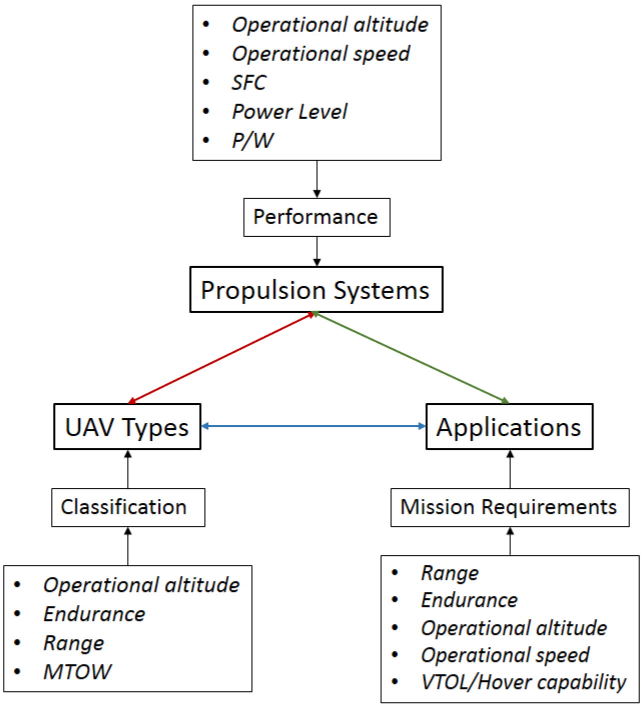

Figure 4.1: Selection process elements and relations layout

The three main blocks and relations implied by the blue arrow have been previously discussed in the Exploration Study. In table 4.1, an effort has been done to categorise typical UAV propulsion systems according to UAV type and power level, determining the red arrow in figure 4.1.

As already discussed, the lack of existing gas turbine engines with power levels below 200 kW constrains the smaller UAV classes to employ reciprocating engines or electric motors. It is therefore interesting to investigate which identified civil applications from the literature review could benefit from a UAV powered by a gas turbine. In figure 4.2, the green arrow is developed as a map of UAV applications areas for which gas turbines could be suitable. High endurance, high speed, long range or high altitude requirements will play a vital role in the conceptual design process of the UAV. Especially the speed requirement will be a dominant factor for both the UAV configuration and the type of propulsion system which is selected (turbojet/fan or turboprop/shaft). For clarity purposes, in figure 4.2 the UAV civil applications have been divided according to the gas turbine engine type(s) whose requirements matched those of the particular application. From the figure, it is clear that certain applications could well benefit from two or even three different kinds of gas turbine engines. This is due to the fact that the definitions of the applications themselves are still at a conceptual phase and only a more detailed evaluation could enable the setting of more specific requirements in these terms.

UAV Type	Engine Type	Power Range (kW)
Micro	Electrical	0.75
Mini/ CR/SR	Piston (2x2)	0.75 - 15
LR/EN	Rotary	15 - 70
MALE	Piston (4x4)	70 - 150
MALE	Turboprop	200 - 370
HALE	Turbo-Jet/Fan	>370

Table 4.1: Engines for UAVs

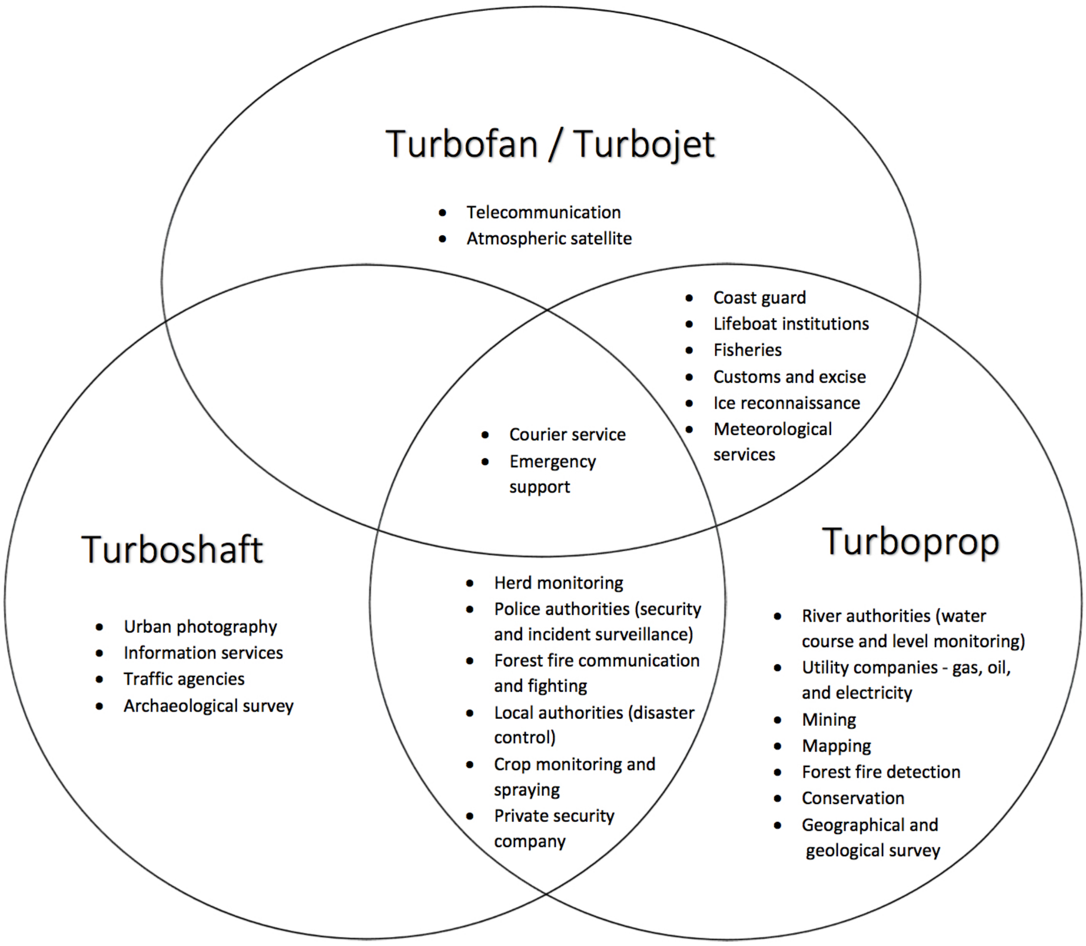

Figure 4.2: Applications divided according to most suitable Gas turbine engine type

As it can be seen, not all the applications presented in 2.1.4 are present in the figure. The reason for this is that applications with very low required speed and/or low altitude are not suitable to be powered by a gas turbine engine. Moreover, in order to reduce unnecessary complexity in the further case study, also UAV applications which required vertical take off an landing (VTOL) and hover capabilities have been excluded from this analysis.
In figure 4.3, UAV civil applications grouped according to similar requirements have been set over the different UAV classes which could accomplish the specific task. In addition, different colors have been used to distinguished which gas turbine engine type(s) is expected to best perform for each case.

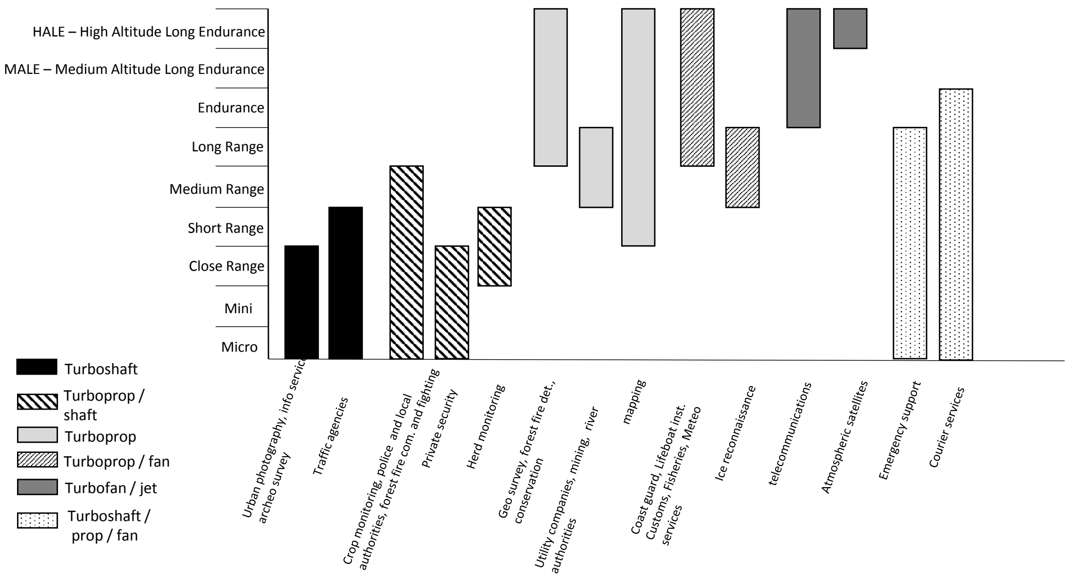

Figure 4.3: UAV civil applications versus UAV types versus gas turbine engine types

As it is shown both in table 4.2 and in figure 4.3, the turboprop configuration appears to be suitable for the broader range of possible applications. Geological surveys, forest fire detection, utility companies support are some of the civil applications recognized with the highest potential in the near future, and which could highly benefit from the implementation of a gas turbine base propulsion system.

4.1.2 Mission Requirements Definition

According to these results, three types of applications are considered suitable for a Case Study. These are:

1. Power and Pipeline Inspection

2. Package Delivery
3. Forest Fire Support / Mining Exploration

Power and Pipeline monitoring is much in demand in Russia, U.S., Canada, and in many other counties worldwide. Oil and gas pipelines and power lines are fixed located. That is why allocation, concordance and authorization of limited controlled airspace over the pipelines and power lines for UAVs flights, especially at a low altitude, could be realistic in near-term outlook. Numerous international oil companies have sponsored UAV demonstrations focused on facility and pipeline inspection, surveillance and monitoring. Currently, many areas of high risk to pollution and high environmental sensitivity are monitored daily by costly manned aircraft surveillance; UAVs can replace or augment these manned air vehicles, providing a cost effective alternative that also reduces human risks.
There are several reported activities of this kind involving the use of UAVs. Quoting *UAV Systems: The Global Perspective 2005* by Blyenburgh & Co, "Aeronautics Defense Systems is using its short range Aerostar UAV to provide protection and patrol services for Chevron Texacos operations in Angola, under a two year contract awarded last year and reportedly worth US$ 4 million. The Aerostar carries a payload of up to 50 kg and has an endurance of 14 hours. Moreover, Fugro Airborne Surveys [1] reported on the development and deployment of the Fugro GeoRanger, a 18 kg UAV based on the InSitu Scan Eagle [2], used in magnetic surveys. It has an endurance of up to 10 hours and a cruise speed of 75 km/hr. The maximum fuel and payload weight is 5.4 Kg. Another example is the MagSurvey Prion [3], a 30 kg UAV targeted for use in magnetic field surveys which makes use of a very sensitive Cesium magnetometer. Furthermore, according to a written statement by Terzah Poe of Shell Oil [4], "Shell may enlist pilotless planes to aid in exploration [...]. Drones are being investigated as an alternative to manned aerial flights for marine mammal monitoring in order to reduce the safety risk to humans associated with flights over remote stretches of Arctic Ocean. The unmanned aerial vehicle, or drone aircraft, would be used to monitor and track marine mammals in the areas where we are operating."
Requirements for each application have been identified in table 4.2 according to the results of the Exloration Study and, when required, practical estimations to meet the mission goals. For example, *Package delivery* range value has been selected by considering the average distance between African capitals. This choice was determined as a proper reference example of a typical point-to-point mission where lack of infrastructure could hinder the deliver of high value goods such as medicines or emergency items. In the same case, high cruise speed is advantageous, compared to the lower required speed for applications 1 and 3. This has been estimated according to the need of quick intervention of application 2 opposed to the required accuracy for the cameras which can only be achieved at a flight speed inferior to 100 km/h. Similar reasoning have been elaborated for the missions requirements when not available in the literature.

For the mission requirements estimation in table 4.3, the reasoning in [23] has been followed. Regarding pipelines, one of the longest oil pipelines in the world is the 1768

[1] www.fugroairborne.com, Accessed: 04-10-2014
[2] www.insitu.com, Accessed: 10-04-2014"
[3] www.magsurvey.co.uk, Accessed: 10-04-2014"
[4] www.alaskajournal.com, Accessed: 10-04-2014"

Application	*1- Power and Pipeline Inspection*	*2- Package Delivery*	*3- Forest Fire Support or Mining Exploration*
Description	Routine inspections: –100+ km stretches of power & pipeline –timely detect leaks, disruptions or problems –Longest line 1768 km	Goods delivering to areas with limited or difficult access; –Issue of landlockedness in developing countries –Point-to-point	–Identify forest fires in gather intelligence; –Locate potential mining areas; –surveys for oil and gas
Range	1800 km	1100 km (average distance between African capitals)	400 km (100 km above forest + 300 km travel distance)
Cruise speed	100 km/h	>300 km/h	100 km/h
Endurance	20 h	4 h	30 + h
Altitude	1000 m	>5000 m	5000 m (high enough to avoid hot and turbulent air)
Payload	10 kg (IR and day camera)	100 kg	10 kg (IR and day camera)

Table 4.2: Applications Proposal

km long Baku-Tbilisi-Ceyhan (BTC). On the other hand, a development survey typically covers an area of 400 km^2, whereas an exploration survey can cover up to 10000 km^2 [5]. For a 400 km^2 development survey of a region 200 km from a suitable UAV take-off and landing strip, with a line scan spacing of 200 m it has been calculated that 2 flights are needed, each flight covering 1569 line km in about 16 hours, for a UAV cruising at 100 km/hr. For an exploration survey covering a 10000 km^2 region, 200 km from a take-off and landing strip, with a line scan spacing of 400 m, a requirement for 24 flights, each flight covering 1560 line km and lasting about 16 hours, at a cruising speed of 100 km/hr has been calculated. From the above considerations, a UAV with a range of 1800 km, flying at 100 km/hr for 18 to 21 hours per flight would be suitable for both geophysical survey and pipeline monitoring work.

Requirements	
Range	1800 km
Cruise speed	100 km/h
Endurance	20 hr
Payload	10-50 kg

Table 4.3: Requirements established for the selected Case Study Application

[5] BP Frontiers Magazine: Issue 18, April 2007: Surveys in silicon.

4.2 Reference UAV

Investigation of the potential of a micro gas turbine engine propulsed UAV for the selected mission starts with the identification of a reference existing UAV. This reference UAV needs to showcase similar mission performance to that established for the Case Study Application. Once such a UAV is selected, it can be modeled and its mission performance can be studied when different engine models are implemented.
In the definition of the Case Study, the exploration of a class of gas turbine based engines which is not currently available in the market has to be guaranteed. To prove it to be a competitive technology compared to the current propulsion systems employed, the preferred output power of gas turbine based propulsion system for a high potential civil UAV application should be selected in the range of 30-60 kW, a value expected to be further updated during the research process. This conclusion has been drawn according to the discussion of the Exploration Study results with the Delft University's Propulsion and Power group.
Appendix D presents all the existing UAVs within the selected power range with their specifications. Almost all the existing UAVs in this power class make use of reciprocating engine, mainly due to the lack of reliable gas turbine engines with the same output power available in the market. Moreover, the selected power range is considered to be appropriate for most of the missions identified which might be potentially powered by a turboprop/turboshaft engine. As shown in figure 4.4, no evident trends in terms

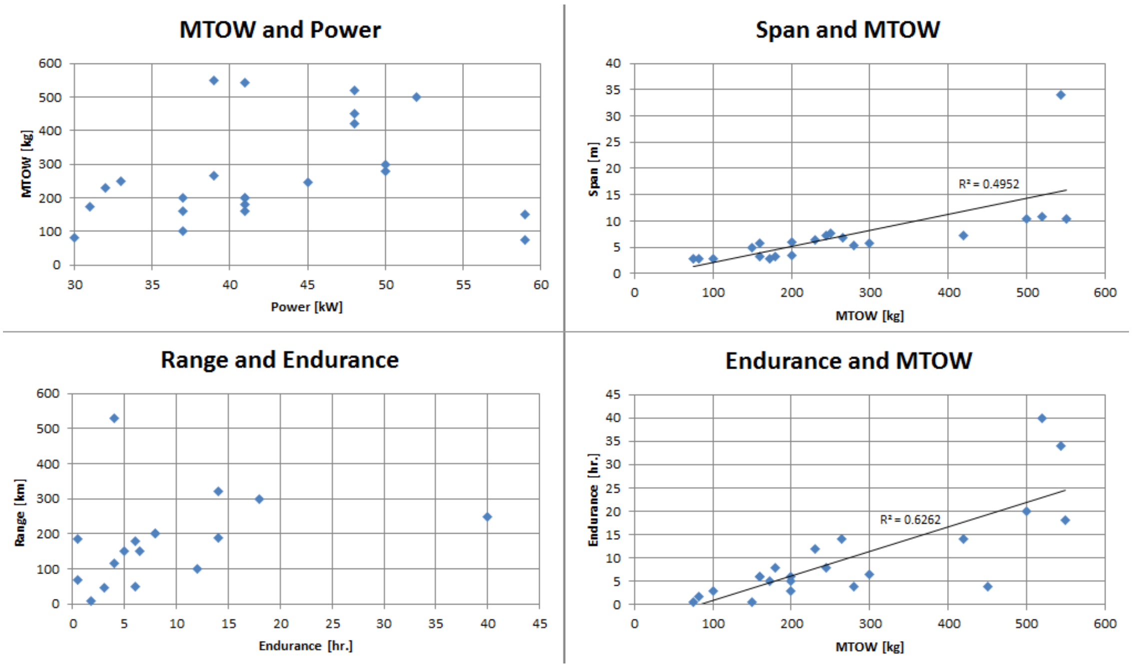

Figure 4.4: Design and system performance trends evaluation of existing UAVs

of maximum take off weight, wing span, mission requirements, and, in general, in UAVs design could be identified from the analysis of the existing UAVs in the selected power range. This definitely shows the great variety and possibilities enabled by this new kind of technology, indicating that each new system requires a tailored design according to the specific mission to be performed.

According to the analysis of the existing UAVs in section 2.1.5, the EADS Harfang has been chosen as reference. Harfang is a medium-altitude, long-endurance (MALE) unmanned air vehicle system principally designed and developed for the French Air Force to perform Intelligence, Surveillance, Target Acquisition and Reconnaissance (ISTAR) missions at strategic, operative and tactical levels. It is manufactured by EADS, France, and Israel Aerospace Industries (IAI) further aided in manufacturing the aerial platform and subsystems.
The Harfang design is based on IAI's Eagle 1/Heron TP platform, in figure 4.5. It can perform a range of missions encompassing surveillance, reconnaissance and target designation. It transmits data or images captured by the optronics sensor and airborne radar through a satellite link. The drone features a high wing, equipped with shutters and de-icing systems stabilised by a twin-boom. It can carry a maximum payload of 250 kg to 7500 m for 24 hours without refuelling. Table 4.4 summarizes the UAV specifications which are discussed in more detailed in the following subsections. The Harfang is powered by a single four-stroke liquid air-cooled Rotax 914 F turbocharged engine [37]. It was manufactured by Austrian aircraft engine supplier BRP-Rotax. The engines drive a two-bladed propeller in pusher configuration at the rear of the fuselage nacelle. It can produce 115 hp (86 kW) of output power, a value further used as reference for the modeling of the gas turbine engine. It is expected that two different propulsion systems (reciprocating and turbine engines) with the same power output will unlikely showcase the same performance (in terms of specific fuel consumption), especially considering their diverse power-to-weight ratios.

Figure 4.5: EADS Harfang UAV views, from [2]

4.3 Reference Gas Turbine Engine

The engine model further used as a baseline engine for the Case Study is a TP100 turboprop with output shaft power of 180 kW built by PBS Velká Bíteš, [38]. This engine is a dual shaft turboprop set-up with a gas generator module on one shaft and a free power turbine on the other. Exhaust gases from gas generator drives the single stage

EADS Harfang Technical Data	
Country of Origin	France
Manufacturer	EADS - Netherlands / IAI - Israel
Initial Year of Service	2008
Production	4
Length	30.51 ft (9.30 m)
Width	54.46 ft (16.60 m)
Height	7.55 ft (2.30 m)
Weight (Empty)	14455 lb (660 kg)
Weight (MTOW)	2756 lb (1250 kg)
Powerplant	1 x Rotax 914F turbocharged engine (115 hp)
Maximum Speed (true air speed)	127 mph (204 km/h, 110 kts)
Endurance	24 h
Loiter time	12 h at 550 nm
Maximum Range	621 miles (1000 km)
Service ceiling	24934 ft (7600 m)
Payolad	250 kg - sensors, optics and communications equipment

Table 4.4: EADS Harfang Specifications

power turbine, and the power is subsequently transmitted through a gearbox to a three blades propeller with constant speed. The engine can be installed in both pusher and tractor mode. Pusher configuration is designed for experimental aircraft or UAV, and it will be further considered in accordance with the original reciprocating engine configuration of the Reference UAV in section 4.2. The gas generator is made up by a single stage radial compressor and an axial turbine. Centrifugal compressors are able to achieve higher pressure ratios than their axial counterparts. However, compressor disk diameter increases quite rapidly with increasing mass flow, making a centrifugal compressor unsuited for larger gas turbine engines, but attractive for the MGT in this study. Both the gas generator and power turbines are axial turbines. The free power turbine is connected to a gearbox which reduces the axial speed to a suitable speed for the propeller. In the case of the TP100 the gas turbine is connected to a three bladed constant speed propeller. TP100 Specifications are described in table 4.5.

TP100 Technical Data	
Manufacturer	PBS Velká Bíteš - Czech Republic
Output Shaft Power	180 kW (Sea Level Static Conditions)
Dry Weight	61.6 kg
Engine Length	887 mm
Width x Depth (without exhaust)	330 x 398 mm
Fuel	JET A, A1, B, TS-1, T2, RT
Operational Ceiling	9000 m

Table 4.5: TP100 Engine Specifications

Chapter 5

Model Development

5.1 Micro Gas Turbine Performance Model

As highlighted by the Explorations Study, the design of a small gas turbine is a challenging task, since MGT performance and losses are dependent on engine size. When an engine of one size (power output) has been designed, one can estimate some of the design parameters for an engine of a different size through a type of scaling which depends on the assumption that compressor pressure ratio, turbine inlet temperature, and efficiencies do not change from one design to the other. The first conclusion is that the mass flow of air through the engine would vary in direct proportion to power. If similar geometry are also assumed, then dimensions such as the wheel diameter scale with the square root of power, and rotational speed varies inversely to the square root of power.
Despite careful attention to detail at the design stage and during manufacture, small turbomachines always have lower efficiencies than larger geometrically similar machines. The primary reason for this is that it is not possible to establish perfect dynamical similarity between machines of different size. According to Dixon [39], exact geometric similarity cannot be achieved for the following reasons:

- the blades in the scaled machine will probably be relatively thicker than in the original one;
- the relative surface roughness for the scaled machine blades will be greater;
- leakage losses around the blade tips of the scaled machine will be relatively greater as a result of increased relative tip clearances.

The starting point for the modeling of the MGT is therefore the downscaling process of the reference turboprop engine described in 4.3.
The main requirement when scaling down a gas turbine is to preserve the characteristics of the thermodynamic cycle. This means that the same enthalpy change in the compressor and turbine should be preserved, but at a smaller mass flow. The thermodynamic cycle

analysis can be then used to predict the performance of the engine in terms of efficiency and power output for a given mass flow rate. The thermodynamic performance of a gas turbine cycle at design point conditions is mainly a function of three parameters:

- Turbine inlet temperature (TIT)
- Compressor pressure ratio
- Component efficiencies

Turbine Inlet Temperature Next to gas parameters several other parameters are needed. These parameters include:

- Inlet pressure, temperature, and mass flow ($\dot{m}_a$);
- Combustion efficiency (η_b), and fuel heating value (LHV);
- Gas Generator Turbine shaft mechanical efficiency(η_m);
- Power Turbine shaft mechanical efficiency(η_m), exit-to-ambient relative pressure drop (dP_{pt});
- Exhaust Nozzle efficiency (η_n) and effective area;
- Propeller diameter (D_{pr}), dynamic and static efficiency (η_{pr}, $\eta_{prSTATIC}$).

Most of this values are available for the reference turboprop engine, while propeller diameter has been selected according to the Reference UAV manufacturer data, and propeller static and dynamic efficiency have been implemented according to the ideal propeller theory as further explained in appendix C.
The choice of engine flow path and components type will be based on a series of experiments performed with the NLR's Gas turbine Simulation Program.

5.1.1 Downscaling Approach

A preliminary micro turbine design can be drafted by scaling from an existing reference model using the appropriate non-dimensional parameters. As a first step, the design air flow will be scaled down to obtain the required power output by changing the turbomachinery diameter, since inlet mass flow is proportional to the second power of the diameter, and roughly proportional to output Power:

$$\dot{m}_a \propto D^2 \propto PW \tag{5.1}$$

Moreover, design efficiencies need to be corrected for the downscaling effects. Efficiencies generally decrease with decreasing scaling factor according to complex non-linear relations. The effects of scaling on the efficiency will be implemented through efficiency drops. The corrected inlet flow parameter reflects the physical size of the turbine nozzle throat, and controls flow capacity. However, for a particular turbine design the efficiency is also dependent upon velocity ratio, blade solidity, vane and blade profiles, Mach and

Reynolds numbers. Conservation of Reynolds number conflicts with the conservation of enthalpy change when changing the dimensions of the rotor. A reduction of Reynolds number with decreasing dimensions is unavoidable unless also the viscosity and/or pressure level of the fluid are modified.
The downscaling technique adopted in this study is here outlined:

1. Identification of a scaling factor (SF) based on the expected shaft output power at specified engine cycle conditions (ambient temperature and pressure, PR_c, and TIT): Scaling Factor
$$SF = \frac{PW_{Desired}}{PW_{REF}} \tag{5.2}$$

2. Identification of required air mass-flow based on selected SF:
$$\dot{m}_{a,scaled} = \dot{m}_{aREF} * SF \tag{5.3}$$

3. Complete cycle calculation assuming component efficiencies as size-dependent variables according to the relations explained in section 5.1.2.

Since mass flow rate and power are expected to drop disproportionally with size due to increasing boundary layer and loss effects, an iterative process is required to adjust $\dot{m}_a$, SF, and components efficiency, in order to reach the desired output power.
Therefore, in this work different scales mainly refer to different engine mass flow rate rather than different output power. This is because changing compressor pressure ratio and turbine inlet temperature at the same ambient conditions will effect the power output of the engine, even though the inlet air mass flow is kept constant. This will be further discussed in Chapter 6.

5.1.2 Components Efficiency Calculation

Despite careful attention to detail at the design stage and during manufacture, it is a fact that small turbomachines always have lower efficiencies than larger geometrically similar machines. The primary reason for this is that it is not possible to establish perfect dynamical similarity between turbomachines of different size. Components efficiencies can be estimated with empirical loss models and correlations, which can eventually include size as a variable for performance change prediction with engine dimension.
The component efficiencies are influenced by:

- The rotor/impeller sizes;
- Velocity ratio ($\frac{u_t}{v_{0t}}$), ratio of rotor tip speed to theoretical spouting velocity;
- Exit Flow coefficient ($\frac{c_m}{u_t}$), ratio of exit meridional velocity to tip speed;
- Clearance gaps;

The velocity ratio is direct measure of the blade loading. The exit flow coefficient is an indirect measure of the specific speed. Radial turbine design is dictated by criteria like specific speed and/or velocity ratios. For smaller turbines the size of the turbine wheel needs to be reduced and, thus, the rotational speed increased in order to reach a high efficiency.
Various simple corrections have been devised to allow for the effects of size (or scale) on the efficiency. One of the simplest and best known method is that due to Moody and Zowski [40], also reported by Addison [41] and Massey [42], which applied to the efficiency of turbines is:

$$\frac{1-\eta_c}{1-\eta_{cREF}} = \left(\frac{D_{cREF}}{D_c}\right)^n = \left(\frac{1}{\sqrt{SF}}\right)^n \tag{5.4}$$

Where the index n is in the range of 0.2 to 0.25.

To improve fuel economy there is a strong incentive to increase cycle pressure ratio. Higher stage pressure ratios are realized by increasing rotor tangential velocities, and are accompanied, therefore, by larger Mach numbers both at the rotor entry and exit. The aerodynamic problems associated with diffusion from these larger Mach numbers must then be solved concurrently if efficient high pressure ratio operation is to be obtained. These problems involve careful selection of the blading solidity, thickness chord ratios, nose radius, hub and shroud contours, appropriate rotor and diffuser diffusion ratios, and strict control of the design dimensions. It is not feasible to maintain the desired aerodynamic blading properties as size is diminished because of manufacturing tolerance limitations. Blade-edge thickness cannot be continually decreased in proportion to diameter and contour envelope accuracy must be compromised. The inducer section of small radial compressors is particularly sensitive to Mach and Reynolds number effects as a consequence of the strong suction surface diffusion near optimum incidence. As a result of all these factors, the decrease of compressor efficiency with increasing pressure ratio can be approximated by the empirical relationship:

$$\Delta\eta_c = \frac{Constant}{\sqrt{\gamma_c R}}\left(\frac{P_2}{P_1} - 2.0\right) \tag{5.5}$$

PPressurePressure The value of the constant is usually of the order 0.1-0.13, where '0.13' is for current small compressor designs, with zero inlet air pre-rotation and is the value which is further implemented in the model. R is the gas constant in [ft lb/lb degR] and is gas dependent, therefore 53.3 was used for air.
The losses resulting from clearance gaps are basically related to the ratio of the effective clearance gap to blade height. Due to a lack of blade height and clearance gap data on different sizes of turbines, these effects are not included in this study. This will obviously induce some error in predicting the complete effect on the efficiency loss due to size decrease. However, previous work estimated that this effects do not exceed 1% ([35]).
The final equations for the compressor and turbine isentropic efficiency are:

$$\eta_c = \left[1-(1-\eta_{ref})\left(\frac{1}{\sqrt{SF}}\right)^{0.2}\right] + \left[0.040415 - \left(\frac{0.13}{\sqrt{\gamma R}}\right)(PR_c - 2)\right] \tag{5.6}$$

Equation 5.6 is arranged to break down to the design compressor efficiency of the reference TP100 when the scaling factor SF is 1 and PR_c is 4.6794. Again, the first expression in

the square brackets represents the size effects, while the second expression is a measure of the pressure ratio effects.
Turbines do not exhibit significant Mach number and pressure ratio penalties providing pressure ratios are lower than approximately 5.0. Therefore, the final relation for the gas generator and power turbine is:

$$\eta_t = \left[1 - (1 - \eta_{ref}) \left(\frac{1}{\sqrt{SF}}\right)^{0.2}\right] \tag{5.7}$$

5.1.3 Technology Levels

In order to get a high power output, a high turbine inlet temperature (TIT) is needed. Given the small scale of the engine, a high TIT will lead to high overall temperature of the engine structure, and several safety measurement will be needed. The TIT is determined by the rotor alloy stress rupture and low cycle fatigue strengths, duty cycle, and cooling options. Compromises are made in turbine design to achieve the optimum balance of power, efficiency, cost, engine life, and other factors. For example, an engine that can operate at a higher TIT than previous models (due to improved materials and design) will allow for increased power and improved efficiency while adding higher cost for the direct cooling of the first turbine stage airfoils and other components. Current microturbine inlet temperatures are generally quite low to enable the use of relatively inexpensive materials for the turbine wheel. Previous works have indicated that turbine inlet temperatures up to 1250 K are feasible with the customary Inconel 713 material. With advanced materials, such as MAR-M247, TIT can be raised up to 1300 K [43].
On the other hand, increasing cycle pressure ratio is attracting in order to improve engine fuel economy. Therefore, choice of compressor pressure ratio is a major design consideration. Small gas turbines have been designed with overall pressure ratios ranging from 2.5 to 8.0 with both single stage centrifugal, mixed flow, multistage axial compressors, and combinations of the above. The centrifugal is the least sensitive to clearance losses, and is therefore capable of wide surge margins with high inlet flow distortion tolerance. Higher stage pressure ratios are attained by increasing rotor tangential velocities, and are accompanied, therefore, by larger Mach numbers both at the rotor entry and exit. The aerodynamic problems associated with diffusion from these larger Mach numbers involve careful selection of the blading solidity, thickness chord ratios, nose radius, hub and shroud contours, appropriate rotor and diffuser diffusion ratios, and strict control of the design dimensions. It is not feasible to maintain the desired aerodynamic blading properties as size is diminished because of manufacturing tolerance limitations. The inducer section of small radial compressors is particularly sensitive to Mach and Reynolds number effects as a consequence of the strong suction surface diffusion near optimum incidence. However, at higher pressure ratios, compressor surge and engine matching do not always allow operation at peak compressor efficiency. Therefore, engine design point compressor efficiency may be one to two percentage points below peak efficiency dependent upon compressor flow range characteristics.

The choice of TIT effects the turbine specific power, while compressor pressure ratio PR_c influences the specific fuel consumption. This means that engine size and dry weight is dependent upon specific power, while engine wet weight is dependent on SFC.
The focus of improving gas turbine technology is centered on combinations of higher temperatures and finding the corresponding optimum compressor pressure ratios. For the scope of engine performance analysis, each combination of design TIT and design PR_c is defined as a certain "Technology Level", which implies specific turbine material and cooling options, and specific compressor design and manufacturing limitations.

5.1.4 Weight Estimation

Once a new engine is assumed to be a scaled version of an existing one, with some performance improvement due to the use of newer technologies, a preliminary engine weight estimation needs to be performed. This is required because the integration of an engine with reduced weight and size effects the aerodynamic performance of the UAV. This effect should be taken into account for further mission performance analysis when different engine technologies are compared.
Two preliminary weight estimations methods depending on turboprop power output have been selected. The first one, developed by Raymer [44], follows the scaling equations defined in table 5.1. Weight is in pounds, length and diameter in inches.

Scaling Law for turboprop engines	
X_{scaled}=$X_{actual}SF^b$, b from table values	
$SF = \frac{PW_{scaled}}{PW_{actual}}$	, PW in hp
X	b
Weight	0.803
Length	3.73
Diameter	0.12

Table 5.1: Scaling laws for turboprop engines

In reference [45], an empirical model was formulated for the specific weight of a turbine, which is the weight of the engine per kilowatt produced. This empirical expression is given as follows:

$$W_t = a * (PW)^{-0.292} + 0.985^{\Delta Y} \tag{5.8}$$

Where:
W_t: specific weight in (kg/kW)
a: coefficient
PW: shaft power required (kW)
ΔY: years from 1958

The value of the coefficient for the required shaft power has been adapted based on the data for the reference turboprop engine TP100: with 180 kW max power, 2009 year of production, and 61.6 kg of engine dry weight, the above formula takes the form:

$$W_t = -0.54859 * (PW)^{-0.292} + 0.985^{\Delta Y} \tag{5.9}$$

By multiplying the specific weight with the turbine output power, the final weight is obtained. For the scope of this study, a rough weight and size estimation is assumed acceptable. Engine installation weight is also not considered at this stage. Therefore, the two aforementioned methods have been applied for weight calculation and the average of the results has been further considered in the model, as shown in the example for different scaled models in table 5.2:

PW [kW]	**Estimated Weight 1 [kg]**	**Estimated Weight 2 [kg]**	**Averaged Weight [kg]**
86	34	23	**29**
70	29	18	**24**
60	25	15	**20**

Table 5.2: Weight Estimation Methods for different scaled models in the selected power range

5.1.5 GSP Implementation

The GSP *Gas turbine Simulation Program* [46] cycle code is used to predict engine performance scale effects in terms of efficiency and power output.
GSP is a component based modeling environment developed by Dutch National Aerospace Laboratory NLR and Delft University of Technology. GSP allows steady state and transient simulation of different gas turbine architectures for performance prediction, control system performance analysis, diagnostics/prognostics, failure analysis, structural and thermal load prediction, and life prediction.
Besides being a performance prediction tool, GSP is especially suitable for parameter sensitivity analysis such as: ambient (flight) condition effects analysis, preliminary design analysis, installation loss effects analysis, analysis of effects of certain engine malfunctioning, component deterioration effects analysis, emissions and jet noise.
GSP is primarily based on 0-D modeling of the thermodynamic gas turbine cycle, whereas the gas model is based on NASA's CEA program for the thermodynamic properties of gas chemical composition. As a zero dimension model, in GSP the flow properties are averaged over the flow cross section areas at the interface surfaces of the component models (inlet and the exit). Component model stacking is used to create the thermodynamic cycle of the engine of interest, where the exit gas condition of a component forms the inlet gas condition of the next component in the configuration.

In this study, both Design Point Performance and Off-Design Performance analysis are performed. In the cycle Design Point (cycle reference point) all the mass flows, the total pressures and total temperatures at the inlet and exit of all components of the engine are given. When appropriate Mach numbers at the component boundaries are selected, then all aero-thermodynamic important dimensions of the gas turbine are fixed. Thus, selecting a cycle DP defines the geometry of the gas turbine and cycle design point studies compare gas turbines of different geometries.
Furthermore, off-design performance is required to check the steady state performance of gas turbines when their operational conditions are changed. For an off-design simulation, components maps are required. The maps are scaled before the off-design calculation commences in such a way that they are consistent with the cycle design point.
The design operating point for the TP100 is take-off power at runway conditions. An overview of the design model parameters is described in table 5.3.

Reference Engine Design Point parameters			
Description	**Symbol**	**Value**	**Unit**
Inlet pressure	Pt1	101325	[N/m2]
Inlet temperature	Tt1	288.15	[K]
Inlet mass flow	$\dot{m}_a$	1.424	[kg/s]
Compressor isentropic efficiency	η_c	0.805	[-]
Compressor pressure ratio	PRc	4.6794	[-]
Fuel mass flow	$\dot{m}_f$	0.026	[kg/s]
Combustion efficiency	η_b	0.958	[-]
Fuel lower heating value	LHV	42.916	[MJ/kg]
Gas generator turbine isentropic efficiency	η_{ggt}	0.836	[-]
Power turbine isentropic efficiency	η_{pt}	0.825	[-]
Shaft mechanical efficiency (both shafts)	η_m	0.99	[-]
Power turbine power delivered	Pw_{shaft}	190	[kW]

Table 5.3: TP100 design point parameters

This model is further improved with the implementation of the downscaling method as explained in 5.1.1, and it is extended with the addition of the propeller component model. The final architecture for the baseline MGT analysed in this study is shown in figure 5.1.

In this figure, the gas generator consists of an inlet (8), a compressor (9), a combustor (11) and the high pressure turbine(12). The gas generator exit gas is expanded in the low pressure power turbine (13). In the exhaust nozzle (14) the power turbine exit gas,

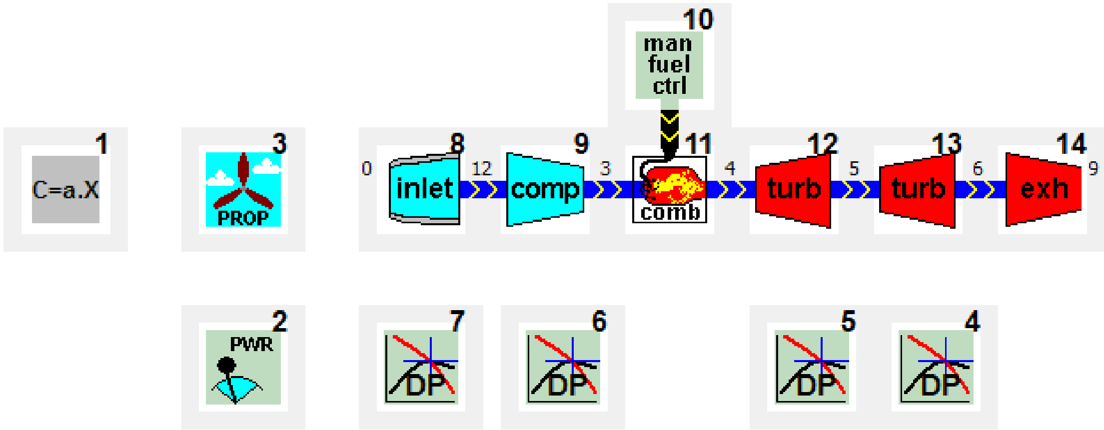

Figure 5.1: GSP model of the MGT

which still has some over pressure, is expanded into a jet at the nozzle exit station (9), providing a small percentage of the total thrust. Since there is no divergent nozzle, part nozzle throat station (8) is equivalent to exit station (9) in the GSP model. The propeller component (3) receives power from the power turbine shaft and translates it to thrust, as further explained in section 5.1.6. The manual fuel controller (10) is a component required by GSP that enables direct specification of off-design fuel flow to the combustor component. Fuel flow also can be specified as a 'free state' in order to calculate an off-design operating point with user specified combustor exit temperature TIT, or other power setting conditions such as turbine rotor speed and/or power load.
The next step is to configure the component models with their design data and performance characteristics. Component(1) is used to set the constant scaling factor SF as defined in 5.1.1, while component (4), (5), (6), and (7) are DP equation components which add relations among input parameters. In the scheduling component (7), the inlet mass flow rate is imposed with according to SF as shown in figure 5.2. Components (4), (5) and (6) are used for implementing the scaling relationship for turbines and compressor efficiencies. Equation 5.10 shows the final implementation of the compressor design efficiency. Here, the scaling laws developed in section 5.1.2 have been implemented together with the trasformation from isentropic efficiency into polytropic efficiency. A compression or expansion process can be characterized by either isentropic or polytropic efficiencies. In case of calculating gas turbine cycle performance for a range of compression ratio values as is typical for cycle analysis and optimisation, using polytropic efficiency is most practical. Morevoer, the air specific heat ratio has been averaged between γ_{12} at station 12 and γ_3 at station 3. R is the gas constant in [ft lb/lb degR] and is gas dependent, therefore 53.3 was used for air. Figure 5.3 shows how this is implemented in the GSP Design Scheduler.

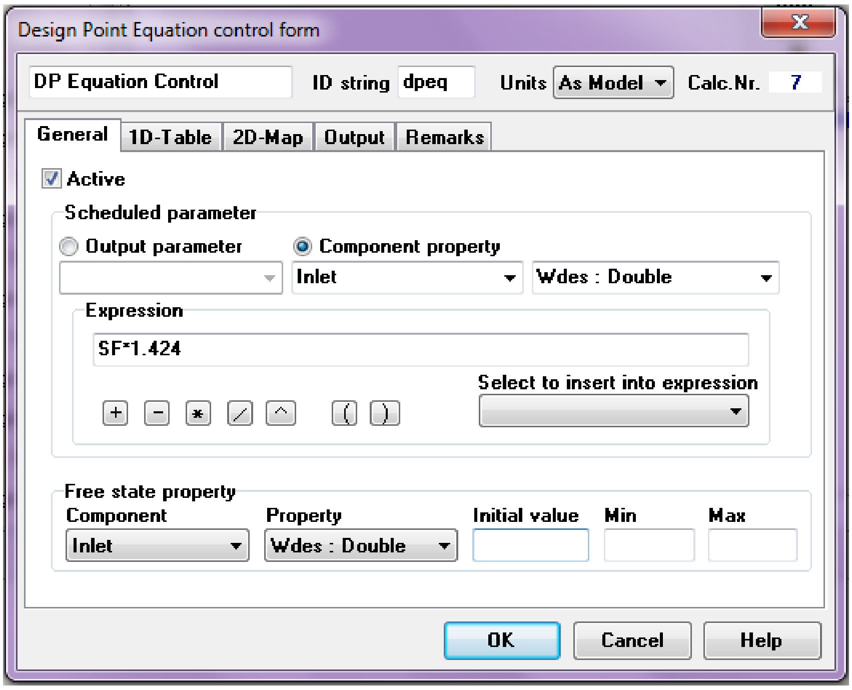

Figure 5.2: Design Point Equation Scheduler for Inlet air mass flow

$$\eta_{\infty c} = \eta_{cDes} = \frac{ln PR_c^{\left(1-\frac{2}{\gamma_{12}+\gamma_3}\right)}}{ln\left[1+\frac{PR_c^{\left(1-\frac{2}{\gamma_{12}+\gamma_3}\right)}-1}{1-(1-\eta_{cRef})\left(\frac{1}{\sqrt{SF}}\right)^{0.25}+\left[0.0404105-\frac{0.13}{\sqrt{\frac{\gamma_{12}+\gamma_3}{2}R}}(PR_c-2)\right]}\right]} \tag{5.10}$$

The same applies for the gas generator turbine (5.11) and power turbine (5.12):

$$\eta_{\infty t} = \eta_{tdes} = \frac{ln\left(1+\left(\frac{1}{PR_t}\right)^{\frac{\gamma_4+\gamma_5-2}{\gamma_4+\gamma_5}}-1\right)\left[1-(1-\eta_{tref})\left(\frac{1}{\sqrt{SF}}\right)^{0.31}\right]}{ln\left(\frac{1}{PR_t}\right)^{\frac{\gamma_4+\gamma_5-2}{\gamma_4+\gamma_5}}} \tag{5.11}$$

$$\eta_{\infty pt} = \eta_{ptDes} = \frac{ln\left(1+\left(\frac{1}{PR_{pt}}\right)^{\frac{\gamma_5+\gamma_6-2}{\gamma_5+\gamma_6}}-1\right)\left[1-(1-\eta_{ptRef})\left(\frac{1}{\sqrt{SF}}\right)^{0.31}\right]}{ln\left(\frac{1}{PR_{pt}}\right)^{\frac{\gamma_5+\gamma_6-2}{\gamma_5+\gamma_6}}} \tag{5.12}$$

5.1.6 Propeller Model

The propeller component can be used simulate various types of propellers:

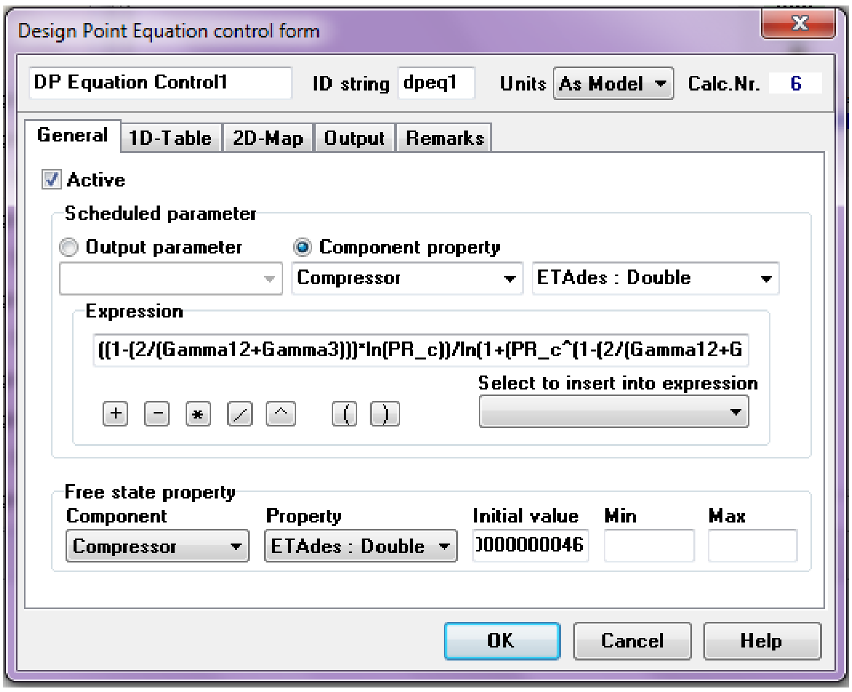

Figure 5.3: Design Point Equation Scheduler for Compressor Design Efficiency

- propellers with a user specified propulsion efficiency based on the ideal propeller theory;
- fixed pitch propellers with varying shaft speeds;
- variable pitch propellers at constant shaft speeds.

Since a performance map was not available for the propeller component, ideal propeller theory with user specified propulsion efficiency has been used:

$$\eta_{prop} = \frac{TV_0}{PW} \tag{5.13}$$

erformance of propellers with an user specified efficiency at flight-conditions (no map) are described with actuator disk (or ideal propeller) theory. A detailed explanation of this method is developed in appendix C. The actuator disk is a model for an ideal propeller. The energy given by the actuator disk to the flow is fully transformed into the kinetic energy of the slip stream. The propulsion or so-called Froude efficiency is given by:

$$\eta_{FR} = \frac{TV_0}{PW} = \frac{2}{1 + \frac{V_{j,ideal}}{V_0}} \tag{5.14}$$

Where $V_{j,ideal}$ is the ideal jet velocity and V_0 is the true air speed.
In GSP, η_{FR} is calculated and compared with the user specified efficiency. If the user specified efficiency is higher than η_{FR}, it is lowered to this value. If the user specified efficiency is lower than η_{FR}, that user defined value is directly used to calculate the

propeller thrust.
A distinction is made between static and in-flight conditions. The reason is that at static conditions $\eta_{FR} = 0$ by definition, since $V_0 = 0$. Therefore, at static conditions the propeller efficiency is defined as η_{st}:

$$\eta_{st} = \frac{\frac{dE_{kin,x}}{dt}}{PW_{delivered}} \tag{5.15}$$

The numerator in equation 5.15 is the kinetic energy production rate in the slip stream based on the axial velocity component.
To avoid singularity problems, a propeller with virtual rotational speed N as power setting variable is introduced and the propeller diameter is chosen to be equal to the diameter of the actuator disk. The virtual rotor speed is used as scaling parameter. The power delivered to the propeller is given by:

$$PW = C_{pw}\rho N^3 D^5 \tag{5.16}$$

from which the power coefficient C_{pw} is obtained, with N propeller rotational speed in $[s^{-1}]$ and D propeller diameter in [m]. The propeller net thrust T is defined by:

$$T = C_t \rho N^2 D^4 \tag{5.17}$$

where C_t is propeller thrust coefficient. Therefore the kinetic energy conversion efficiency $\eta_{kin,x} = \eta_{st}$ as defined in equation 5.15, becomes:

$$\eta_{kin,x} = \frac{\frac{dE_{kin,x}}{dt}}{PW} = \frac{T\frac{V_{j,ideal}}{2}}{PW} = \frac{C_t^{3/2}\rho N^3 D^5 \sqrt{\frac{2}{\pi}}}{C_{pw}\rho N^3 D^5} = \frac{C_t^{3/2}}{C_{pw}\sqrt{\frac{\pi}{2}}} \tag{5.18}$$

The value of $\eta_{kin,x} = \eta_{st}$ is user specified, and it is used to calculate the thrust coefficient C_t:

$$C_t = \left(\eta_{st} C_{pw} \sqrt{\frac{\pi}{2}}\right)^{2/3} \tag{5.19}$$

The static thrust T_{st} is then calculated as:

$$T = \left(\eta_{st} D \sqrt{\rho \frac{\pi}{2}} PW\right)^{2/3} \tag{5.20}$$

Limitations of this method are discussed in chapter 6.

MGT Design Point Parameters			
Description	**Symbol**	**Value**	**Unit**
Scaling Factor	SF	0.473	[-]
Inlet pressure	Pt0	101325	$[N/m^2]$
Inlet temperature	Tt0	288.15	[K]
Inlet massflow	$\dot{m}_{air}$	0.67434	[kg/s]
Compressor Polytropic Efficiency	$\eta_{\infty c}$	0.8269	[-]
Compressor Pressure Ratio	PR_c	4.6794	[-]
Turbine Inlet Temperature	TIT	1144.46	[K]
Fuel lower heating value	LHV	42916	[kJ/kg]
Fuel massflow	$\dot{m}_{fuel}$	0.01224	[kg/s]
Combustion Efficiency	η_b	0.958	[-]
Gas Generator Turbine Polytropic Efficiency	$\eta_{\infty t}$	0.7996	[-]
Power turbine Polytropic Efficiency	$\eta_{\infty pt}$	0.7911	[-]
Exit to Ambient relative Pressure Drop	dP_{pt}	0.08	[-]
Shaft Mechanical Efficiency (both shafts)	η_m	0.99	[-]
Power Turbine Shaft Power	PW_{shaft}	85.704	[kW]
Thrust	FN	3.055	[kN]

Table 5.4: MGT Design Point Performance Parameters

Design Point

The first step in modeling the performance of a gas turbine is the Design Point, which represents a desired performance at a specified operating point. Table 5.4 present the DP cycle parameters of the MGT after the downscaling procedure, at full take-off power and static sea-level conditions.

As explained in section 5.1.3, different combinations of TIT and PR_c should be analyzed for engine design point performance analysis using carpet plot output. Series of Design Points ('DP sweep') can be calculated in GSP in conjunction with a Loop Case Control component. This component can be used as the central storage for specific case input data. The looped input series of TIT and PR_c shown in figure 5.4 have been performed.

Off Design Performance

It is only after DP analysis that a first engine geometry is defined. In order to estimate the performances under various ambient conditions and thrust settings, it is necessary to

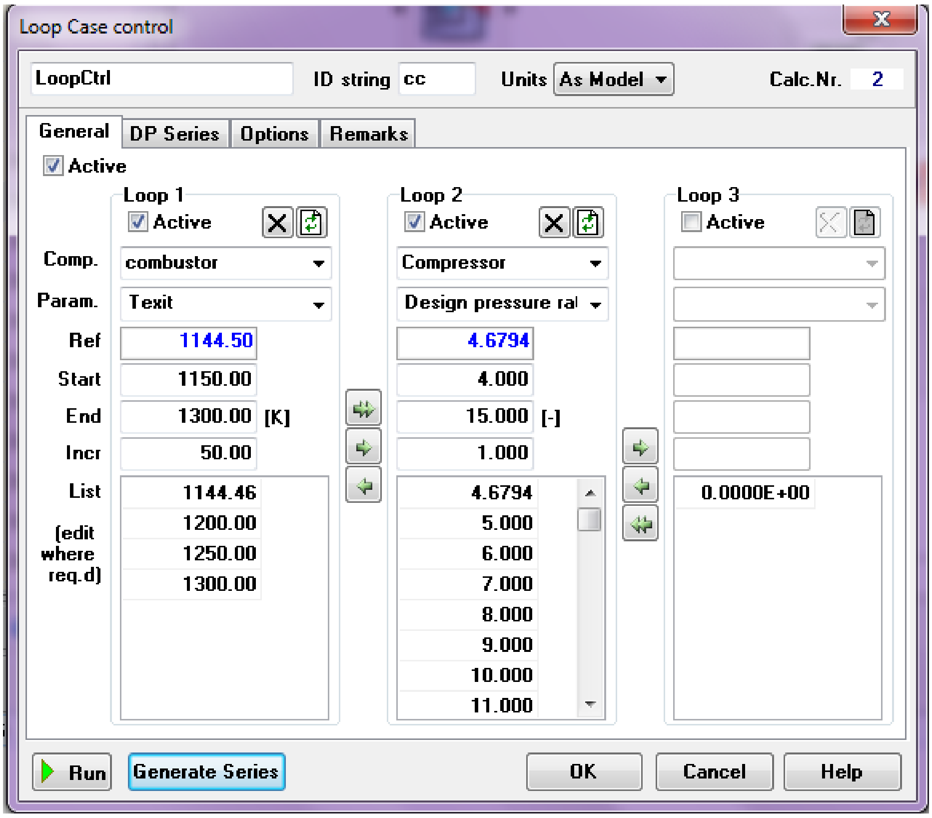

Figure 5.4: Loop Case Control input series for DP analysis

create an off design model. The off-design performance calculations are fundamental to ensure that the engine is capable of operating throughout its flight envelope and power range in a safe, stable and efficient manner. The data from the DP cycle is first used to create a thermodynamic model and is subsequently extended with a control suite.
The Off-design performance (OD) in this study concerns the operating point change with varying altitude and flight speed, as it is further explained in section 5.1.6. In GSP, off-design performance is an iterative process which requires additional information with respect to the DP simulation. This information is included in the model by the component maps. These enable prediction of off-design corrected mass flows, pressure ratios, efficiencies, relative shaft speeds, etc. However, the component characteristic maps are often hard to obtain or need to be scaled from available standard/similar maps. High quality maps are a requirement for accurate simulations, especially for the compressor. In the GSP reference model, the actual compressor map from the manufacturer was used. For the gas generator turbine the standard generic GSP map was scaled, and for the power turbine the map of a similar (but larger) engine power turbine was used. Manufacturer data points have then been used to tune the model of the TP100 engine by adjusting the specific data inputs in the data entry windows of the GSP model components.
The selected operating conditions to be varied are the ambient conditions and thrust setting. The next two sections will explain both in more details.

Flight Envelope

The flight envelope describes the range of altitude and Mach number within which the engine is intended to operate. There are four speed limits that restrict the flight envelope. For altitudes between 0 and 3048 m (10000 ft), it extends to zero speed. This altitude is commonly cited in engine performance studies and is usually the acceleration altitude during the en route climb in a typical flight mission of a civil transport airplane. Above 3048 m, the left boundary of the flight envelope is limited to the minimum calibrated airspeed (CAS). The maximum speed is set by the maximum CAS and the maximum Mach number (lowest is used). In a conceptual flight envelope design, the minimum CAS is chosen slightly less than the minimum en route stalling speed calculated for the airplane model at sea level for the weight equal to the typical operating empty weight. This is to guarantee that the left border of the engine flight envelope will never conflict with the airplane stall limit. The maximum speed should not exceed the maximum operating Mach number usually given in the airplane specifications. The maximum operating altitude in the engine envelope is taken higher or equal to the airplane maximum certified altitude. Figure 5.5 shows how the flight envelope looks like once the above mentioned considerations have been implemented. Engine operating maximum altitude is 8000 m, while operating true air speed varies between 0 and 0.19 Mach, with minimum CAS of 27 m/s above 3048 m, and maximum CAS equal to 38 m/s.

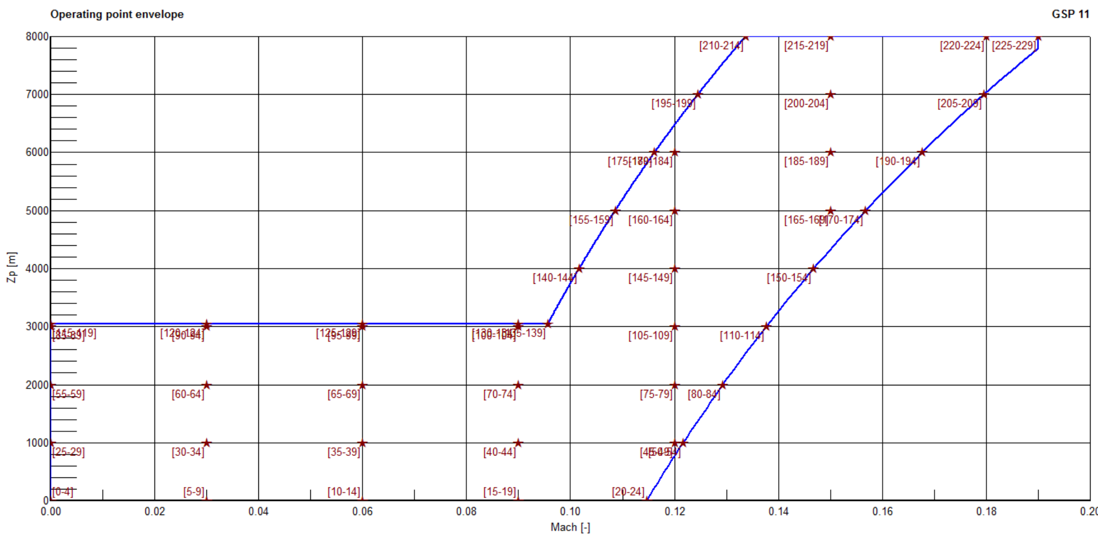

Figure 5.5: Flight Envelope for the Off-Design Simulations

Thrust Ratings

A thrust aero-engine has to ensure delivery of the required level of thrust at given operating conditions. This thrust is attained by controlling the engine with a certain measurable engine parameter (control parameter) associated with predefined thrust setting for each particular mission phase. In this study, the turbine inlet temperature TIT has been selected as control parameter.

Thrust ratings are used to describe the maximum available thrust under standard rating definitions. These are the maximum take-off (MTO), maximum continuous (MCT), maximum climb (MCL), and flight idle ratings in a normal operation, described as:

Maximum Takeoff thrust(MTO) This is the maximum thrust that the engine can deliver for 5 minutes in the take-off envelope of the aircraft. Peak thrust is usually achieved when the engine is static. This condition usually generates the highest stresses and temperatures in the engine, hence use of this rating is only permitted for up to 5 minutes of operation. It is used, as the name suggests, for take-off when the aircraft is at its heaviest and has to be accelerated to take-off speed in a finite runway distance. The higher the thrust available from the engine, the shorter the runway can be, or the greater the aircraft payload can be. As an alternative to payload, a higher thrust rating allows more fuel load to be carried into the air, so extending range of operation. These trade-offs between available thrust, runway length, aircraft weight and range may need to be assessed for each flight. An aircraft may take-off with less than maximum take-off thrust to reduce wear on the engine and extend its life. This is usually termed a 'reduced thrust' take-off, and is used to reduce engine maintenance costs.

Maximum Continuous thrust (MCT) Outside the MTO flight envelope, the MCT rating defines the maximum thrust that can be demanded from the engine. As such, it has particular significance with respect to engine failure in flight, as the aircraft will have to proceed to its destination or nearest diversion airport at max continuous thrust.

Maximum Climb thrust (MCL) This is the thrust rating to be used during the climb phase and it may be the same as max continuous thrust. The top of the climb phase is typically the most challenging condition for an engine outside the take-off regime, and is a critical design requirement. De-rate can be applied to MCL thrust to extend engine life, but at the cost of a slower time to climb and slightly increased trip fuel consumption.

Flight Idle The idle rating is the minimum thrust that can be used whilst the aircraft is in flight. It is largely defined by the requirement to keep the engine running, possibly supplying secondary services to the aircraft such as hydraulic and electrical power. The flight idle rating is important in that the lower it is, the quicker the aircraft can descend (without going into a dive). It is often determined by stability considerations such as flutter and surge margin.

For the sake of uniformity in performance modeling and reporting, the Society of Automotive Engineers (SAE) defined rating code (RC) assignments. The standard Rating Code numbers are 50 = max takeoff, 45 = max continuous, 40 = max climb, and 20 = low idle.

5.2 Models Coupling

A typical aircraft performance model sets the net thrusts required at specific points of the operational envelope of the aircraft. On the other hand, the engine designer establishes for each phase the net thrust available by the engine as a function of a certain physical characteristic of the engine, referred to as control parameter (usually either EPR or TIT), ambient conditions and flight speed. Rating codes and measured ambient conditions are converted with the Thrust Management Tables into the value of the control parameter corresponding to the required thrust. The system also sets the fuel flow rate as required to maintain the control parameter value.
When applied to this case study, the thrusts available at each SAE rating code have to be established by modeling at a number of points which discretely represent the engine flight envelope, as explained in 5.1.6. In the current case, they are obtained from engine OD simulation according to the following line of reasoning: the value of the control parameter TIT is calculated corresponding to a certain percentage of maximum thrust. OD simulations are run for the Flight Envelope where the control setting is achieved through a Power (or thrust) Control component. In this component, Power Codes are defined according to the thrust rating codes in 5.1.6. To each Power Code is assigned the respective TIT. The results of the simulations are the above mentioned Thrust Management Tables. Each rating table contains the variation of 'fractional thrust' with Mach number and altitude. 'Fractional thrust' is the thrust divided by reference-thrust-per-engine (sea-level static thrust, also called fn*). The factors used for different Rating Codes (RC) are available in table 5.5. In the Thrust Management Tables (figure 5.6), each RC stands a matrix of net

Thrust Rating	Code	fn/fn*
Maximum Take-Off	RC 50	1
Maximum Continuos	RC 45	0.9
Maximum Climb	RC 40	0.85
Flight Idle	RC 20	0.2

Table 5.5: Thrust Rating Codes Assignment

thrusts and a matrix of fuel flows obtained from engine system simulation. Each row in the engine performance matrixes contains a sweep of either thrust or fuel flow rate values corresponding to a constant Mach number and varying flight altitude. Each column, in its turn, is composed of either thrust or fuel flow rate values for a fixed altitude and a range of Mach number.

Firstly, the rating command is applied to provide unique throttle positions for the mission phases where thrust modulation is not normally required, as at takeoff and climb. For the cruise and descent phase, interpolation of the thrust values (and hence fuel flows) available between RC 45 and RC 20 is required, according to the Aircraft Performance model results.

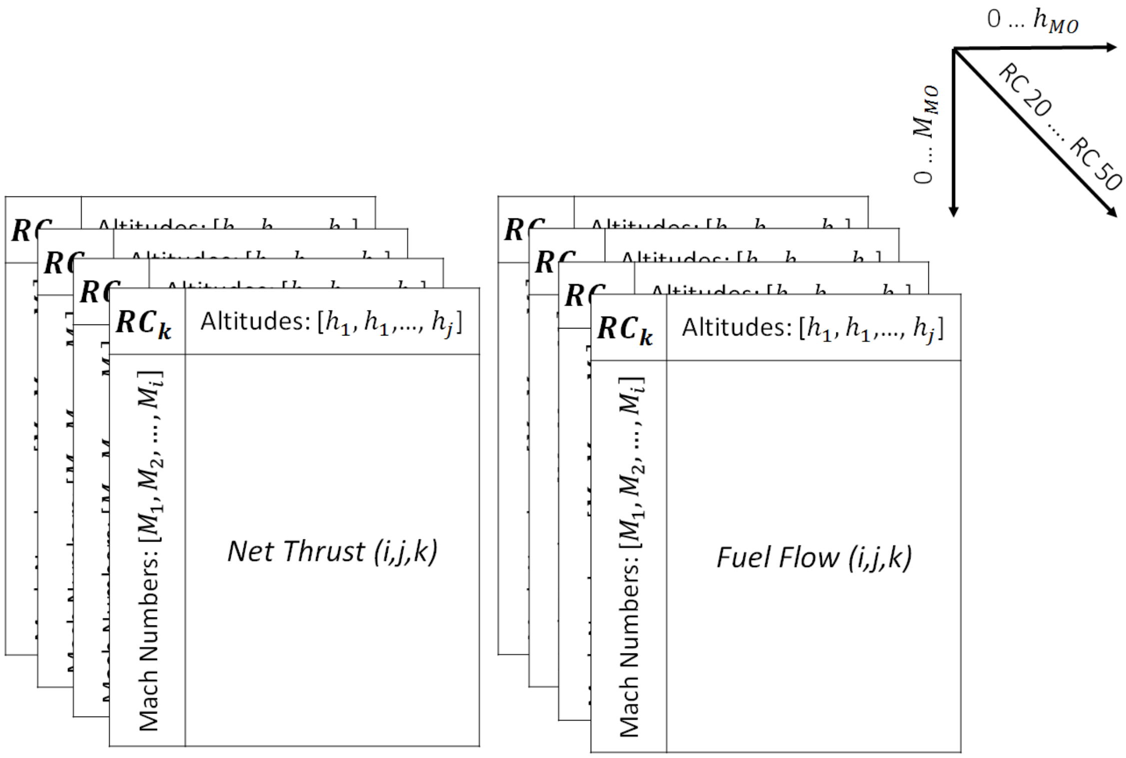

Figure 5.6: Thrust Management Tables structure

5.3 Aircraft Performance Model

An Aircraft Performance Model is developed in a parallel Thesis Project. The model is able to estimate mission performance for the reference UAV platform described in 4.2, where the baseline reciprocating engine model is implemented. This is further used as reference for the evaluation of possible mission performance improvements with other gas turbine designs. In fact, different gas turbine designs can be compared in the Aircraft Performance model through implementation of the aforementioned Thrust Management Tables.
Detailed description of the model is out of the scope of this Thesis, and the reader is suggested to refer to Beuselinck's work [36] for a more elaborated explanation.

Chapter 6

Analysis

In this chapter, the results of the engine model are analysed. The effect of different technology levels, size, and components efficiency on the engine model performance is discussed, both at design point and off-design. It is important to remember that the design point has been selected at sea level static conditions. This choice has been made considering that the combined takeoff-climb phases are those where the engine is assumed to produce the maximum thrust force, therefore the most critical in the flight envelope.
A final section presents the results of the Aircraft Performance model with different engine models implemented.

6.1 Technology Level Effects

Different design points for a specific size (in terms of inlet air mass flow) but different combinations of TIT and compressor pressure ratio can be visualized in a so-called carpet plot. A carpet plot is a fundamental tool for a comprehensive understanding of the possible design points: the importance and the effects of TIT and PR_c on engine performance are here further discussed.
Figure 6.1 shows the carpet plot for the first technology level variations after the downscaling with a Scaling Factor (SF) of 0.47, value obtained according to the procedure explained in section 5.1.1. The nominal output power obtained with the reference TIT of 1144.46 K and PR_c of 4.6794, once the size effect on the components efficiency have been applied, is 86 kW. This is the same shaft power delivered by the reference reciprocating engine. However, it is clear from the figure that increasing TIT has the direct effect of increasing the power delivered by the engine to the propeller (x axis), while increasing PR_c has the strongest influence in lowering the specific fuel consumption (SFC) of the engine (y axis).

The SFC is defined as the mass of fuel burned by an engine in one hour divided by the power that the engine produces. However, for the scope of this study, a different figure of merit is further selected. The thrust specific fuel consumption (TSFC) refers in fact to

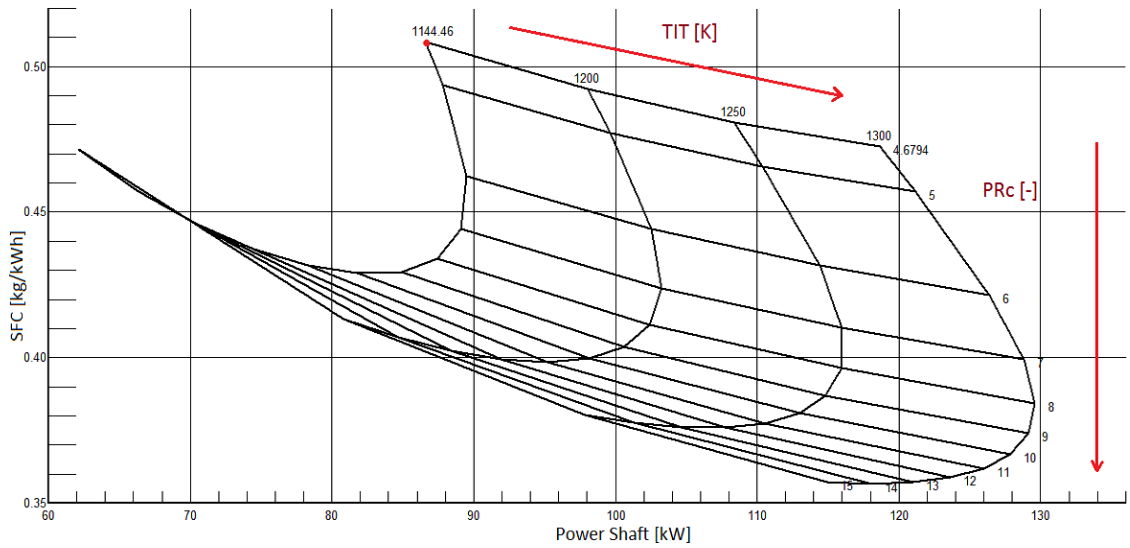

Figure 6.1: Carpet Plot for a Scaling Factor of 0.47 with power output and specific fuel consumption variations for different technology levels (pressure ratio effects on components efficiency not included).

the fuel consumed per unit of thrust produced, providing important information about the performance of a given aircraft engine. Engineers use the TSFC to figure out how much fuel is required for an aircraft to perform a given mission. However, the value of TSFC varies with speed and altitude, because the efficiency of the engine changes with atmospheric conditions. Figure 6.2 reports the values of TSFC over thrust for different possible Technology Levels at sea level static conditions. From this figure, the increase in TIT is not beneficial to the TSFC, which in fact increases. This result is due to the fact that the thrust at the denominator ($TSFC = \frac{\dot{m}_f}{T}$) is calculated using an ideal propeller with constant diameter: this choice is further discusses in the following sections.

At each TIT it is possible to find an 'optimum' value of PR_c, which increases with increasing TIT. These 'optimum' pressure ratios are not the ones which give the minimum TSFC for a selected turbine inlet temperature, as it could be concluded from figure 6.3. In fact, an 'optimum' PR_c for a specific TIT is the one that allows for the best compromise between thrust available and TSFC, represented by the point where a further increase in PR_c starts decreasing the level of generated thrust. To better explain this concept, the choice of 'optimum' PR_c is discussed for the baseline TIT of 1144.46 K. The red dot in figure 6.2 shows the DP at which the engine has been first sized. Clearly, it does not represent an advantageous point neither in therms of thrust available nor in terms of TSFC. The 'optimum' PR_c would preferably be closer to 6. Nevertheless, if the maximum required thrust for the mission is e.g. 3.1 kN, a better option would be to choose $PR_c = 7$, hence reducing even further the TSFC. On the other hand, this choice will also effect the performance of the engine in conditions different than the selected DP, and more information is required for the selection of the best pressure ratio. This information regards the thrust available at different operational thrust settings in several critical points of the flight envelope, where the thrust available is only a certain percentage

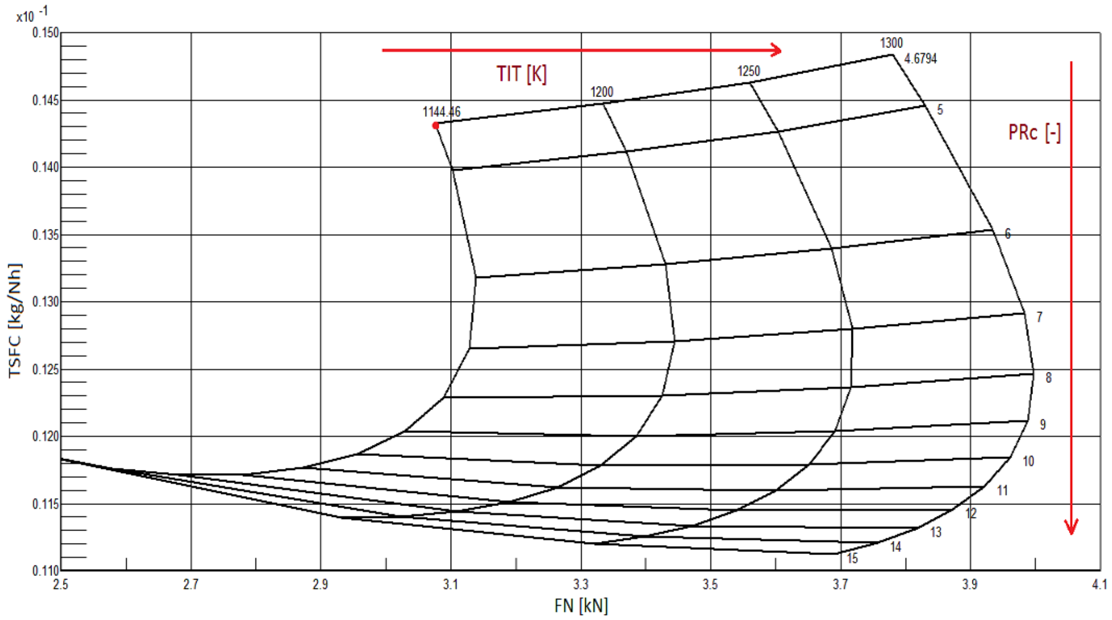

Figure 6.2: Carpet Plot for a Scaling Factor of 0.47 with power output and thrust specific fuel consumption (TSFC) variations for different technology levels (pressure ratio effects on components efficiency not included).

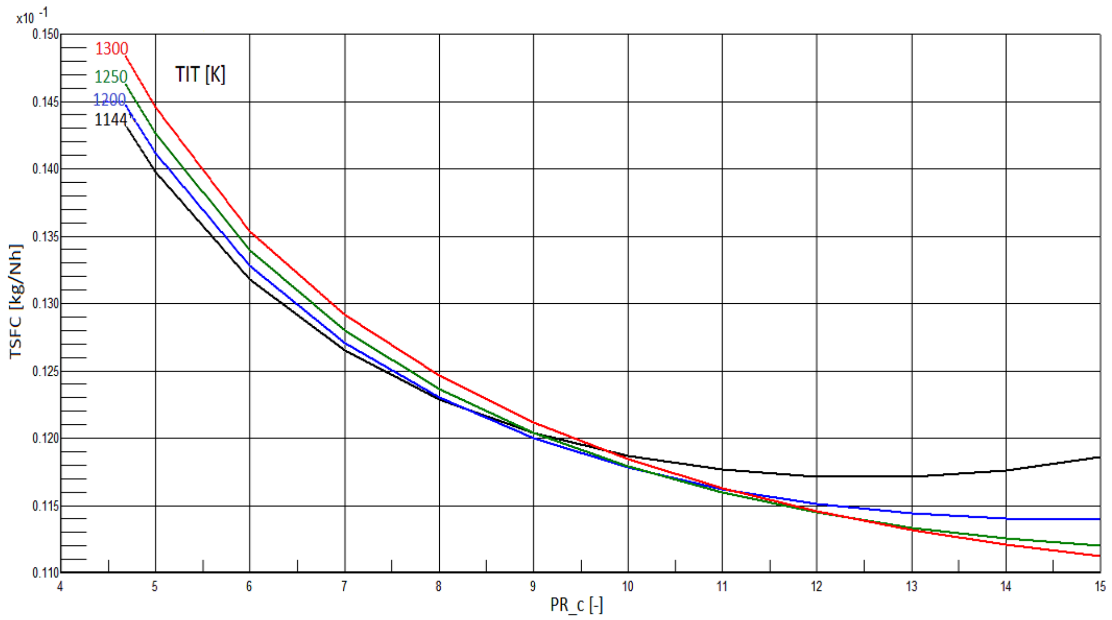

Figure 6.3: Variation of TSFC with compressor pressure ratio for different TIT at DP.

of the maximum thrust. These data can be obtained by running the off design simulations at the conditions of interest, and from the Aircraft Performance model simulations. Based on the available information at this conceptual stage, a preference for reduced TSFC leads to the selection of PR_c slightly higher than the aforedescribed 'optimum' PR_c. TIT step of 50 K is considered a proper representation of engine technology improvement, as already discussed in Chapter 5; TIT equal to 1300 K is not taken into account because of the level of thrust generated exceeding by far the required thrust for the selected mission.

6.2 Size Effects

Excess thrust can be reduced by downscaling the turbine even more. Again, size is chosen to be identified by the inlet air mass flow rate. Hence, different carpet plots can be made for distinct inlet air mass flow rates, as it is shown in figure 6.4. The figure displays the carpet plots trend with downscaling. In the graph, SFC over shaft power is plotted for different combinations of compressor pressure ratio and turbine inlet temperature, whose values increase in the direction shown by the arrows. In the figure, scaling factor (SF) of 0.47 (black), 0.39 (blue) and 0.33 (green) are presented. They correspond respectively to an output power of 86, 70 and 60 kW at DP for the baseline technology level (TIT=1144.46 K and PR_c=4.6794). The red line connects the same baseline design point at different engine scales. It is clear that decreasing size worsen turbine SFC at comparable technology levels, as expected.

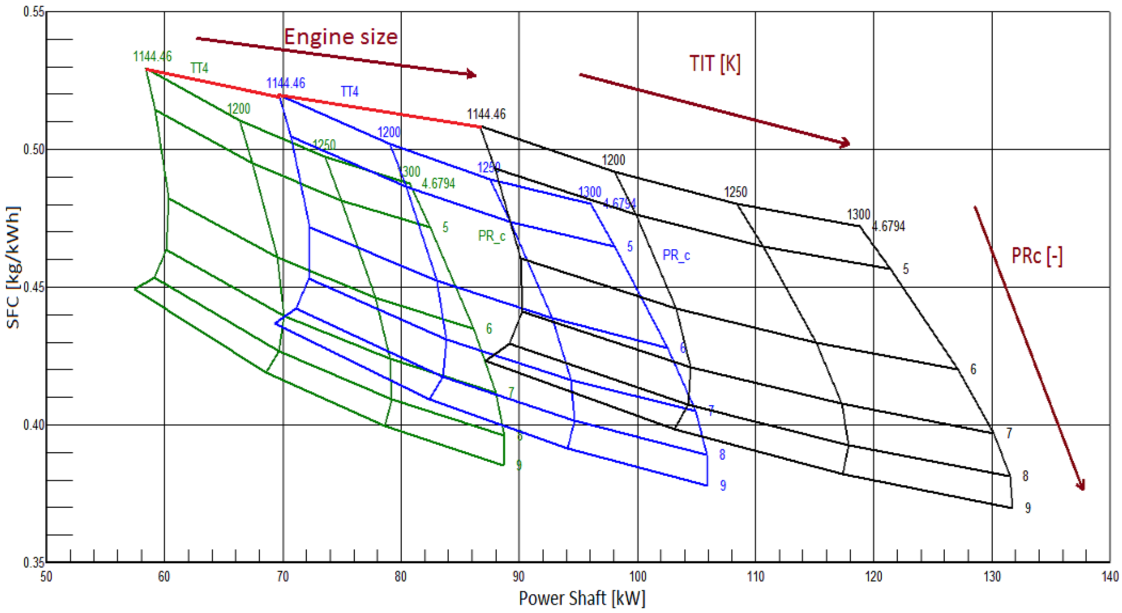

Figure 6.4: Carpets trend (SFC over Power) with engine size reduction. Green plot refers to a scaling factor of 0.33, blue plot to SF=0.39, and black plot to a SF=0.47.

However, a different result is obtained when TSFC is plotted over engine thrust. The same design point at decreasing engine scales showcases improved TSFC, as shown by the red line in figure 6.5. This would mean better performance with downscaling, in contradiction with what expected.

The trend in graph 6.5 is explained by the assumption of the same propeller diameter D for different engine sizes. The assumption of a propeller diameter is reasonable if the same airframe is considered. Ideally, the propeller diameter should be greater for efficient

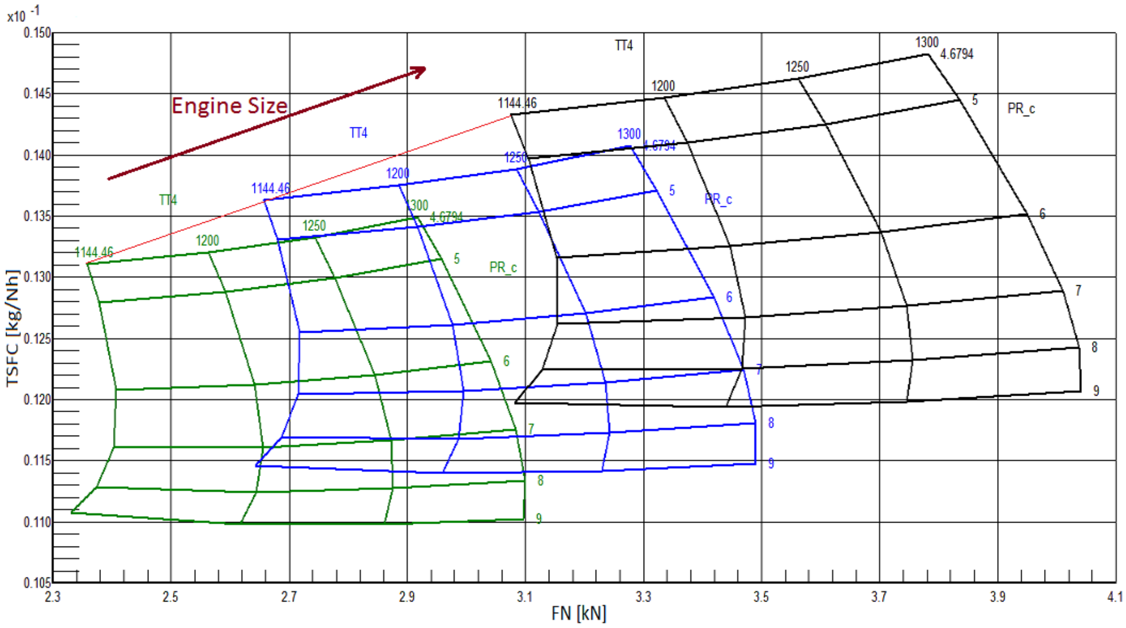

Figure 6.5: Carpets trend (TSFC over FN) with engine size reduction. Green plot refers to a scaling factor of 0.33, blue plot to SF=0.39, and black plot to a SF=0.47.

low airspeed operation, especially for take-off performance. Larger propellers have more surface area, which gives the propeller more thrust for the same amount of input power. In other words, larger diameter propellers are more efficient. This means that reducing the size of the engine (hence the power input to the propeller), but not the propeller diameter, gives higher thrust than what is expected from a turboprop where also the propeller diameter is scaled. As a consequence, SFC ($\frac{Wf}{PW_{input}}$) increases (worsens) at smaller engine size, while TSFC ($\frac{Wf}{FN_{prop}}$) decreases (improves) with size up to a certain flight speed V_0.
The trend of TSFC with increasing DP true air speed is shown in figures 6.6. The graph starts at flight Mach number Ma=0.02, where the transition from static to in-flight conditions occurs. At about Ma=0.11, there is a turning point, meaning smaller scale becomes less efficient (higher TSFC). The limitations of the ideal propeller model are further discussed in Chapter 8.

Figure 6.7 shows the DP performance of different engine scales at the beginning of the climb phase, where ideal propeller theory at in-flight conditions is applied. From this graph, TSFC is increasing with downscaling as expected. Therefore, not the selected figure of merit (TSFC), but SFC is further used as term of performance comparison at sea level static conditions.

6.3 Components Efficiency Effects

Turbmachinery efficiencies play a fundamental role in engine overall performance. The effects of downscaling on components efficiency has already been discussed. When both the effects of size and pressure ratio are included in the calculations of the components

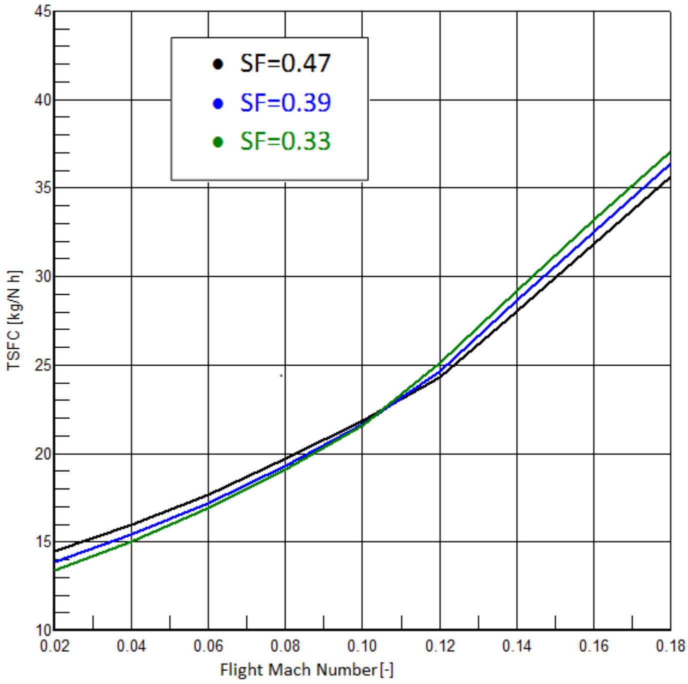

Figure 6.6: TSFC trend for different engine sizes with flight Mach Number at sea level.

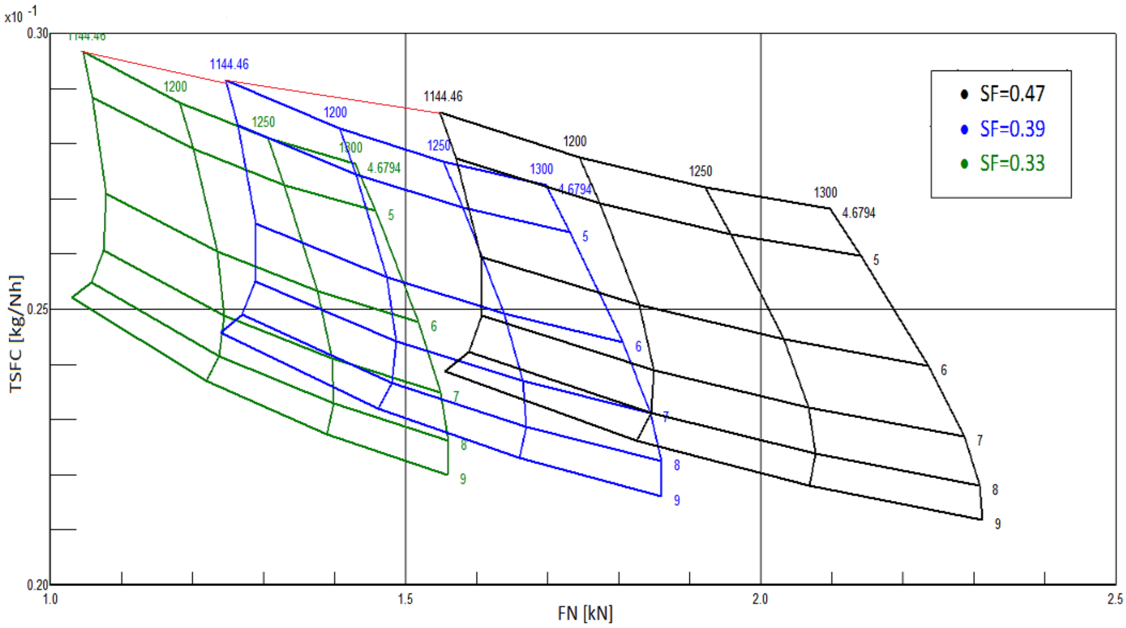

Figure 6.7: Carpets trend (TSFC over Thrust) with engine size reduction

efficiency, the carpet plot discussed in section 6.1 for the first scale (SF=0.47) changes as shown in figure 6.8. Here, the increasing PR_c positively effects TSFC up to a value of about 9. Above this point, the losses in the compressor reduce its efficiency causing very poor overall engine performance. Therefore, higher compressor pressure ratios should be selected only in case appropriate blade and rotor design can be performed and manufacturing techniques will allow to maintain an acceptable level of component efficiency. Moreover, the 'optimum' PR_c at each TIT is lower than in figure 6.3, and TSFC is higher for the same combination of TIT and PR_c. Once the effect of increasing PR_c are included in the estimation of components efficiency with downscaling, the carpet plots at different sizes present the trend for SFC shown in figure 6.9.

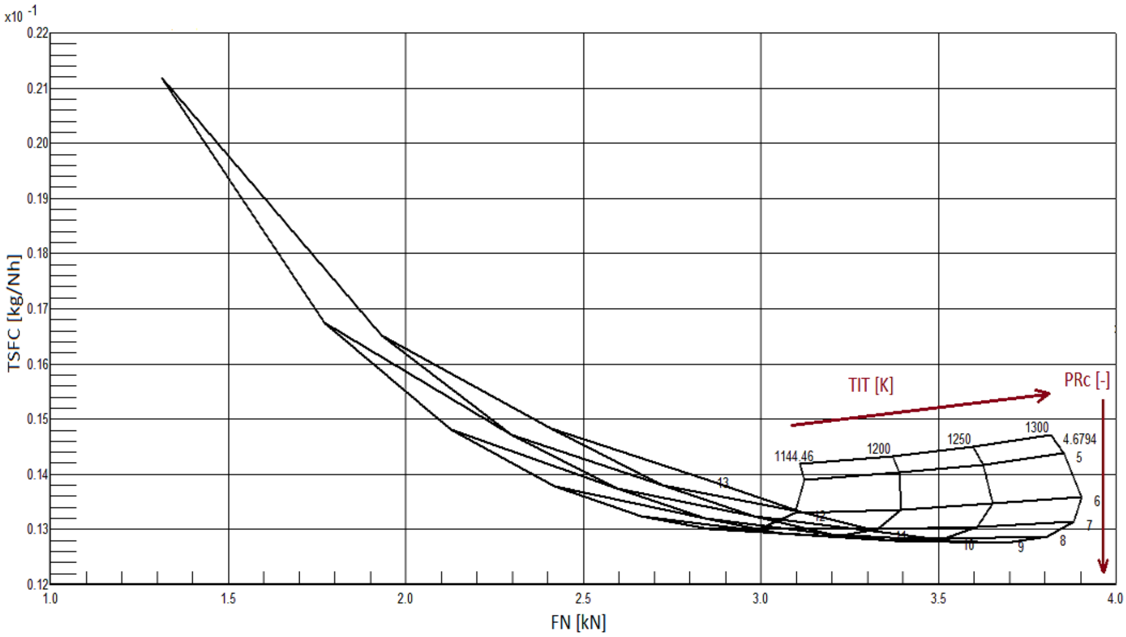

Figure 6.8: Carpet Plot for a Scaling Factor of 0.47, pressure ratio effect on components efficiency is included.

It is of great interest to estimate the gain in engine performance with components efficiency improvement. When a theoretical increase of 2% in the components efficiency is assumed, TSFC and available thrust improve substantially. Figure 6.10 shows the trend in the carpet plot with efficiencies advancement for the smaller size (SF=0.33), at sea level static conditions. In the figure, effects of size and pressure ratio on the efficiency have been included for each DP of the carpet. The values of compressor efficiency at each DP are available in figure 6.11. Turbine efficiency does not vary significantly for different points of the same carpet. For this engine size, the gas generator turbine isentropic efficiency is equal to 0.812 (for each DP of the original carpet), a value improved to 0.826 for the blue carpet (where the components efficiency has been increased by 2%). Similarly, power turbine isentropic efficiency is equal to 0.8 for the original carpet, improved to 0.814 for the blue one.

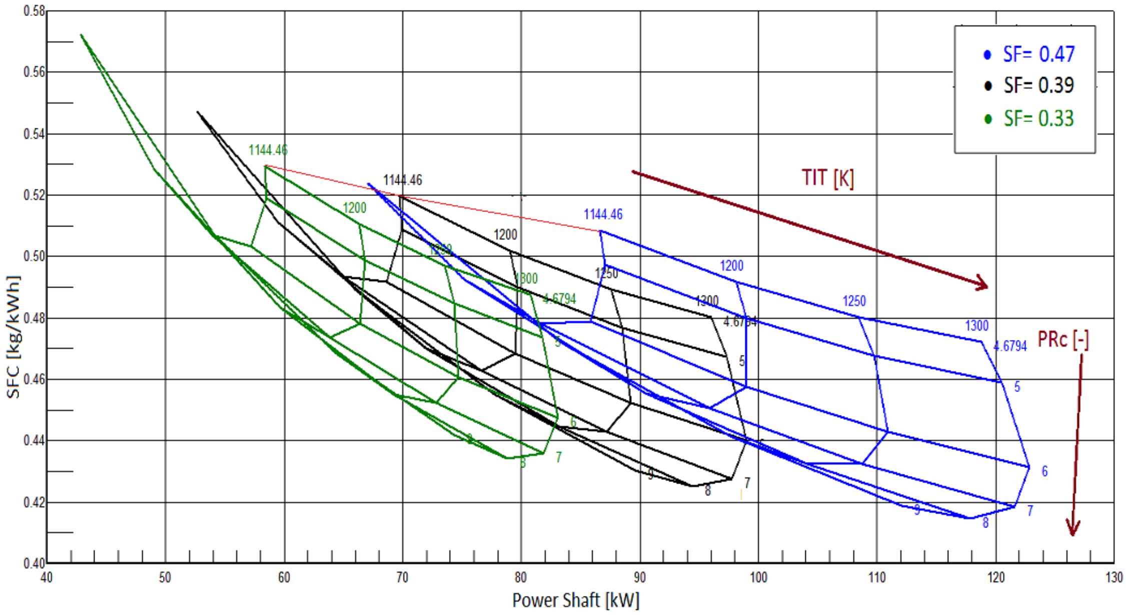

Figure 6.9: Carpet Plot trends with pressure ratio effects on components efficiency included.

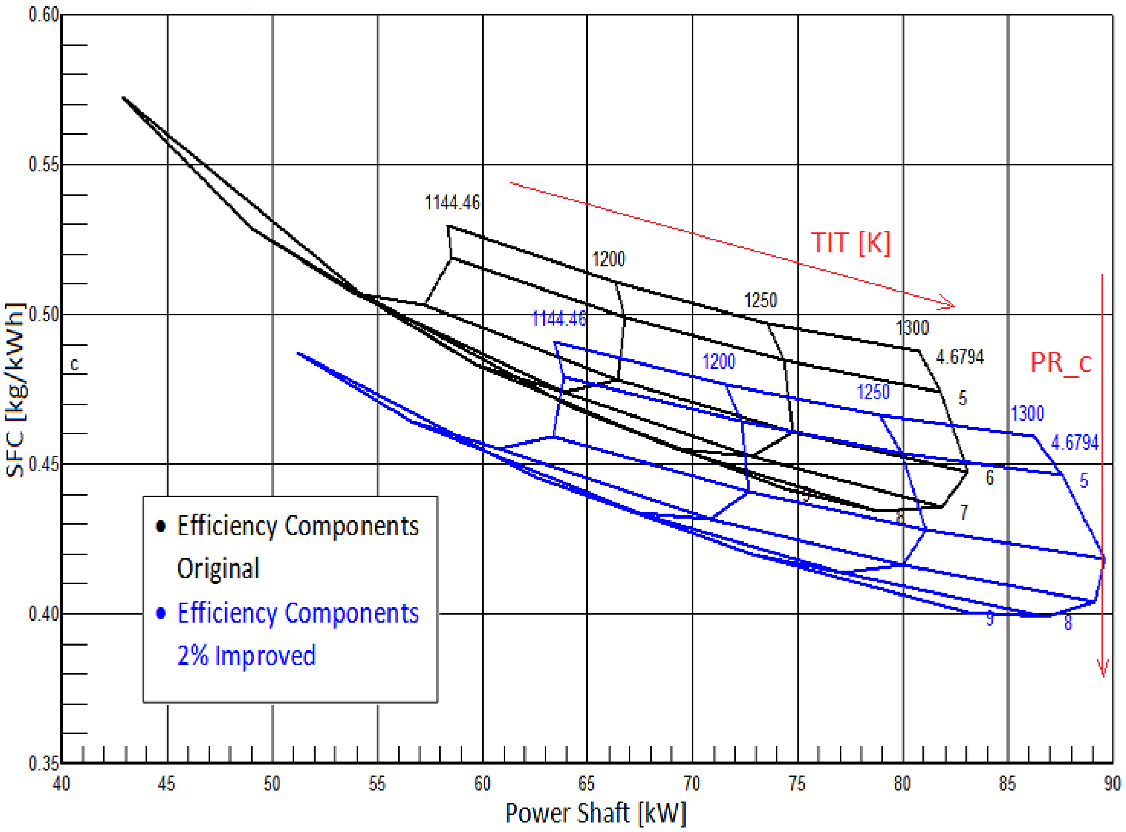

Figure 6.10: Carpet trend with 2% components efficiency improvement for engine scale factor SF=0.33.

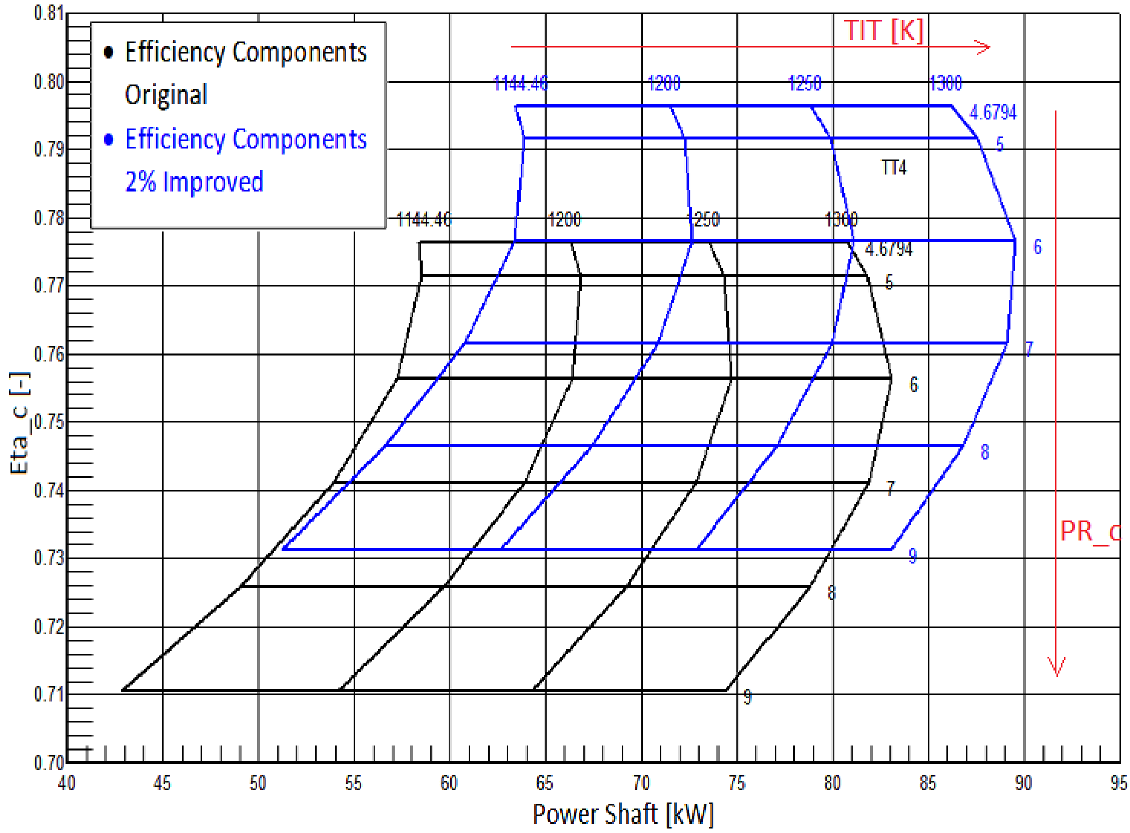

Figure 6.11: Compressor Isentropic Efficiency values for engine scale factor SF=0.33.

6.4 Mission Results

According to the above analysis, three technology levels have been selected in addition to the baseline TL 0 (TIT=1144.46 K with PRc=4.6794) to be further developed as engine models. The reasoning behind these choices as already been discussed. Each of these Technology Levels represents a different engine design. Table 6.1 shows which combinations of TIT and PR_c for different engine size have been preferred. Technology Level 0 and 1 for the scale factor SF=0.33 have not been implemented since their thrust level was too low to perform the mission. Technology Level 3+ refers to TL 3 with components efficiency values increased by 2%. LT

For each engine DP selected in the table, models have been developed at off-design conditions (OD). Thrust Management Tables have been created and implemented into the Aircraft Performance Model.
The mission is divided according to the typical aircraft flight phases: Take-Off, Climb, Cruise, Descent, Loiter, Approach, and Landing. However, the relevant phases used for engine performance comparison are Climb, Cruise, and Descent, where the greatest differences among propulsion systems are evident. For each phase, flight time, distance covered, and fuel consumed data have been compared in table 6.2. The baseline reciprocating engine has been used as reference to estimate relative performance gain or loss with the other gas turbine engine models of different sizes and technology levels. Therefore, the

Scale Factor	Technology Level	TIT [K]	PRc [-]	Power Output [kW]	Eta Compressor [-]	Eta GG Turbine [-]	Eta Power Turbine [-]
0.47	TL 0	1144.46	4.68	86	0.78	0.82	0.80
0.47	TL 1	1144.46	6	86	0.76	0.82	0.80
0.47	TL 2	1200	7	97	0.75	0.82	0.80
0.47	TL 3	1250	8	105	0.73	0.82	0.80
0.39	TL 0	1144.46	4.68	70	0.78	0.81	0.80
0.39	TL 1	1144.46	6	70	0.76	0.81	0.80
0.39	TL 2	1200	7	77	0.74	0.81	0.80
0.39	TL 3	1250	8	83	0.73	0.81	0.80
0.33	TL 2	1200	7	64	0.74	0.81	0.79
0.33	TL 3	1250	8	70	0.72	0.81	0.79
0.33	TL 3+	1250	8	77	0.73	0.82	0.80

Table 6.1: Engine DP selected from carpet plot analysis

results are also given as relative variation (in percentage) with respect to the reciprocating engine. Table 6.3 shows the distance traveled for each mission phase. Finally, table 6.4 summarizes the total mission results in terms of endurance, range, and fuel consumed for each engine model. During climb, optimized PR_c for a specific TIT and engine size gives

Time												
	Climb				**Cruise**				**Descent**			
Engine Type	[h]		**Fuel** [kg/h]		[h]		**Fuel** [kg/h]		[h]		**Fuel** [kg/h]	
Reciprocating Engine	1.1		17.35		22.3		12.92		3.3		8.41	
MGT SF=0.47 TL 0	1.3	21%	65.04	275%	14.7	-34%	14.95	16%	4.8	44%	6.37	-24%
TL 1	1.2	13%	24.33	40%	16.9	-24%	14.28	11%	4.8	45%	12.47	48%
TL 2	0.9	-15%	25.97	50%	19.8	-11%	13.66	6%	3.3	0%	11.73	39%
TL 3	0.8	-28%	27.18	57%	20.8	-7%	13.37	3%	3.0	-11%	11.53	37%
MGT SF=0.39 TL 0	4.4	321%	18.74	8%	15.3	-31%	14.30	11%	2.8	-16%	10.85	29%
TL 1	3.1	198%	18.43	6%	18.6	-16%	13.37	3%	2.6	-21%	10.08	20%
TL 2	1.8	67%	20.41	18%	18.4	-17%	13.32	3%	4.4	34%	11.07	32%
TL 3	1.3	24%	21.84	26%	21.0	-6%	12.92	0%	3.2	-3%	10.33	23%
MGT SF=0.33 TL 2	6.8	548%	15.70	-10%	15.8	-29%	12.46	-4%	3.1	-5%	9.54	13%
TL 3	3.3	216%	17.14	-1%	18.5	-17%	12.62	-2%	4.1	24%	10.15	21%
TL 3+	1.9	77%	18.11	4%	23.0	3%	11.81	-9%	3.2	-4%	8.94	6%

Table 6.2: Mission Phases Endurance: Engine models performance comparison.

a significant improvement both in terms of time and in fuel consumption (per hour of flight). However, the reciprocating engine is performing better than any turbine model in this phase. As technology level increases, time to climb decreases, as expected from the higher level of thrust available at climb power settings. For the scaling factor SF=0.47, TL 2 and 3 are able to climb faster (up to 28%) compared to the reciprocating engine,

Distance [km]						
Engine Type	**Climb**		**Cruise**		**Descent**	
Reciprocating Engine	153		3724		446	
MGT SF=0.47 TL 0	200	31%	2420	-35%	643	44%
TL 1	187	22%	2779	-25%	644	44%
TL 2	142	-7%	3262	-12%	461	3%
TL 3	123	-20%	3420	-8%	414	-7%
MGT SF=0.39 TL 0	684	346%	2521	-32%	380	-15%
TL 1	484	216%	3053	-18%	358	-20%
TL 2	271	77%	3019	-19%	595	33.2%
TL 3	203	32%	3445	-8%	438	-2%
MGT SF=0.33 TL 2	1048	584%	2581	-31%	422	-5%
TL 3	512	234%	3034	-19%	550	23%
TL 3+	287	87%	3766	1%	430	-4%

Table 6.3: Mission Phases Distance: Engine models performance comparison.

Total Mission Results						
Engine Type	**Total Time [h]**		**Fuel Consumption [kg/h]**		**Total Distance [km]**	
Reciprocating Engine	27.6		12.46		4438	
MGT SF=0.47 TL 0	21.5	-22%	15.97	28%	3358	-24%
TL 1	23.7	-14%	14.48	16%	3711	-16%
TL 2	24.6	-11%	13.95	12%	3936	-11%
TL 3	25.1	-9%	13.70	10%	4026	-9%
MGT SF=0.39 TL 0	23.2	-16%	14.81	19%	3663	-17%
TL 1	25.0	-9%	13.74	10%	3968	-11%
TL 2	25.4	-8%	13.51	8%	3985	-10%
TL 3	26.2	-5%	13.11	5%	4168	-6%
MGT SF=0.33 TL 2	26.4	-4%	12.98	4%	4136	-7%
TL 3	26.8	-3%	12.83	3%	4193	-6%
TL 3+	28.7	4%	11.95	-4%	4567	3%

Table 6.4: Total Mission Results.

but their fuel consumption per hour is higher (50 and 55%). For SF=0.33, TL 2 is under powered during climb, resulting in an unacceptable time to climb.

During cruise, endurance and fuel consumption (per hour of flight) increase with increasing technology level and smaller engine size. All technology levels with SF=0.33 have lower fuel consumption [kg/h] than the reciprocating engine. In addition, SF=0.33 TL 3+ is the only gas turbine engine model which has both higher endurance and lower fuel consumption than the reciprocating engine. During descent, fuel consumption improves with engine size reduction.

Total range and total endurance of the turbine engine is increased with smaller engine size and higher technology level. The engine model with SF=0.33 and TL 3+ covers a distance of about 130 km longer than the reciprocating engine, with a total increase in endurance of about 1 hour and 4% reduction in fuel consumption per hour of flight.

These results are further discussed in Chapter 8.

Chapter 7

Conceptual Engine Design

According to the mission results of various engine models, a final gas turbine engine has to be selected based on the Mission Requirements identified in Chapter 4.
The engine model which showcased the best mission performance in Chapter 6 is considered a competitive alternative to the original reciprocating engine. Its conceptual design at DP sea level static conditions derives from the reference TP100 model after the down-scaling process performed with a scaling factor SF=0.33. A turbine inlet temperature of 1250 K and a compressor pressure ratio of 8 have been selected. Effects of size and PR_c have been considered when estimating components efficiency. A theoretical 2% improvement for the polytropic efficiencies has been implemented for the compressor and both turbines. Table 7.1 shows the main parameters of this engine at DP. Engine off-design performance, in the form of Thrust Management Tables, are available in Appendix E.

This engine model is used in the redesign process of the UAV platform. Lower engine weight allows to reduce the UAV maximum take-off weight (MTOW). In return, the fuel required decreases, providing the possibility of optimizing the airframe of the UAV. Without significant configuration changes, wings, fuselage, and empennage can be redesigned in an iterative process, until no more significant fuel saving is achieved.
Table 7.2 presents the results of the redesign process, with comparison between the baseline and the optimized airframes. The redesigned UAV, implemented with the new turbine design, is able to travel an estimate distance of about 4419 km with and endurance of 28.7 hours. A significant fuel reduction of 12.5% is gained compared to the original UAV configuration, which has 18% lower MTOW.

Parameter	Symbol	Value	Unit
Inlet air massflow	Wair	0.47467	[kg/s]
Compressor pressure ratio	PR_c	8	[-]
Compressor Isentropic Efficiency	Eta_c	0.746	[-]
Turbine Inlet Temperature	TT4	1250	[K]
Combustor Efficiency	ETA_b	0.96	[-]
Fuel massflow	WF	0.00886	[kg/s]
Gas Generator Turbine Pressure Ratio	PR_GGT	3.3	[-]
Gas Generator Turbine Isentropic Efficiency	Eta_GGT	0.826	[-]
Power Turbine Pressure Ratio	PR_PT	2.2	[-]
Power Turbine Isentropic Efficiency	Eta_PT	0.814	[-]
Shaft Power Output	Pwshaft	77	[kW]
Propeller Thrust	FNprop	2.762453	[kN]
Total Net Thrust	FN_tot	2.822557	[kN]
Thrust Specific Fuel Consumption	TSFC	0.011	[kg/N h]
Specific Fuel Consumption	SFCshaft	0.414	[kg/kW h]

Table 7.1: Engine Design Point Parameters

	MTOW [kg]	Wingspan [m]	Fuselage length [m]	Fuel [kg]
Baseline UAV	1250	16.6	5.8	343
Optimized UAV	1021	15	5.1	300

Table 7.2: Redesigned UAV platform main parameters after the implementation of the selected engine model.

Chapter 8

Results and Discussion

This Chapter discusses both the results of the different engine models of Chapter 6, and those of the final conceptual engine design implemented in the optimized UAV of Chapter 7.

Firstly, a cycle point analysis has been performed. The engine design point was selected to be at sea level static conditions. From the cycle point analysis, it is concluded that for a determined engine size, increasing TIT has the effect of augmenting the power generated by the engine, at the cost of a higher fuel consumption.
Nevertheless, at each TIT, increasing PR_c improves engine fuel economy, until a certain point is reached which performs minimum SFC with an acceptable level of take-off thrust. On the other hand, decreasing turbine size affects the efficiency of the components. Both scaling factor SF and compressor pressure ratio PR_c have a negative influence on components efficiency. In particular, increasing PR_c has a strong effect on compressor efficiency, which prevents the designer to select values higher than 9, as it is usual for further reducing the specific fuel consumption.
In Chapter 6, the implications of assuming a constant propeller diameter with engine downscaling have been presented. Larger propellers are more efficient, meaning that smaller turboprops with the same propeller diameter have higher thrust than their counterparts with a smaller propeller. The limitations of the ideal propeller model are evident: as the engine is downscaled, while keeping the same propeller diameter D, V_{jet} and the propeller thrust reduce for this model. The kinetic power that is lost and which is proportional to V_{jet}^3 reduces much faster, leading to better thrust efficiency of the propeller at smaller scale. At low speeds, the better thrust efficiency outweighs the opposite effect of decreased turbomachinery efficiencies with size. On the other hand, at higher speeds the effect of the engine components prevails and TSFC becomes larger.
It is important to remember that this thrust is an ideal number that does not account for the losses that occur in practical high speed propellers, like tip losses. The losses must be determined by a more detailed propeller theory, which is beyond the scope of this study. The simple momentum theory, however, provides a good first approximation and can be used for a preliminary design.

In addition, ideal (maximum theoretical) propeller efficiency is adjusted in GSP according to the following reasoning. The η_{ideal} is calculated and compared with a user specified efficiency. The lowest value between the two is further used to calculate the propeller thrust. This method implies that, for an increasing calculated η_{ideal}, the maximum propeller efficiency that can be reached is limited at the value specified by the user, as shown in figure 8.1. In the figure, η_{prop} of different engine scales is plotted over a range of increasing flight velocity at sea level. As previously discussed, better thrust efficiency of the propeller is achieved at smaller scale.

Furthermore, off-design engine performance has been examined. Different phases in the

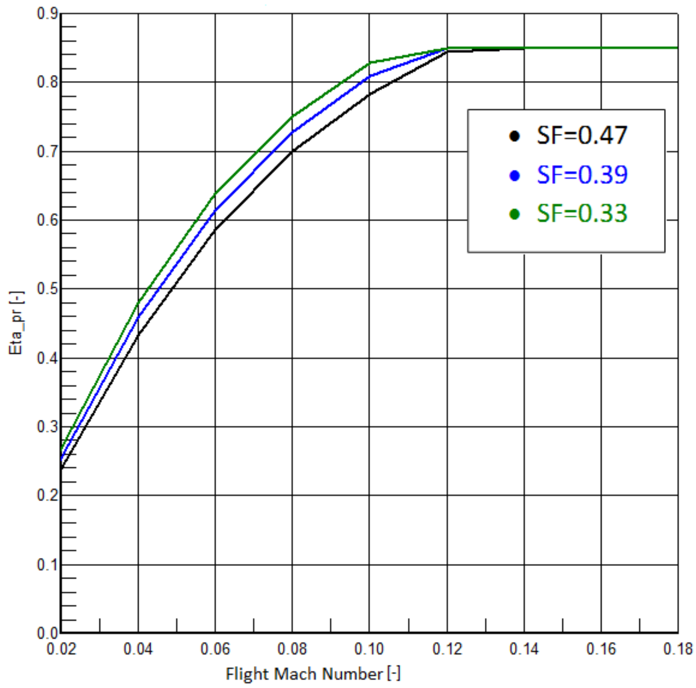

Figure 8.1: Propeller efficiency with V0 at sea level

flight envelope require specific operational settings, hence different thrust ratings.

At climb, fixed power setting has been defined. This means that the same percentage of maximum thrust has been used for each engine models. Available thrust resulted to be critical in the assessment of the engine model performance. As size is reduced, performance becomes poorer because the power available is not sufficient to overcome the aircraft drag. Higher technology levels, meaning greater power available, are fundamental. For a scaling factor of 0.39, technology levels 0, 1, and 2 take up to about 300% more time than the reciprocating engine to reach the cruising altitude, meaning too low thrust available at climb engine setting. At even smaller size (SF=0.33), only TL 3+ is able to climb within an acceptable time. On the other hand, higher technology level means higher thrust at the expenses of a higher fuel consumption. When turbine performance at climb is set over the reference reciprocating engine performance, none of the turboprop models is able to outdo it.

As a matter of fact, the reciprocating engine showcases very good performance at climb due to the effect of the supercharger. Superchargers are a natural addition to aircraft

piston engines that are intended for operation at high altitudes. As an aircraft climbs to higher altitude, air pressure and air density decreases. The output of a piston engine drops because of the reduction in the mass of air that can be drawn into the engine. A supercharger increases the pressure of the air supplied, giving at each intake cycle more oxygen, letting it burn more fuel and do more work, thus increasing power.
At cruise, no fixed engine setting is used. In fact, the aircraft design and mission profile determine the required thrust by the engine and, thus, the power needed by the ideal propeller. The closer the cruise power is to the maximum power of the engine, the better, since turbine cycle efficiency is there at its optimum. A smaller turbine has to cruise at a higher power setting compared to a bigger one in order to achieve the same required thrust, therefore decreasing the specific fuel consumption.
The effect of power setting on cycle efficiency is partially compensating the negative effect of scale on turbine components efficiency. This, in addition to the engine weight reduction, allows a downscaled turboprop engine to arguably showcase overall better mission performance compared to the bigger turbines and the reference reciprocating engine. Moreover, the cruise phase represents the largest portion of the mission, and, correspondingly, the largest opportunity for fuel burn reduction.

Finally, a conceptual engine design has been developed. A turboprop engine is selected with one third of the design point inlet massflow of the original TP100. Engine diameter scales with the square root of the scaling factor. With a scaling factor of 0.33 and the original diameter of about 350 mm, the estimated engine diameter is 20 cm. With a calculated weight of 20 kg, the turbine is 70% lighter than the reciprocating engine. A turbine inlet temperature of 1250 K requires the turbine blades to be made of MAR-M247. A pressure ratio of 8 with isentropic efficiency of 0.74 is feasible for a radial compressor, even though in multistage configuration, due to stress considerations which severely limit the compressor safety, durability and life expectancy. With the current technology, the equivalent flow axial compressor will be less efficient due primarily to a combination of rotor and variable stator tip-clearance losses. Furthermore, a radial compressor offers the advantages of simplicity of manufacturing and relatively low cost. This is due to requiring fewer stages to achieve the same pressure rise.
When this engine model, at a conceptual design phase, is implemented into the UAV platform, engine weight reduction and improved performance compared to the original reciprocating engine allow to modify the UAV airframe and further optimize the mission performance. The aircraft performance simulation estimates an endurance of 28.7 hours, 4% higher than the original UAV configuration for the same payload weight (250 kg).
The Case Study mission requirements established in Chapter 4 consist of a range value of 1800 km, for 18 to 21 hours endurance, suitable for both geophysical survey and pipeline monitoring work. The actual range of the final UAV with the micro gas turbine is about 1.5 times higher, with 40% longer endurance. Moreover, the payload carried by the redesigned UAV goes beyond the one estimated for the Case Study. A payload weight of 250 kg (instead of 50 kg) was chosen due to the performance data available for the reference UAV, which was fundamental for the aircraft model validation. This means that also Application 2 of the Case Study, corresponding to a mission for delivering high value goods to areas with limited access, is feasible.

Chapter 9

Conclusion

The present Master Thesis Research investigated the potential of micro gas turbines employed in small Unmanned Aerial Vehicle for civil applications. The strong growth of the UAV market is expected to come along with the increase in functionalities such as higher endurance, lower noise and emissions, extended mission range, among others.
The type and performance of the UAV is principally determined by the needs of the operational mission. In the Exploration Study, future high potential civil applications have been identified and further developed into a Case Study. Different propulsion concepts have been analysed, and gas turbine engines result having many advantages compared to typical reciprocating engines and electric motors. In particular, turboprops are suitable for UAVs operating between 7 and 15 km height at speeds of less than Mach 0.6. Nowadays, most turboprop engines are intended for large general-aviation aircrafts, regional commercial transports, and military transports, with power output much higher than that required for most UAV applications. Therefore, a gap in the current available technology has been identified which was speculated to be potentially filled by the development of small gas turbine based engines.
Micro gas turbine technology State of the art has been presented, with an extensive discussion of major design considerations. An engine model has been developed, starting from a reference turboprop engine. According to the indications found in the literature, the reference turboprop has been downscaled and effect of size on components efficiency has been estimated. Engine cycle optimization using the Gas turbine Simulation Program (GSP) has been carried out and the effects of turbine inlet temperature, compressor pressure ratio, engine size, and components efficiency have been investigated.
Furthermore, an "Aircraft Study" has been performed in a correlated Master Thesis Project. In this work, the aerodynamic and flight performance model of a baseline UAV has been developed. Results from the turbine model of different engine configurations, in the form of Thrust Management Tables, have been integrated in the UAV mission performance model. The outcome of the simulations consented to determine the best performing engine configuration for the selected mission.
The main challenge of the project was to improve the propulsion system efficiency for specific requirements in terms of range and endurance. When the optimized conceptual

engine design is implemented into the UAV platform, redesigned accordingly to the reduced weight and improved performance, the mission model estimated an endurance of 28.7 hours, with a range of 4419 km and a payload weight of 250 kg, with a significant fuel reduction of 12.5% compared to the original UAV configuration.
The design options which allow a micro turbine to arguably showcase a competitive edge compared to alternative propulsion concepts have been established. The original reciprocating engine showcases 86 kW and a specific fuel consumption of 0.30 kg/kWh at sea level. On the other hand, the micro gas turbine has 77 kW output power and a specific fuel consumption of 0.41 kg/kWh at the same design point. Despite the worse performance at sea level, the effect of power setting at cruise and the engine weight reduction (20 kg un-installed dry weight instead of 70 kg for the reciprocating engine) allows the turboprop to arguably showcase overall better mission performance.
The final engine configuration is a dual shaft turboprop set-up with a gas generator module on one shaft and a free power turbine on the other. The output power is transmitted through a gearbox to a propeller of 1.6 diameter. Turbine inlet temperature equal to 1250 K and a compressor pressure ratio of 8 are selected. The gas generator is made up by a single multistage radial compressor with a design efficiency of 0.75 and an axial turbine with a design efficiency of 0.83.

9.1 Recommendations for future work

Engine modeling and Aircraft Mission Performance modeling required several assumptions which effect the results of the study. In particular, the propeller model should be improved with the implementation of performance maps, and constant or variable pitch propeller configuration should be investigated. Gas generator and power turbine maps should also be developed according to the data of the manufacturer.
Future work could explore lower power levels according to varying mission requirements which can be modified in agreement with other possible UAV civil applications. Optimized mission profiles could be applied for different engine configuration, for a more sensible performance comparison.
Since the cruise phase showcased to be the most influential for the fuel consumption, investigation of a Design Point at cruise conditions is suggested for further engine sizing optimization.
Finally, the technology of the derived conceptual engine model has to be developed into a detailed design. CFD simulations are suggested for the definition of the optimum blades geometry. Different compressor configurations should also be investigated, e.g. combination of multi stage axial and radial compressor.

9.2 Reflection

As a result of the work carried out in this Master Thesis Project, a valuable tool for understanding the contribution of micro gas turbine integration into civil UAV has been developed. The concept of using simulations for performance prediction is becoming increasingly important due to less cost, better prediction and variety of modeling possible also to confirm new design without doing actual experiments. Nevertheless, test and experiments are always required to verify the simulation results before using the model predictions for design purposes. Based on these, empirical correlations can be developed for further strengthening of the simulation estimations. This thesis apart from applying the above mentioned models provides vital insights on the current development of simulations and provides a natural background for planning of relevant experiments and test.

Bibliography

[1] J. Wilson, "Worldwide UAV Roundup," *AIAA, American Institute of Aeronautics and Astronautics*, 2013.

[2] CASSIDIAN, EADS company, "Harfang datasheet," *http://www.defenceandsecurity-airbusds.com/web/guest/harfang-pdf*, Accessed: 10-12-2014.

[3] Merriam-Websters Dictionary, "Drone," *http://www.merriam-webster.com/dictionary/drone*, Accessed: 20-04-2014.

[4] NASA, "Earth observations and the role of uavs: a capabilities assessment," *Civil UAV Assessment Team*, 2006.

[5] J. Gundlach, *Designing Unmanned Aircraft Systems: A Comprehensive Approach.* American Institute of Aeronautics and Astronautics, 2012.

[6] R. Austin, *Unmanned Aircraft Systems.* John Wiley & Sons Ltd, 2010.

[7] M. D. F. Bento, "Unmanned aerial vehicles: an overview," *Inside GNSS*, 2008.

[8] L. Brief, "Growth Opportunity in Global UAV Market," Tech. Rep. March, 2011.

[9] K. Nonami, "Prospect and Recent Research & Development for Civil Use Autonomous Unmanned Aircraft as UAV and MAV," *Journal of System Design and Dynamics*, vol. 1, pp. 120–128, 2007.

[10] S. Tsach, A. Peled, D. Penn, B. Keshales, and R. Guedj, "Development trends for next generation UAV systems," no. May, pp. 1–14, 2007.

[11] T. H. Cox, C. J. Nagy, M. A. Skoog, and I. A. Somers, "Civil UAV Capability Assessment," Tech. Rep. December, NASA, 2004.

[12] M. Lukovic, "The Future of the Civil and Military UAV Market," tech. rep., Frost & Sullivan Market Insight, 2011.

[13] R. a. V. Gimenes, L. F. Vismari, V. F. Avelino, J. a. B. Camargo, J. R. Almeida, and P. S. Cugnasca, "Guidelines for the Integration of Autonomous UAS into the Global ATM," *Journal of Intelligent & Robotic Systems*, vol. 74, pp. 465–478, sep 2013.

[14] "EASA Regulation(EC) No 216/2008," *https://www.easa.europa.eu/document-library/regulations/regulation-ec-no-2162008*, Accessed: 15-04-2014.

[15] ICAO, *Unmanned Aircraft Systems (UAS).* John Wiley & Sons Ltd, 2010.

[16] J. Allen and B. Walsh, "Enhanced Oil Spill Surveillance, Detection and Monitoring Through the Applied Technology of Unmanned Air Systems," *International Oil Spill Conference Proceedings*, no. 1, pp. 113–120, 2008.

[17] D. J. Pines and F. Bohorquez, "Challenges Facing Future Micro-Air-Vehicle Development," *Journal of Aircraft*, vol. 43, pp. 290–305, 2006.

[18] A. Horcher and R. J. M. Visser, "Unmanned aerial vehicles: applications for natural resource management and monitoring," *Proceedings of the Council of Forest Engineering*, 2004.

[19] K. Ro, J. S. Oh, and L. Dong, "Lessons learned: Application of small uav for urban highway traffic monitoring," *AIAA paper*, no. January, pp. 1–19, 2007.

[20] A. V. Koldaev, "Non-military UAV application," *Aero India International Seminar*, no. Fe, 2007.

[21] H. Bendea and P. Boccardo, "Low cost UAV for post-disaster assessment," *The International Archives of the Photogrammetry, Remote Sensing and Spatial Information Sciences*, vol. XXXVII, no. Part B8, pp. 1373–1380, 2008.

[22] Y. Huang, S. J. Thomson, and W. C. Hoffmann, "Development and prospect of unmanned aerial vehicle technologies for agricultural production management," *Int J Agric & Biol Eng*, vol. 6, pp. 1–10, 2013.

[23] J. Barnard, "The use of Unmanned Air Vehicles in Exploration and Production activities," *23rd Bristol International UAV Systems Conference*, no. Apr, 2008.

[24] J. Everaerts, "The use of unmanned aerial vehicles (UAVs) for remote sensing and mapping," *The International Archives of the Photogrammetry, Remote Sensing and Spatial Information Sciences*, vol. XXXVII, 2008.

[25] R. Decuypere and D. Verstraete, "Micro Turbines from the Standpoint of Potential Users," *Micro Gas Turbines - Educational Notes RTO-EN-AVT-131, Paper 15*, pp. 15–1 – 15–14, 2005.

[26] H. Oron, "UAV Engines in the next decade-Turbine Engines, Piston Engines and the newly Combat Proven Rotary Engine," *A Lecture at the 6th Symposium on Jet Engines and Gas Turbines, "Elbit Systems"*, 2006.

[27] J. Larminie, A. Dicks, and M. S. McDonald, *Fuel cell systems explained*, vol. 2. Wiley New York, 2003.

[28] "Protonex Technology Corporation," *http://www.protonex.com/*, Accessed 25-04-2014.

[29] A. H. Epstein, S. D. Senturia, G. Anathasuresh, A. Ayon, K. Breuer, K. Chen, F. E. Ehrich, G. Gauba, R. Ghodssi, C. Groshenry, S. Jacobson, J. H. Lang, C. Lin, A. Mehra, J. M. Miranda, S. Nagle, D. J. Orr, E. Piekos, M. A. Schmidt, G. Shirley, M. S. Spearing, C. S. Tan, Y. Waitz, and I. Tzeng, "Power Mems And Microengines," *International Conference on Solid-State Sensors and Actuators*, no. June, pp. 753–756, 1997.

[30] J. Peirs, D. Reynaerts, and F. Verplaetsen, "A microturbine for electric power generation," *Sensors and Actuators*, vol. 113, pp. 86–93, June 2004.

[31] C. Rodgers, "Turbofan Design Options for Mini UAV's," *AIAA*, no. July, 2001.

[32] P. A. Pilavachi, "Mini- and micro-gas turbines for combined heat and power," *Applied Thermal Engineering*, vol. 22, pp. 2003–2014, dec 2002.

[33] S. A. Jacobson, "Aerothermal challenges in the design of a microfabricated Gas Turbine Engine," in *29ˆth AIAA Fluid Dynamics Conference*.

[34] R. A. Van den Braembussche, "Micro Gas Turbines - A Short Survey of Design Problems," *Micro Gas Turbines - Educational Notes RTO-EN-AVT-131, Paper 1*, pp. 1–1 – 1–18, 2005.

[35] A. J. Head and W. Visser, "Scaling 3-36kw microturbines," in *ASME Turbo Expo 2012: Turbine Technical Conference and Exposition*, pp. 609–617, American Society of Mechanical Engineers, 2012.

[36] S. M. Beuselinck, "Exploration of the potential of civil unmanned aerial vehicles powered by micro gas turbine propulsion system."

[37] BRP-Powertrain, "Operator's manual for rotax engine type 914 series," *http://www.rotax-owner.com/en/support-topmenu/engine-manuals*, Accessed: 20-09-2014.

[38] P. V. Bíteš, "TP100 turbopropeller engine," *http://www.pbsvb.com/customer-industries/aerospace/aircraft-engines/tp-100-turboprop-engine*, Accessed: 20-08-2014.

[39] S. L. Dixon, *Fluid Mechanics and Thermodynamics of Turbomachinery.* 1998.

[40] L. Moody and T. Zowski, "Hydraulic machinery. handbook of applied hydraulics, 26-19," 1969.

[41] H. Addison, *Applied hydraulics.* Chapman & Hall, 1964.

[42] B. Massey, "Mechanics of fluids, 1989."

[43] W. Visser, S. Shakariyants, and M. Oostveen, "Development of a 3 kw microturbine for chp applications," *Journal of Engineering for Gas Turbines and Power*, vol. 133, no. 4, p. 042301, 2011.

[44] P. R. Daniel, "Aircraft design: a conceptual approach," *Published by American Institute of Aeronautics and Astronautics Inc*, pp. 515–552, 1992.

[45] J. K. Berner, *Space power conversion systems using a Modified Ericsson cycle with turbomachinery*. 1985.

[46] W. P. J. Visser and M. J. Broomhead, "GSP - A generic object-oriented gas turbine simulation environment," *ASME Turbo Expo 2000*, no. May, 2000.

Appendix A

Turboprop Thermodynamic Cycle

This appendix contains the mathematical model for the turboprop thermodynamic cycle analysed in the thesis. It looks as follows:

Figure A.1 represent a two-shaft turboprop engine configuration.

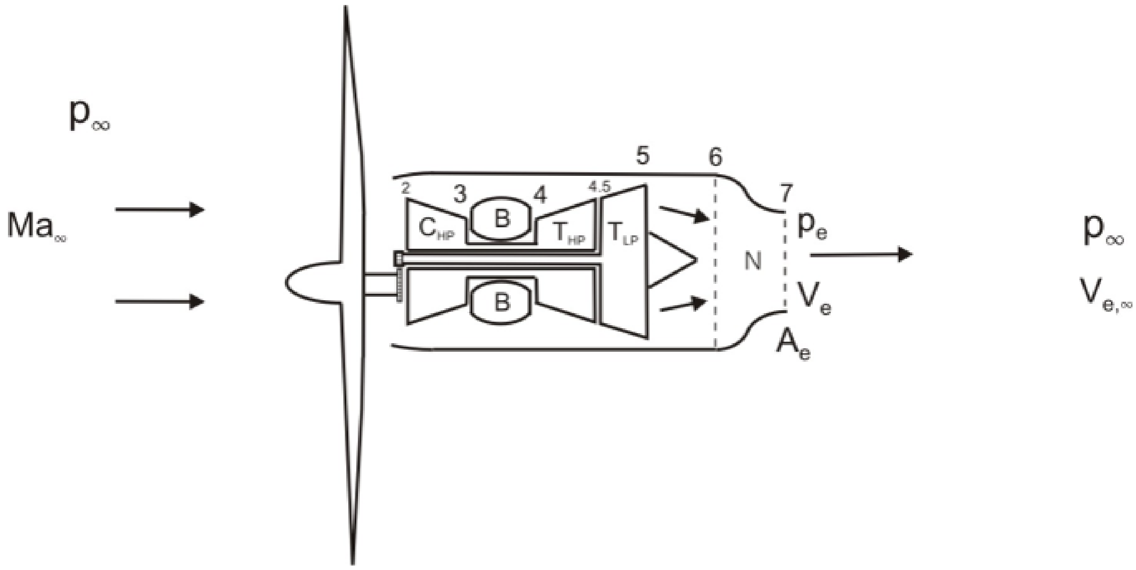

Figure A.1: Turboprop Layout and Station Numbering

Where C_{HP} indicates the high pressure compressor, B the burner (or combustor), T_{HP} the gas generator turbine, T_{LP} the power turbine (low pressure), and N the nozzle.
The power output of the free turbine (to the speed reduction gearbox) can be estimated as follows:

$$P_{shaft} = \eta_m \dot{m}_g c_{p,g} \left(T_{04,5} - T_{05}\right) \tag{A.1}$$

With η_m shaft mechanical efficiency, $\dot{m}_g$ gas mass flow at station (4,5), $c_{p,g}$ gas specific heat at constant pressure, T total temperature at the specified station.

The temperature drop $(T_{04,5} - T_{05})$ in the power turbine can be calculated using both isentropic or polytropic efficiency. With the polytropic efficiency $\eta_{\infty,PT}$, it becomes:

$$T_{04,5} - T_{05} = T_{04,5}\left[1 - \left(\frac{p_{05}}{p_{04,5}}\right)^{\frac{\gamma_g - 1}{\gamma_g}\eta_{\infty,PT}}\right] \tag{A.2}$$

With γ_g ratio of specific heat for the gas coming from the gas generator, p total pressure at the specified station.
The upstream HP turbine must drive the main compressor, such that:

$$\dot{m}_a c_{p,a}\left(T_{03} - T_{02}\right) = \eta_m \dot{m}_g c_{p,g}\left(T_{04} - T_{04,5}\right) \tag{A.3}$$

So that:

$$T_{04,5} \approx T_{04} - \frac{1}{\eta_m}\left(T_{03} - T_{02}\right) \tag{A.4}$$

$$p_{04,5} \approx p_{04}\left[\frac{T_{04,5}}{T_{04}}\right]^{\frac{\gamma_g}{(\gamma_g - 1)\eta_{\infty,GGT}}} \tag{A.5}$$

Downstream:

$$T_{05} = T_{04,5} - \frac{P_{shaft}}{\eta_m \dot{m}_g c_{p,g}} \tag{A.6}$$

Where P_{shaft} is the power delivered to the propeller:

$$P_{shaft} = CP\rho N^3 D^5 \tag{A.7}$$

With N rotational speed of the propeller, D propeller diameter, ρ air density, and CP power coefficient.
The resulting propeller thrust is:

$$F_{prop} = CT\rho N^2 D^4 = \frac{\eta_{prop} CP}{J}\rho N^2 D^4 = \frac{\eta_{prop} P_{shaft}}{V_0} \tag{A.8}$$

Where CT is the propeller thrust coefficient, J is the propeller advance ratio, and V_0 is the aircraft flight velocity.
Once T_{05} is known:

$$p_{05} \approx p_{04,5}\left[1 - \frac{1}{\eta_t}\left(1 - \frac{T_{05}}{T_{04,5}}\right)\right]^{\frac{\gamma_g}{\gamma_g - 1}} \tag{A.9}$$

Only in this formula, isentropic efficiency η_t instead of polytropic has been shown. Appendix B further discusses the relations between the two definitions.
In the typical case where a turboprop would not be using an afterburner, one can transfer

flow property values immediately from station (5) to station (6) for the nozzle entry. The core exhaust jet is usually unchoked, such that for a simple convergent nozzle with station (7) as the exit plane:

$$p_7 \to p_\infty \tag{A.10}$$

$$\frac{T_7}{T_{06}} = \left(\frac{p_\infty}{p_{06}}\right)^{\frac{\gamma_g - 1}{\gamma_g}} \tag{A.11}$$

$$\rho_7 = \frac{p_\infty}{RT_7} \tag{A.12}$$

With R gas constant.
The exit jet velocity becomes:

$$V_{jet} = \sqrt{2\eta_n c_{p,g} T_{06} \left[1 - \left(\frac{p_\infty}{p_{06}}\right)^{\frac{\gamma_g - 1}{\gamma_g}}\right]} \tag{A.13}$$

Finally, cycle thermal efficiency and turboprop overall efficiency can be calculated:

$$\eta_{th} = \frac{P_s}{\dot{m}_f LHV} \tag{A.14}$$

Where $\dot{m}_f LHV$ is the product of fuel mass flow and fuel lower heating value.

$$\eta_{TP} = \eta_{pr}\eta_{th} \tag{A.15}$$

The definition of η_{pr} is explained in appendix C.
Overall thrust is calculated by:

$$F_{overall} = F_{prop} + F_{jet} = \frac{\eta_{pr} P_{shaft}}{V_0} + \dot{m}_a \left([1 + f] V_{jet} - V_0 \right) \tag{A.16}$$

Where f is the ratio of air over fuel mass flows.

Appendix B

Compressor and Turbine Efficiency

Radial flow turbomachinery handles the small volumetric flows of air and combustion products (0.2 to 2 kg/s) with reasonably higher component efficiency compared to their axial counterparts. These components are usually more efficient at low pressure ratios due to their uncomplicated design, robustness and insensitivity to flaws. The compression and expansion in the real process are not irreversible and adiabatic, which means the relation between temperature and the pressure ratio is not fixed. Figure B.1 shows the compression and expansion processes in the temperature-entropy diagram. The relation between temperature and pressure can be expressed in terms of the ratio of work for the ideal versus the real process in the form of the isentropic efficiency.

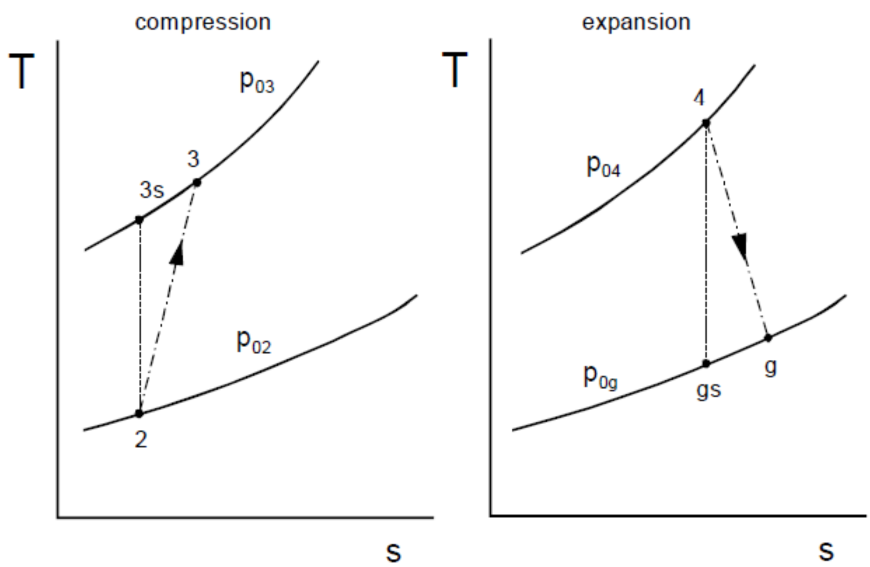

Figure B.1: Non-isentropic compression and expansion respectively.

Using the concept of total enthalpy or temperature, which accounts for the kinetic energy changes of the fluid between inlet and exit of the component, isentropic efficiency is defined as follows:

$$\eta_{is,compressor} = \frac{\left(\frac{p_{03}}{p_{02}}\right)^{\frac{k_{air}-1}{k_{air}}} - 1}{\frac{T_{03}}{T_{02}} - 1} \tag{B.1}$$

$$\eta_{is,turbine} = \frac{\frac{T_{0g}}{T_{04}} - 1}{\left(\frac{p_{0g}}{p_{04}}\right)^{\frac{k_{air}-1}{k_{air}}} - 1} \tag{B.2}$$

A problem arises when gas turbine cycles are analysed with varying compression ratios. In practice, changing pressure ratio means modifying the number of compressor or turbine stages. A compressor generally has a number of successive stages in series with similar characteristics, i.e. similar isentropic efficiency. Geometry is changing and blade length is decreasing, because of increasing density with increasing pressure of the medium downstream. Design rules for the variation of geometry usually make flow losses and thereby also stage isentropic efficiency remain rather constant. Figure B.2 shows a compressor with three stages.

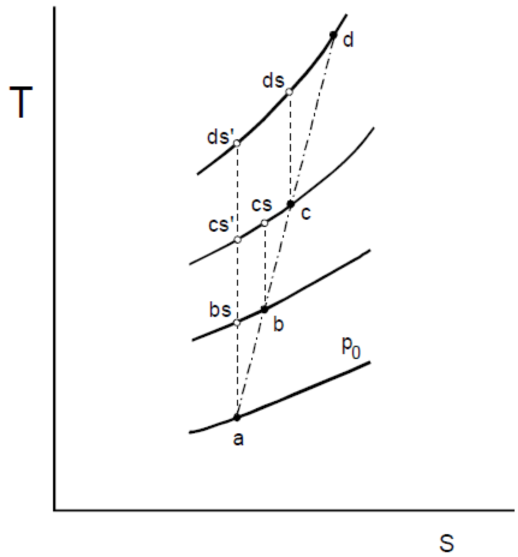

Figure B.2: Turboprop Layout and Station Numbering.

If we divide the compression phase into an infinite number of infinitely small compression stages, with equal isentropic efficiencies, the result is a polytropic compression process with a constant value for the polytropic exponent n_{air}.
As an alternative for the isentropic efficiency, the polytropic efficiency is defined as the isentropic efficiency of an infinitely small compression step with the assumption that it is constant for throughout the compression phase. The polytropic efficiency can be

calculated:

$$\eta_{\infty,c} = \frac{dT_{0,s}}{dT_0} = \frac{\frac{k_{air}-1}{k_{air}}}{\frac{n_{air}-1}{n_{air}}} \tag{B.3}$$

For a compressor, polytropic efficiency can be expressed as:

$$\eta_{\infty,c} = \frac{\ln\left(\frac{p_{03}}{p_{02}}\right)^{\frac{k_{air}-1}{k_{air}}}}{\ln\left(\frac{T_{03}}{T_{02}}\right)} \tag{B.4}$$

For the expansion process, a similar relation can be formulated:

$$\eta_{\infty,t} = \frac{\ln\left(\frac{T_{0g}}{T_{04}}\right)}{\ln\left(\frac{p_{0g}}{p_{04}}\right)^{\frac{k_{gas}-1}{k_{gas}}}} \tag{B.5}$$

For a turbine, isentropic stage efficiency is smaller than overall isentropic efficiency.
A compression or expansion process can be characterized by either isentropic or polytropic efficiencies. The relation between the two can be derived combining B.1 with equations B.4 (B.2 with B.5 for the turbine). In case of calculating gas turbine cycle performance for a range of compression ratios as is typical for cycle analysis, using polytropic efficiency is most practical and has further been implemented in this work.

Appendix C

Ideal Propeller Theory

Ideal Propeller Theory, or Momentum Theory, was originally intended to provide an analytical means for evaluating ship propellers.
Momentum Theory is also known as Disk Actuator Theory. This theory assumes that:

- Mach number is low so that the flow behaves as an incompressible fluid;
- the flow is inviscid and steady (ideal flow), therefore the propeller does not experience energy losses due to frictional drag;
- also the rotor is thought of as an actuator disk with an infinite number of blades, each with an infinite aspect ratio;
- the propeller can produce thrust without causing rotation in the slipstream;
- the flow outside the propeller streamtube has constant stagnation pressure (no work is imparted to it);
- Across the actuator disk, assume that the pressure changes discontinuously, but the velocity varies in a continuous manner.

Since most of these assumptions are unrealistic, this theory is only useful in predicting ideal or maximum propeller efficiency.

In figure C.1, the flow is proceeding from left to right. Stations 0 and J are assumed to be far upstream and downstream of the propeller respectively, and the location of the actuator disk is identified by the subscript D.
From the basic thrust equation, the amount of thrust depends on the mass flow rate through the propeller and the velocity change through the propulsion system (the only force on the control volume is due to the change in momentum flux across its boundaries). Hence, T is equal to the mass flow rate ($\dot{m}$) times the difference in velocity (V):

$$T = \dot{m}\Delta V = \dot{m}\left(V_j - V_0\right) \tag{C.1}$$

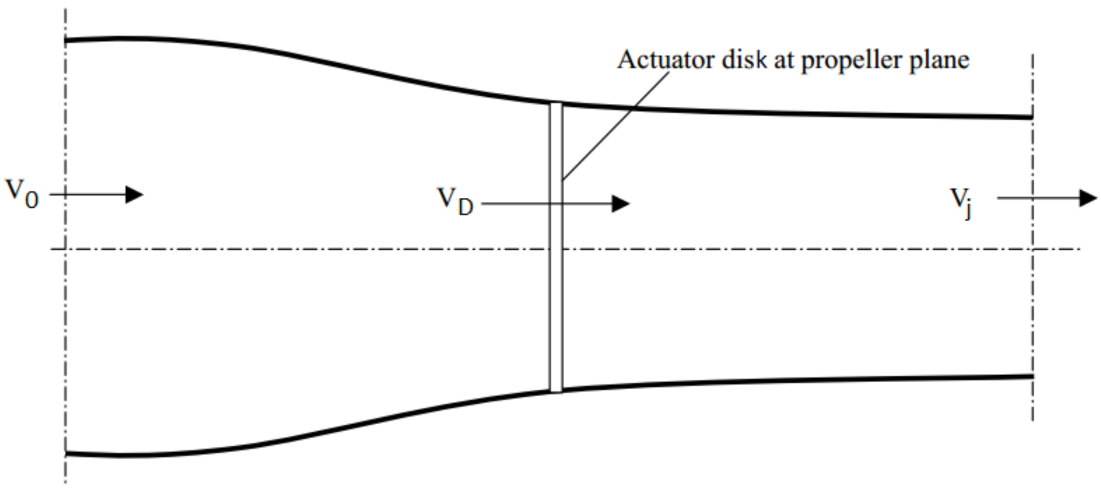

Figure C.1: Actuator disk representation

There is no pressure-area term because the pressure at J is equal to the pressure at 0. The mass of air passing through the propeller (per unit of time) is:

$$\dot{m} = \rho A_{disk} V_D \tag{C.2}$$

Where:
ρ = air density
$A_{disk} = \pi \frac{D^2}{4}$ propeller disk area
V_D = velocity through propeller

The power P_{input} absorbed by the propeller is given by the change in kinetic energy:

$$P_{input} = \frac{1}{2} \dot{m} \left(V_j^2 - V_0^2 \right) = \frac{1}{2} \rho A_{disk} V_D \left(V_j^2 - V_0^2 \right) \tag{C.3}$$

However, delivered power P_{input} is also equal to the work done by the thrust force:

$$P_{input} = T V_D = \rho A_{disk} V_D \left(V_j - V_0 \right) V_D \tag{C.4}$$

By comparing equations C.3 and C.4, the velocity at the propeller position becomes:

$$V_D = \frac{1}{2} \left(V_j + V_0 \right) \tag{C.5}$$

If V_D and V_j are expressed in terms of flight velocity V_0, then:

$$V_j = V_0 + v_2 \tag{C.6}$$

$$V_D = V_0 + v_1 \tag{C.7}$$

where v_1 and v_2 are known respectively as the increases in the velocities at the propeller disk and in the position far downstream. As a consequence, the slipstream must contract between the conditions existing far upstream and those existing downstream in order to satisfy the continuity equation:

$$Q_0 = Q_D = Q_j \tag{C.8}$$

$$\rho V_0 A_0 = \rho V_D A_{disk} = \rho V_j A_j \tag{C.9}$$

$$V_0 A_0 = (V_0 + v_1) A_{disk} = (V_0 + v_2) A_j \tag{C.10}$$

Where:

$$A_{disk} = \pi \frac{D_{disk}^2}{4}, A_0 = \pi \frac{D_0^2}{4}, A_j = \pi \frac{D_j^2}{4} \tag{C.11}$$

Hence,

$$D_0^2 = \frac{V_0 + v_1}{V_0} D_{disk}^2 \tag{C.12}$$

$$D_j^2 = \frac{V_0 + v_1}{V_0 + v_2} D_{disk}^2 = C_A D_{disk}^2 \tag{C.13}$$

where C_A is called the contraction factor.

The law of conservation of momentum equates the force exerted on the fluid with the net outflow of momentum. The control volume is the stream tube from A_0 to A_j. The mass per unit time through A_0 is $\rho V_0 A_0$ and the momentum inflow is $\rho V_0^2 A_0$. Similarly, the momentum outflow through A_j can be written and the conservation of momentum requires that:

$$\rho V_0^2 A_0 - \rho \left(V_j + v_2\right)^2 A_j + T = 0 \tag{C.14}$$

Using equations C.13 and C.12, this becomes:

$$T = \rho \pi \frac{D_{disk}^2}{4} \left(V_0 + v_1\right) v_2 \tag{C.15}$$

On the other hand, the thrust can also be written as $T = \Delta p A$. Bernoulli's equation can be used to relate the pressure and velocity upstream and downstream of the propeller disk, but not through the disk. For the upstream and downstream of the disk in figure C.2, respectively:

$$p_1 + \frac{1}{2} \rho \left(V_0 + v_1\right)^2 = p_0 + \frac{1}{2} \rho V_0^2 \tag{C.16}$$

and

$$p_2 + \frac{1}{2}\rho\left(V_0 + v_1\right)^2 = p_0 + \frac{1}{2}\rho\left(V_0 + v_2\right)^2 \tag{C.17}$$

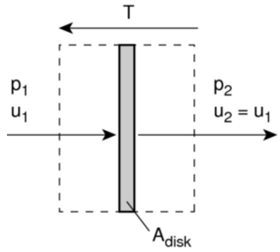

Figure C.2: Control volume around the actuator disk.

Subtracting the above equations:

$$\Delta p = \frac{1}{2}\rho\left(2V_0 v_2 + v_2^2\right) \tag{C.18}$$

Therefore, another formulation for the propeller thrust is:

$$T = \rho\pi\frac{D_{disk}^2}{4}\left(V_0 + \frac{v_2}{2}\right)v_2 \tag{C.19}$$

Combining the two definitions of T C.15 and C.19, it is derived that:

$$v_2 = 2v_1 \tag{C.20}$$

This shows that half of the acceleration takes place before the propeller disk and the remaining half after the propeller disk. In other words, the axial induced velocity at the propeller (v_1) is half the axial induced velocity at J. The relation between the propeller thrust and the axial induced velocity is:

$$T = \rho\pi\frac{D^2}{4}\left(V_0 + v_1\right)2v_1 \tag{C.21}$$

The propeller thrust is made non-dimensional with the propeller area and the inflow velocity V_0:

$$C_T = \frac{T}{\pi\frac{D^2}{4}\frac{1}{2}\rho V_0^2} \tag{C.22}$$

where C_T is a thrust coefficient indicating the propeller loading. The following correlation between actuator disk parameters holds:

$$\frac{2v_1}{V_0} = \sqrt{1 + C_T} - 1 \tag{C.23}$$

The induced velocity V_D in the slipstream represents the energy supplied to the flow behind the propeller. This is due to the fact that the fluid gives way when a thrust is exerted to it. The loss of the energy is reflected in an efficiency which is lower than 1. To formulate the efficiency, the propeller disk moves with a velocity V_0 and exerts a force T. The propulsive power is therefore:

$$P_{prop} = TV_0 \tag{C.24}$$

In the slipstream, a velocity $2V_D = V_j - V_0$ is present. With the mass flow expressed as the mass flowing through the propeller disk, which is equal to that flowing through the slipstream, this represents an energy of:

$$E_{lost} = \pi \frac{D^2}{4} \rho \left(V_0 - V_D\right) \left(2V_D\right)^2 \tag{C.25}$$

Hence, the efficiency of the propeller can be written as:

$$\eta_{prop} = \frac{P_{prop}}{P_{input}} = \frac{TV_0}{TV_0 + E_{lost}} \tag{C.26}$$

Which becomes:

$$\eta_{prop} = \frac{2}{1 + \frac{V_j}{V_0}} \tag{C.27}$$

This represents the maximum efficiency which is theoretically possible in an inviscid flow with a propeller not introducing any rotation in the slipstream. It is therefore called the ideal propeller efficiency.

Appendix D

Analysed existing UAVs

Table D.1 presents all the existing UAVs analysed in Chapter 4 within the selected power range with their specifications.

Country	Prime	Designation	Status	Launch	Propulsion	Type	Endurance (hr)	Range (km)	Ceiling (m)	Power (kW)	MTOW (kg)	Payload (kg)	Max speed (km/h)	Cruise speed (km/h)	Wing/Rotor span (m)
Austria	Schiebel Camcopter S-100	Camcopter S-100	In production		Reciprocating	VTOL	6	180	5500	41	200	50	222	185	3.4
	Diamond Aircraft	Diamond Hero	In development		Reciprocating		6.5			40		113			
India	Kadet Defense Systems	MSAT-500/NG	Deployed	Bungee catapult or pneumatic	Reciprocating	delta wing	1.75	10	5000	30	82				2.75
Israel	UVision Global Aero Syst	Butterfly	Under way		Reciprocating	Paraglider	4	115		48	450	230		55	
Italy	Selex Galileo Avionica	Falco	In production	Ground launched, catapult launched	Reciprocating	MALE TUAV	14	190	6500	48	420	70	216		7.2
Malaysia	Composite Technology Research	Aludra Mk 1	Deployed	Ground launched	Reciprocating	Fixed Wing	3	48	3658	37	200	25		220	6
Netherlands	High Eye B.V.	HEF150	Under way	Ground launched	Reciprocating	VTOL	7			41		50			3.15
Norway	CybAero	APID 60	Under way	Ground and ship launched	Reciprocating	VTOL	8	200		41	180	50	150	90	3.3
Pakistan	Satuma	Flamingo	Completed	Ground launched	Reciprocating	Fixed Wing	8	200	4267	45	245	35	130		7.32
Russia	Enics	E08	Under way	Catapult launched	Pulse Jet	Canard	0.5	70	3000	59	150		300	200	5
		E95M	Under way	Catapult launched	Pulse Jet	Fixed wing	0.5	187	3000	59	75		300	200	2.9
	Kamov	Ka-137	Under way	Ground and ship launched	Reciprocating	VTOL	4	530	5000	50	280	80	175	145	5.3
Serbia	Military Technical Institute	Pegaz 101	In development	Ground launched	Reciprocating	Fixed wing	12	100	3000	32	230	40	200	150	6.34
Spain	INTA	Siva	Under way				6.5	150	4000	50	300	49	190	115	5.8
Sweden	CybAero	APID 55	Under way		Reciprocating	VTOL	6	50	3000	41	160	55	90	60	3.3
		Vantage	Under way		Reciprocating	VTOL	5		2400	31	173	16	185		2.77
	Saab defense	Skeldar V-200	In production			VTOL	5	150	4500	41	200	40	130		
Turkey	Turkish Aerospace Industries	Karayel	In production		Reciprocating	Fixed wing	20		6858	52	500	70		148	10.5
UAE	ADCOM Military Industries	Yabhon RX	Under way	Catapult launched	Reciprocating	Fixed wing	6		5500	37	160	50	240	204	5.8
		Yabhon-N	Under way	Catapult launched	Reciprocating	Flying wing	3		6000	37	100	40	420	107	2.75
UK	Warrior (Aero-Marine Ltd.)	GULL 68 UXV	Under way	Ground or Water Lauched	Reciprocating	Seaplane		2081		33	250	94	185		7.6
US	AAI	Shadow 600	Completed		Reciprocating	Fixed wing	14	322	1487	39	265	41	200	148	6.8
	Atair	LEAPP Type II	Under way	Ground Lauched	Reciprocating	Paraglider	34		5182	41	544	91			34
	Elbit Systems of America	Hermes 450	Deployed	Ground Lauched	Reciprocating	Fixed wing	18	300	5486	39	550	180	176	130	10.5
	General Atomics Aeronautical Systems	I-GNAT ER/Sky Warrior	Deployed		Reciprocating	MALE	40	250	7620	48	520	91	192		10.75

Table D.1: Existing UAVs in the 30-60 kW power range, from 2013 Worldwide UAV Roundup,AIAA [1]

Appendix E

Thrust Management Tables

This appendix contains the Thrust Management Tables of the conceptual engine design of Chapter 7. Each table shows a set of net thrust values or fuel values for the specified rating code as defined in Chapter 5. In the tables, rows represent thrusts or fuel flows available at different flight Mach numbers, while each column indicate a different flight altitude.

RC 20	**0**	**1000**	**2000**	**3000**	**4000**	**5000**	**6000**	**7000**	**8000**
0	794	801	793	778	759	750	713	684	643
0.03	666	684	688	684	676	670	662	634	591
0.06	489	510	522	527	528	527	521	514	483
0.09	337	359	376	388	398	410	412	415	393
0.12	257	274	286	295	302	309	319	316	304
0.15	209	223	233	239	244	250	258	255	245
0.18	178	187	197	202	206	210	212	213	206
0.19	170	180	187	192	196	200	201	202	196

Table E.1: RC 20 Net Thrust [N]

RC 20	**0**	**1000**	**2000**	**3000**	**4000**	**5000**	**6000**	**7000**	**8000**
0	11.14	10.49	9.84	9.20	8.60	8.08	7.49	6.95	6.38
0.03	11.14	10.50	9.84	9.21	8.61	8.06	7.55	6.98	6.36
0.06	11.17	10.51	9.86	9.22	8.62	8.05	7.50	6.99	6.37
0.09	11.20	10.54	9.89	9.25	8.64	8.09	7.51	7.00	6.38
0.12	11.25	10.59	9.93	9.28	8.67	8.09	7.59	7.02	6.42
0.15	11.31	10.64	9.98	9.32	8.70	8.12	7.62	7.04	6.43
0.18	11.39	10.69	10.04	9.37	8.75	8.15	7.58	7.03	6.46
0.19	11.42	10.74	10.06	9.39	8.76	8.17	7.59	7.04	6.47

Table E.2: RC 20 Fuel Flow [kg/h]

RC 40	**0**	**1000**	**2000**	**3000**	**4000**	**5000**	**6000**	**7000**	**8000**
0	2419	2247	2075	1904	1739	1586	1437	1293	1161
0.03	2302	2146	1989	1831	1677	1533	1394	1256	1131
0.06	1937	1814	1688	1560	1434	1316	1200	1085	979
0.09	1617	1523	1423	1319	1217	1121	1026	930	842
0.12	1318	1254	1184	1108	1032	956	878	798	724
0.15	1063	1012	956	894	833	775	717	655	598
0.18	894	851	804	752	701	652	604	552	504
0.19	849	808	764	715	666	620	575	525	479

Table E.3: RC 40 Net Thrust [N]

RC 40	**0**	**1000**	**2000**	**3000**	**4000**	**5000**	**6000**	**7000**	**8000**
0	26.46	24.45	22.49	20.60	18.78	17.08	15.45	13.88	12.43
0.03 26.47	24.45	22.50	20.61	18.78	17.08	15.46	13.91	12.43	
0.06	26.49	24.48	22.53	20.63	18.80	17.10	15.47	13.92	12.45
0.09	26.53	24.52	22.57	20.67	18.84	17.13	15.50	13.92	12.48
0.12	26.59	24.57	22.62	20.72	18.89	17.18	15.56	13.96	12.52
0.15	26.66	24.65	22.70	20.78	18.95	17.24	15.60	14.01	12.56
0.18	26.75	24.76	22.78	20.86	19.03	17.31	15.68	14.08	12.62
0.19	26.79	24.77	22.82	20.89	19.06	17.33	15.72	14.10	12.64

Table E.4: RC 40 Fuel Flow [kg/h]

RC 45	0	1000	2000	3000	4000	5000	6000	7000	8000
0	2568	2370	2176	1992	1819	1650	1488	1338	1204
0.03	2453	2273	2095	1922	1760	1600	1446	1305	1176
0.06	2076	1932	1787	1644	1511	1378	1248	1130	1021
0.09	1743	1630	1513	1396	1288	1179	1070	971	881
0.12	1439	1359	1273	1185	1099	1009	918	835	759
0.15	1161	1097	1028	957	891	824	754	690	632
0.18	976	923	865	806	750	694	635	581	532
0.19	927	877	822	766	713	660	604	553	506

Table E.5: RC 45 Net Thrust [N]

RC 45	0	1000	2000	3000	4000	5000	6000	7000	8000
0	28.29	26.01	23.84	21.79	19.87	17.99	16.20	14.56	13.07
0.03	28.27	26.02	23.87	21.81	19.87	17.99	16.22	14.57	13.08
0.06	28.30	26.05	23.89	21.83	19.90	18.02	16.23	14.59	13.09
0.09	28.33	26.10	23.94	21.87	19.93	18.09	16.26	14.62	13.12
0.12	28.39	26.16	24.00	21.93	19.98	18.15	16.31	14.66	13.15
0.15	28.47	26.25	24.08	22.02	20.05	18.19	16.37	14.71	13.20
0.18	28.57	26.35	24.18	22.09	20.13	18.26	16.45	14.78	13.26
0.19	28.61	26.39	24.21	22.12	20.17	18.30	16.50	14.81	13.28

Table E.6: RC 45 Fuel Flow [kg/h]

RC 50	0	1000	2000	3000	4000	5000	6000	7000	8000
0	2823	2590	2371	2150	1947	1760	1590	1434	1291
0.03	2719	2500	2296	2086	1893	1716	1553	1404	1268
0.06	2321	2142	1972	1796	1634	1484	1348	1221	1106
0.09	1968	1821	1682	1536	1401	1276	1162	1056	959
0.12	1662	1550	1436	1315	1201	1097	1001	913	831
0.15	1341	1252	1167	1074	987	906	832	763	700
0.18	1128	1053	982	905	831	763	701	643	589
0.19	1072	1001	933	860	790	726	666	611	560

Table E.7: RC 50 Net Thrust [N]

RC 50	**0**	**1000**	**2000**	**3000**	**4000**	**5000**	**6000**	**7000**	**8000**
0	31.94	29.29	26.80	24.31	22.02	19.90	17.96	16.19	14.56
0.03	31.95	29.31	26.82	24.31	22.02	19.91	17.96	16.19	14.57
0.06	31.98	29.34	26.85	24.34	22.05	19.93	17.99	16.21	14.58
0.09	32.04	29.39	26.88	24.39	22.09	19.96	18.02	16.24	14.61
0.12	32.12	29.47	26.97	24.46	22.15	20.02	18.07	16.26	14.65
0.15	32.23	29.56	27.06	24.56	22.24	20.10	18.14	16.32	14.70
0.18	32.36	29.69	27.17	24.68	22.34	20.18	18.22	16.38	14.76
0.19	32.40	29.73	27.22	24.72	22.37	20.22	18.24	16.44	14.79

Table E.8: RC 50 Fuel Flow [kg/h]